Novel functions of *Drosophila melanogaster* Argonaute2 for miRNA mediated silencing and early embryonic development

Inaugural-Dissertation
zur Erlangung des Doktorgrades
der Mathematisch-Naturwissenschaftlichen Fakultät
der Heinrich-Heine-Universität Düsseldorf

vorgelegt von

Wibke Johanne Meyer
aus Leer

März 2006

Aus dem Institut für Genetik
der Heinrich-Heine Universität Düsseldorf

Gedruckt mit der Genehmigung der
Mathematisch-Naturwissenschaftlichen Fakultät der
Heinrich-Heine-Universität Düsseldorf

Referent: Dr. H.-A. J. Müller
Koreferent: Prof Dr. R. Simon

Tag der mündlichen Prüfung: 23. April 2007

Für meine Familie

Abstract

Gene silencing mediated by small RNAs is a mechanism of post-transcriptional gene regulation. It is common for many eukaryotic cells. Argonaute proteins are essential components of RNA mediated silencing pathways. Unlike in other model organisms, in *Drosophila* different Argonaute proteins have been assigned to different RNA silencing pathways. It was shown that Argonaute1 (Ago1) is essential for microRNA (miRNA) mediated silencing while Argonaute2 (Ago2) is required for silencing triggered by small interfering RNAs (siRNAs).

This thesis investigated a mutant allele of *ago2*, the female sterile mutation *ago2*^{dop}. *ago2*^{dop} mutations cause developmental defects in cellularisation and microtubule-based transport in early embryos. *Drosophila* Ago2 contains an unusual amino-terminus with two types of imperfect glutamine-rich repeats (GRRs) of unknown function. This thesis demonstrates that the GRRs of Ago2 are essential for the normal function of the protein. The *ago2*^{dop} alleles show an altered number of GRRs. The main question was to find out how Ago2 as the key enzyme of the siRNA mediated silencing pathway is involved in early embryogenesis. This thesis provides evidence that the phenotypes of *ago2*^{dop} mutant embryos are not a consequence of siRNA mediated silencing. *ago2*^{dop} mutants are still able to respond to siRNA triggers. Therefore Ago2 must have at least one other important function and might act in another regulatory pathways.

This thesis identified a new isoform of Ago2 that lacks the GRRs, which was named Ago2^{short}. The genetics of the *ago2*^{dop} alleles suggests that mutant Ago2^{dop} protein might negatively interfere with the function of Ago2^{short}. Ago2^{dop1} also interacts genetically with all other members of the Argonaute protein family. *ago2*^{dop1} homozygous embryos that are reduced in *ago1*, *piwi* or *aubergine* (*aub*) activity show an enhancement of the cellularisation phenotype in early embryos.

I propose that the developmental defects are caused by an inability to degrade maternal transcripts at mid-blastula transition (MBT). The MBT is marked by switch from solely maternal to zygotic control of embryogenesis. Downregulation of maternal genes is required at this stage of development. Maternal transcripts might be degraded through a miRNA mediated silencing pathway. In this thesis evidence is presented that miRNA *miR-9a* might be one possible regulator of maternal transcript degradation.

Furthermore genetic analyses demonstrate that Argonaute proteins act in a partial redundant fashion in early development. Ago1 and Ago2 have overlapping functions in the establishment of segment polarity. In protein extracts, Ago1 and Ago2 can be coprecipitated suggesting that they are present in the same protein complex. Genetic analysis revealed that Ago1 and Ago2 act in a partially redundant manner to control the expression of the segment-polarity gene *wingless* in the early embryo.

Taken together, this work demonstrates novel functions for Ago2 and argues strongly against a strict separation of Ago1 and Ago2 functions. Furthermore, the data suggest that different Argonaute proteins might act together to control key steps of embryonic development.

Zusammenfassung

Die Argonaut-Proteinfamilie besteht aus Proteinen, die essentiell für RNA vermittelte post-transkriptionale Genregulation sind. Im Gegensatz zu anderen Modellorganismen wurde für *Drosophila* gezeigt, dass verschiedene Argonaut-Proteine eine hohe Spezifität für verschiedene RNA Regulationswege besitzen. So wurde das Modell kreiert, dass Argonaute1 (Ago1) ausschließlich in der microRNA (miRNA) vermittelten Genregulation agiert und dass Argonaute2 (Ago2) essentiell für die Genregulation ist, die durch small interfering RNAs (siRNAs) ausgelöst wird.

Diese Doktorarbeit untersuchte die weibliche Sterilmutation *ago2^{dop}* in *Drosophila melanogaster*. *ago2^{dop}*-Mutationen führen zu Entwicklungsdefekten in der Zellularisierung und dem Mikrotubuli-abhängigen Transport von Organellen in frühen Embryonen. Das Ago2-Protein in *Drosophila* besitzt einen ungewöhnlichen Aminoterminus. Er besteht aus zwei Mustern nicht-perfekter Glutamin-reichen Wiederholungen (GRRs). Die Funktion der GRRs war bisher nicht bekannt. Diese Arbeit konnte zeigen, dass die GRRs für die korrekte Funktion von Ago2 essentiell sind. *ago2^{dop}*-Allele besitzen eine verringerte Anzahl der GRR-Wiederholungen. Ein Hauptpunkt dieser Doktorarbeit war, zu klären, welche Rolle Ago2 als wichtigstes Enzym des siRNA vermittelten Regulationsweges in der frühen Embryogenese spielt. Da der siRNA-Regulationsweg in *ago2^{dop}*-Embryonen funktionsfähig ist, kann der *ago2^{dop}*-Phänotyp nicht auf Defekte in diesem Mechanismus zurückzuführen sein. Ago2 muss daher noch mindestens eine weitere wichtige Funktion besitzen und könnte in anderen Regulationsmechanismen eine wichtige Rolle spielen. In dieser Arbeit konnte eine neue Ago2-Isoform identifiziert werden, die Ago2^{short} genannt wird und der die amino-terminalen GRRs fehlen. Eine detaillierte genetische Untersuchung legt nahe, dass die embryonalen Defekte auf eine negative Interaktion zwischen Ago2^{dop} mit Ago2^{short} zurückzuführen sind. Ago2^{dop1} interagiert auch mit anderen Argonaut-Familienmitgliedern: *ago1*, *piwi* und *aubergine* (*aub*). *ago2^{dop1}*-homozygote Embryonen, die eine verminderte Genaktivität von *ago1*-, *piwi*- oder *aub*-Aktivität besitzen, zeigen einen verstärkten Phänotyp.

Die Ergebnisse dieser Arbeit führten zu dem Modell, dass die Defekte während der frühen Embryogenese daher resultieren, dass maternale Transkripte in *ago2^{dop1}*-Mutanten während des sogenannten Mid-blastula-Übergangs (MBT) nicht degradiert werden können. Der MBT zeichnet sich dadurch aus, dass die Embryogenese nicht mehr von maternalen sondern von zygotischen Genen gesteuert wird. Maternale Genprodukte werden während des MBT abgebaut und die Degradierung maternaler Transkripte könnte durch miRNA-abhängige Prozesse erfolgen. Genetische Daten in dieser Arbeit sprechen dafür, dass die miRNA *miR-9a* am Abbau maternaler Transkripte beteiligt sein könnte.

Ago1 und Ago2 besitzen sich überschneidende Funktionen im Aufbau und Erhalt der Segmentpolarität. Ago1 und Ago2 co-immunoprezipitieren in Proteinextrakten, was nahe legt, dass beide Proteine im gleichen Proteinkomplex vorliegen. Desweiteren agieren Ago1 und Ago2 genetisch redundant in der Regulation des Segmentpolaritätgenes *wingless* im frühen Embryo. Die Daten dieser Arbeit zeigen, dass Ago1 und Ago2 nicht zwei verschiedenen Regulationsmechanism zugeordnet werden können, sondern zusammen arbeiten, um entscheidende Schritte der Embryonalentwicklung zu steuern.

Index

Introduction

Developmental biologists are interested in understanding how a complex multi-cellular organism develops from a single cell. Developmental Biology has its origin in classic embryological studies and tries to understand the control of cell growth, cell differentiation and cell specification of different cell types, which then give rise to tissues and organs. The key questions in developmental biology are: Which genes are involved in the patterning of the body plan? How are the different morphogenetic processes controlled? To study embryonic development in the animal kingdom model organisms such as the mouse *Mus musculus*, zebrafish *Danio rerio* or the African clawed frog *Xenopus laevis* are utilised. But also invertebrates are subject to study such as the nematode *Caenorhabditis elegans* or the fruit fly *Drososphila melanogaster*. These animals were chosen because they are easy to grow in large amounts, easy to look at and have a short life cycle. Additionally, they have a relatively simple body plan and are easy to manipulate genetically and molecularly. Despite the evolutionary distance between these model organisms and human it has been shown that animal development follows common rules. Related genes in *Drosophila melanogaster* and vertebrates have similar functions during development. Therefore, studying genetically accessible model organisms like *Drosophila melanogaster* can reveal detailed insight into the general molecular mechanisms necessary for embryonic development.

1.1 The development of *Drosophila melanogaster*

1.1.1 Cellularisation

The early *Drosophila* embryo undergoes 13 rapid mitotic division cycles, which are not accompanied by cytokinesis, and forms a multi-nucleated syncetial embryo. Entering mitotic cycle 14 a polarised epithelium is formed in a process called celluarisation. Division cycles 0-9 occur in the interior of the embryo (Figure 1A). During division cycles 8-10 most nuclei start to migrate to the periphery (Figure 1B) and arrange in a single layer below the cell membrane (Figure 1C). Some nuclei remain in the central yolk. At the cortex the nuclei divide four times (Figure 1D). After mitotic cycle 14 the embryo contains approximately 6000 nuclei and is called the stage of the “syncytial blastoderm”. Interphase of mitotic cycle 14 is prolonged and lasts over 60 minutes in which cellularisation takes place. Cellularisation starts when membrane invaginates in between the cortical nuclei and forms cleavage furrows which are also called furrow canals (Fullilove and Jacobson, 1971). New membrane is inserted apical into the former egg membrane (Figure 1F). The former egg

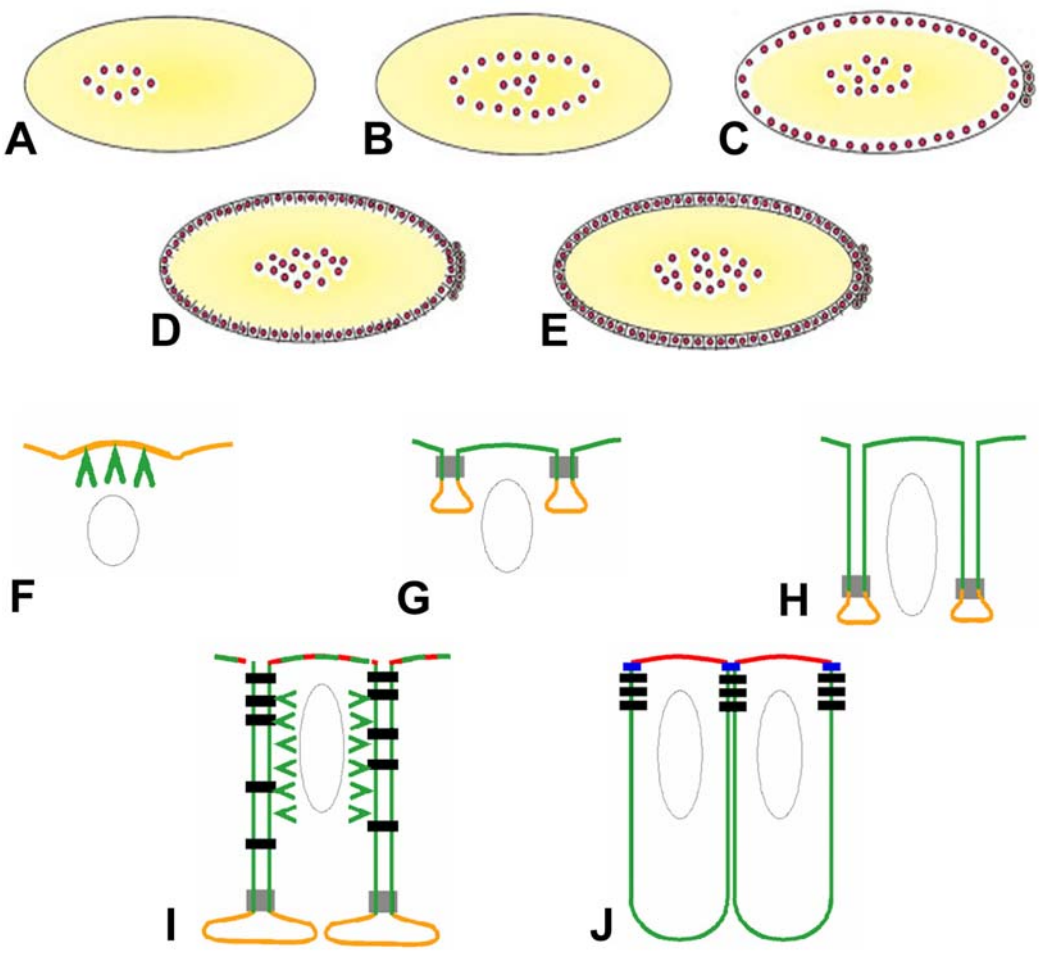

Figure 1: Cellularisation in *Drosophila melanogaster*

Drosophila melanogaster mitotic cycles during early embryogenesis (A-E). In preblastoderm stages during mitotic cycles 1-9 nuclei are localised in the anterior of the embryo (A). During cycle 8-10 nuclei migrate to the periphery (B). By the end of cycle 10 nuclei have arrived at the cortex. Some nuclei remain in the central yolk and form polyploidy yolk nuclei. Pole cells are formed at the posterior of the embryo (C). Nuclei at the cortex divide three times and form the syncytial blastoderm (D). Cellularisation begins at the interphase cycle 14 (E). Cellularisation (F-J): Syncytial blastoderm entering cycle 14. New membrane (green arrowheads) is inserted into the original egg membrane (orange, F). The original egg membrane is shifted into the furrow canal (orange) and the basal junction (grey bar) is formed (G). Membrane growth occurs at a relatively slow speed (slow phase, H). Membrane growth accelerates to a fast speed at the time when the furrow canals pass the basal level of the nuclei (fast phase, I). Spot adherens junctions (black bars) form along the lateral cell surfaces with a bias towards the apical region. The predominant site for membrane insertion is at the lateral membrane domain (green arrowheads). After cellularisation, a polarised epithelium is formed with apical (red) and basolateral (green) membrane domains. A zonula adherens (black bars) and an adjacent subapical region (blue bars) has formed at the border of the two membrane domains (J). (Mazumdar and Mazumdar, 2002; Müller, 2001)

membrane is shifted into the furrow canals, which by continuous membrane growth move radial around the nuclei (Figure 1G). The ingrowth of the furrow canals can be divided into a slow phase and a following fast phase (Turner and Mahowald, 1976). During slow phase membrane is inserted apical of the nuclei at a relatively slow speed (Figure 1H). Nuclei elongate during slow phase. When the furrow canals have reached the basal level of the nuclei membrane growth accelerates considerably which is therefore named fast phase. In fast phase membrane insertion takes place laterally (Figure 1I) (Lecuit and Wieschaus, 2000). During fast phase the newly generated cells close at the basal side and form a monolayer of approximately 6000 blastoderm cells (blastoderm epithelium). After cellularisation, a polarised epithelium is formed with apical and basolateral membrane domains (Figure 1J) (Foe et al., 1993; Mazumdar and Mazumdar, 2002). All future tissues are derived from this single epithelial layer at the cellular blastoderm.

The driving force for invagination of cell membranes results from a dynamic change of the microtubule network and the actinmyosin cytoskeleton. Centrosomes are arranged pairwise on the apical side of the cell. Long microtubules arise from the centrosomes and extend the plus ends to the anterior of the embryo. The nuclei are encompassed by the microtubules and cover the nuclei as inverted baskets (Callaini and Anselmi, 1988; Kellogg et al., 1991; Mazumdar and Mazumdar, 2002). The basal end of the invaginating furrow concentrates actin and myosin II which form an actinmyosin contractile ring around each nucleus (Fullilove and Jacobson, 1971). During slow phase of membrane invagination the rings are tightly connected such that they form a hexagon around each nucleus. As invagination progresses during fast phase the rings dissociate from each other and become rounder. The diameters of the rings narrow gradually until the basal closure forms the blastoderm cells (Foe et al., 1993; Theurkauf, 1994).

Yet it is not fully understood what precisely triggers cellularisation. It is known that maternal as well as zygotic genes are involved in this process. Maternal genes are expressed by the mother during oogenesis. The maternal gene products are deposited in the oocyte and are essential for early embryonic development. Maternal effect mutations show phenotypes in oogenesis or embryogenesis. Zygotic genes are expressed by the genome of the embryo itself. Transcription of zygotic genes starts with cycle 11 and increases dramatically during cycle 14. Cellularisation of the blastoderm is the first morphogenetic process, which depends on the contribution of zygotic transcription. The switch from solely maternal to zygotic control of embryogenesis is also known as midblastula transition (MBT). Additionally, MBT is accompanied by the downregulation of maternal gene products (Bashirullah et al., 1999). Seven zygotic genes have been identified this far that are required for cellularisation: *nullo* (Postner and Wieschaus, 1994; Rose and Wieschaus, 1992), *serendipity-*α (*sry* α) (Schweisguth et al., 1990), *slow-as-molasses* (*slam*) (Lecuit et

al., 2002; Stein et al., 2002), *bottleneck* (*bnk*) (Schejter and Wieschaus, 1993), *frühstart* (*frs*) (Grosshans et al., 2003), *kurzkern* (*kur*) (Brandt et al., 2006) and *kugelkern* (*kuk*, also known as *charleston* (*char*)) (Brandt et al., 2006; Pilot et al., 2006). *nullo*, *sry* α and *slam* are required for the stabilisation of the furrow canals. *bnk* ensures the correct timing of the basal closure of the cells. *frs* is necessary for the interphase 14 arrest. *kur* and *kuk/char* are required for nuclear elongation (Brandt et al., 2006; Grosshans et al., 2003; Lecuit et al., 2002; Pilot et al., 2006; Postner and Wieschaus, 1994; Rose and Wieschaus, 1992; Schejter and Wieschaus, 1993; Schweisguth et al., 1990; Stein et al., 2002).

The identification of only few zygotic regulators suggests that most of the cytoskeletal components required for cellularisation might be maternal gene products. Examples for maternally transcribed genes are actin binding proteins as myosin or the *Drosophila* profilin homologue Chickadee (Giansanti et al., 1998), membrane and Golgi associated proteins like α-Spectrin (Sisson et al., 2000), myosin components like Zipper (Myosin II) (Miller and Kiehart, 1995) or Jaguar (Myosin VI) (Mermall and Miller, 1995) and molecules of signal transduction pathways like Rho1 or Cdc42 (Crawford et al., 2001; Grosshans et al., 2005; Thomas and Kiehart, 1994). While the functional dissection of zygotic genes have been reported in some detail, some of the precise roles of maternal contributions remain unanswered as they also appear to be required in the earlier stage of meiotic cytokinesis.

1.1.2 Setting up the body plan in *Drosophila melanogaster*

When the embryo has reached the blastoderm stage gastrulations begins. At the onset of gastrulation cells at the ventral midline start to invaginate into the interior of the embryo and later differentiate to the mesoderm. During gastrulation the ventral blastoderm, also called germ band, extends, driving the posterior trunk region onto the dorsal side. During this movement the pole cells, which are the precursors of the germ line, are internalised through the posterior midgut. After this movement only neuro-ectodermal cells are at the surface of the embryo. The germ band later retracts as embryonic development is completed. At the time of germ band extension the first external signs of segmentation can be seen which later respond to the segments of the larvae and the adult fly.

How is the body plan established in the *Drosophila* embryo? Within the syncytial blastoderm embryo gradients of transcription factors are formed and regulate downstream genes (Lawrence and Struhl, 1996; Pankratz and Jäckle, 1993). The antero-posterior and dorsal-ventral axes are already determined in the oocyte by a group of maternal genes called coordinate genes (Figure 2). Some of these maternal mRNAs are highly localised at distinct positions in the oocyte and become translated locally in the zygote. During

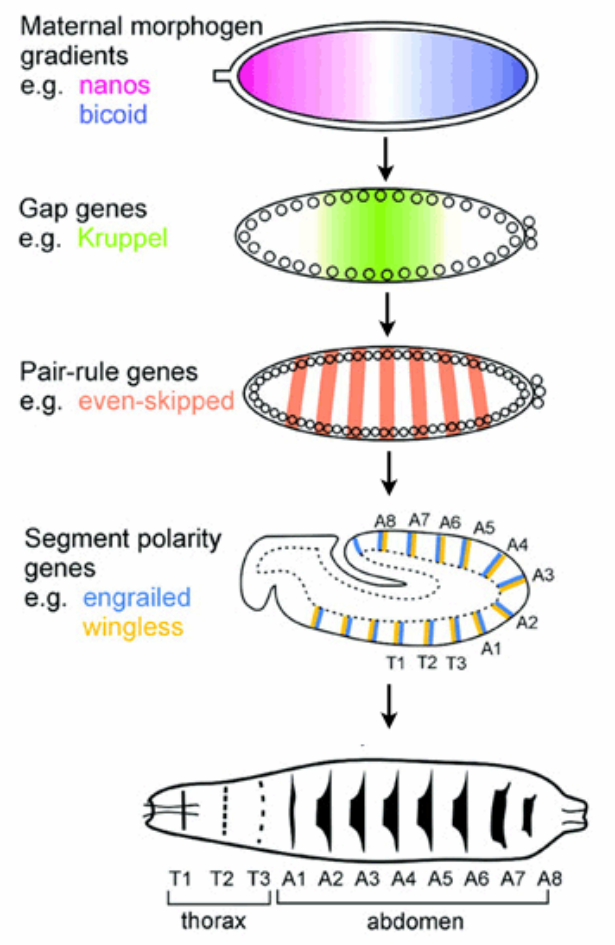

Figure 2: Patterning along the antero-posterior axis of the *Drosophila* embryo

A cascade of maternal and zygotic genes is activated in the syncytial embryo to subdivide the blastoderm into smaller domains. The embryo cellularises and undergoes gastrulation after activation of the pair-rule genes. The segment polarity genes are controlled by the pair-rule genes Segment polarity genes control the antero-posterior polarity of each individual segment of the future larva. After (Sanson, 2001)

syncytial blastoderm four protein gradients of maternal gene products are set up: Bicoid (Bcd) and Hunchback (Hb) determine the anterior structures of the embryos by an anterior to posterior gradient whereas Nanos (Nos) and Caudal (Cad) determine the posterior parts trough a posterior to anterior gradient (Figure 2). Bcd and Nos gradients emerge from diffusion, degradation and translational control while Hb and Cad gradients are maintained by translational inhibition trough Bcd and Nos (Driever and Nusslein-Volhard, 1988a, b, 1989; Irish et al., 1989; Lehmann and Nusslein-Volhard, 1987; Nusslein-Volhard et al., 1987; van Eeden and St Johnston, 1999). However, these proteins then activate zygotic expression of the gap genes along the antero-posterior axis (Figure 2). The gap genes *hb* and *giant* (*gt*) are localised anteriorly and are activated together with *Krüppel* (*Kr*) and *Knirps* (*Kni*) in the central area of the embryos. All four are expressed in overlapping regions. Interaction between the gap genes identifies their borders of expression (Rivera-

Pomar and Jackle, 1996; Struhl et al., 1992). Gap gene expression then establishes the next set of gene expression, the pair-rule genes (Figure 2). Each pair-rule gene is expressed in seven stripes. Their expression is depending on the expression ratio of the gap genes. For the primary pair-rule genes the expression domain of each stripe is determined individually. Primary pair-rule genes are *hairy* (*h*), *even-skipped* (*eve*) and *runt* (*run*). To maintain the expression pattern the activity of secondary pair-rule genes is required. Secondary pair-rule genes are *fushi-tarazu* (*ftz*), *odd-paired* (*opa*), *odd-skipped* (*odd*), *sloppy-paired* (*slp*) and *paired* (*prd*). The expression of the pair-rule genes determines the anterior boundary of each of the 14 parasegments. Different pair-rule genes are expressed in alternating parasegments. Pair-rule gene mutants show a characteristic

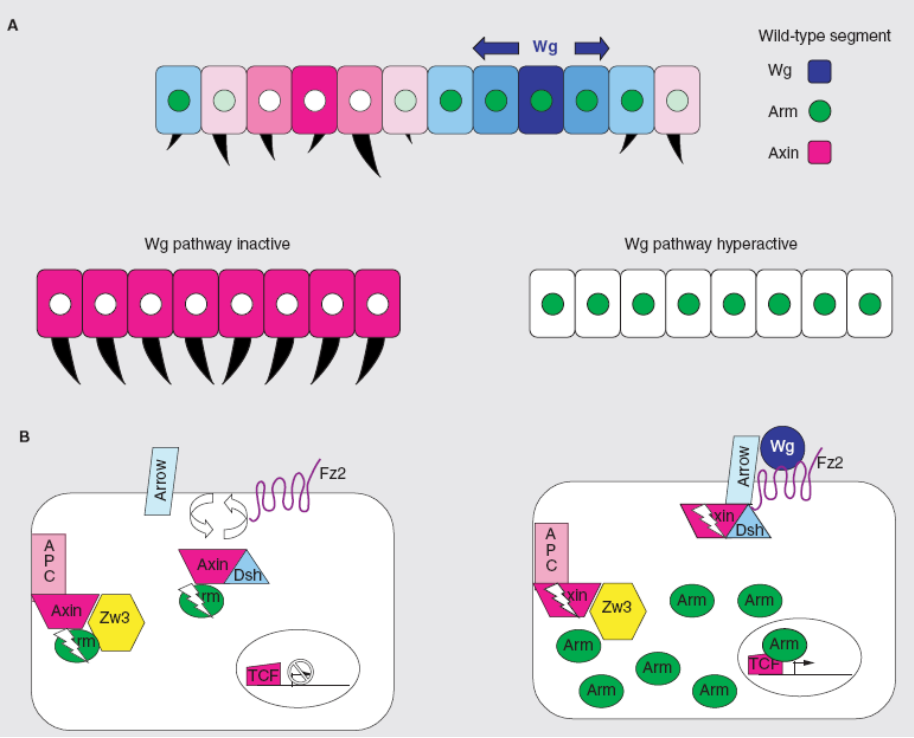

Figure 3: The Wingless signalling pathway

Wg expressing cells (blue) accumulate high levels of cytoplasmic Arm (green). Axin protein levels are down-regulated in response to Wg signalling (pink) (A). Aberrant conditions that result in pathway inactivation show loss of Arm accumulation and uniform high levels of Axin (A, left panel). Those animals exhibit a larval epidermis that is covered with denticles. Conversely, conditions that hyperactivate the pathway show loss of Axin accumulation and uniform high levels of Arm (A, right panel). Consequently the cuticle will not form any denticles. The schematic diagram shows how Dsh may be required for the cycling of Axin to the plasma membrane where it can be bound and degraded by the activated form of Arrow. In the absence of Wg signalling (left panel) destruction complexes constitutively target Arm for degradation. In the presence of Wg signalling (right panel) Arrow and Fz2 are brought together into an active receptor complex, which can bind Axin as it cycles to the membrane. This degrades the cytosolic pool of Axin and allows accumulation of Arm, which can translocate to the nucleus and provide an activation domain for the TCF transcription complex. After (Jones and Bejsovec, 2003).

cuticle pattern. Every second abdominal segment is absent (Hafen et al., 1984; Hiromi et al., 1985; Kuroiwa et al., 1984; Small and Levine, 1991). Coordinate, gap and pair-rule genes all encode for transcription factors.

Towards the end of gastrulation the activity of maternal, gap and pair-rule genes drops and the proteins disappear. But before they are degraded segment polarity genes are activated. Segment polarity genes like *engrailed* (*en*), *wingless* (*wg*) and *hedgehog* (*hh*) are expressed in 14 stripes, one in each parasegment (Figure 2). *en* has a key role in segmentation and is expressed initially in a single line of cells at the anterior margin of each parasegment. The expression of *en* is directly dependent on *ftz* and *eve*: *en* is activated in cells with high levels of the transcription factors Ftz or Eve. *wg* is activated only in those cells that receive little or no Eve or Ftz protein. Therefore, *wg* is only transcribed in cells directly anterior of *en* expressing cells. The expression of *wg* and *en* are mutual controlled. Wg maintains En expression in adjoining cells, and En-expressing cells secrete Hh, which in turn maintains Wg expression in neighbouring cells (DiNardo et al., 1988; Hidalgo and Ingham, 1990; Martinez Arias et al., 1988). This results in a permanent stabilisation of segment and parasegment boundaries. During late embryogenesis, the epidermis secretes a protective cuticle, which has a repeating pattern of ventral structures known as denticles. Wg and Hh instruct cell identity within the embryonic epidermis with Wg directing the naked cell fate and Hh determining the cells that will form denticles. Mutations in these genes lead to defects in segmentation across each parasegment. While the ventral cuticle of a *wild-type* embryo displays denticle belts alternating with naked regions, the cuticle of a *wg* mutant embryo is completely covered with denticles (Figure 3A) (Klingensmith and Nusse, 1994; Perrimon, 1994).

In the absence of Wg signalling Dishevelled (Dish) is continuously cycling the destruction complex from cytoplasm to the plasma membrane. The destruction complex is thought to be consisting of the serine/threonine kinase Zeste-White 3 (Zw3), Axin and adenomatous polyposis coli protein (APC). As a consequence, the destruction complex promotes the continuous degradation of Armadillo (Arm), the fly homologue of β-catenin (Figure 3B). In contrast in the presence of Wg signalling, cells that receive the Wg signal assemble the receptor complex consisting of Arrow and *Drosophila* frizzeld2 (*D*fz2). Dsh shuttles the destruction complex to the membrane where it binds to Arrow. This inhibits the destruction complex and allows Arm to accumulate in the cytoplasm, to bind to other proteins and to translocate to the nucleus. There it provides an activation domain for the transcription factor TCF and activates the expression of Wg target genes (Figure 3B) (Jones and Bejsovec, 2003).

1.2 The maternal effect mutation *drop out*

Many questions of early embryogenesis remain unanswered. To date it is not clear how cellularisation is controlled, which gene products are required and how they interact with each other. To address some of these questions the maternal effect mutation *drop out* (*dop*) has been studied in this thesis. *dop* was identified in an EMS induced screen for female sterile mutations in *Drosophila* (Galewsky and Schulz, 1992). The *dop* mutation allows homo- and hemizygous mothers to survive and produce normal amounts of embryos, but these embryos exhibit severe defects during cellularisation. The authors named this mutant *drop out* because many nuclei “drop out” from the cortex of the blastoderm during cellularisation. This results in cells that do not contain a nucleus at the cellular blastoderm stage. Consequently, these embryos have problems during gastrulation and produce variable amounts of defective cuticles. *dop* is located on the left arm of the third chromosome and is uncovered by the chromosomal deletion *Df(3L)BK10*. Complementation tests using different chromosomal deletions could narrow the interval down to the genomic region 71D1-3. This interval is uncovered by the deficiency *Df(3L)XG9* (Figure 4A). Which gene is affected by the *dop* mutation? Six genes are predicted for this genomic region (Figure 4B) from which only two genes remained as potential candidate genes for *dop*: *CG7739* and *argonaute2* (*ago2*) (Schreiber, 2003). Rescue constructs containing the full length cDNA for both gene products were generated and only *ago2* transgenes were able to rescue female sterility (see page 39 et seq.).

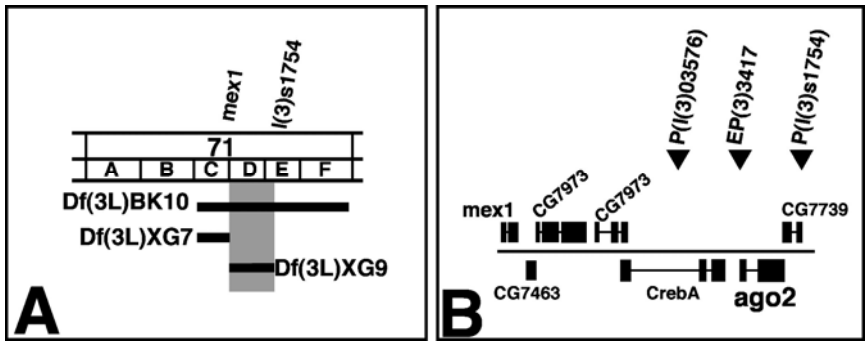

Figure 4: Genetic and molecular analysis of the *dop* locus

The female sterile mutation *dop* was initially mapped to the genomic region covered by the deficiency *Df(3L)BK10* (Galewsky and Schulz, 1992; Schreiber, 2003). Black bars represent the deleted regions. Further deletion mapping identified the cytological interval 71D1-E1 as the region uncovering the *dop* locus which is represented by the deficiency *Df(3L)XG9* (grey box, A). The 45kb region 71D1 to 71E3 contains 6 predicted genes and three P-element-insertions (*mex1* is located outside the *Df(3L)XG9* deficiency) (B). After (Schreiber, 2003)

1.3 RNA silencing mechanism guided by small RNAs

Over the past years RNA silencing mechanisms have not only become a powerful tool in cell biology but it has also been shown that they play a crucial role in gene regulation throughout development in many organisms from nematodes and insects to plants and humans. Ago2 has been shown to be the key enzyme in the RNA interference pathway (RNAi). Therefore, it would be very interesting to find out more about a potential role of Ago2 and RNA silencing pathways at the MBT.

In many eukaryotic cells RNAi is a mechanism of gene silencing mediated by short double stranded RNAs (dsRNAs). Basically, the short RNA is complementary to the mRNA of a target gene and binds to the target mRNA. Binding either inhibits its translation or target mRNA is degraded. Consequently, no protein is made from the target mRNA and the gene is silenced. This mechanism was first known as co-suppression and is also known as post-transcriptional gene silencing (PTGS) in plants or quelling in fungi (Nakayashiki, 2005; Napoli et al., 1990; Qi and Hannon, 2005).

For their work on RNAi in *C. elegans* the scientists Andrew Fire and Craig Mello have been awarded the Nobel Prize in Physiology and Medicine 2006 (Fire et al., 1998). However, the phenomenon of RNAi was discovered earlier by plant scientists in 1990 (Napoli et al., 1990). The researchers around Jorgensen wanted to produce petunia petals with an improved flower colour. Therefore, they over-expressed the gene for a pigment-enhancing enzyme. Unexpectedly, the flowers were much less coloured than the parental violet flowers or even white. They found out that the mRNA levels produced by this gene were 50fold decreased in transgenic plants in comparison to parental strains. They termed this phenomenon co-suppression but the mechanisms were not understood. Guo and Kemphuis made similar observations. They wanted to silence genes specifically by injecting antisense RNA into *C. elegans*. The idea was that antisense RNA hybridises with the endogenous mRNA and inhibits its translation. Injection of antisense RNA caused a dramatic downregulation of gene expression. But to their surprise silencing was as efficient when sense RNA was injected (Guo and Kemphues, 1995). Some years later Andrew Fire, Craig Mello and co-workers discovered the molecular mechanisms behind this phenomenon. To the researcher's surprise, double stranded RNA induced silencing even more effective than either strand alone. But this discovery was groundbreaking. Fire, Mello and colleagues termed this phenomenon RNA interference. It was then Zamore and colleagues who shed more light onto the molecular mechanism of RNAi. They found out that both strands of the dsRNA are processed to RNA segments of 21-23 nt length. The target mRNA is then also cleaved into 21-23 nt pieces. Therefore, Zamore and colleagues suggested that the 21-23 nt fragments guide the cleavage (Zamore et al., 2000).

Extensive research has been done since to understand the mechanisms of RNAi and other RNA silencing pathways. These studies led to the identification of distinct RNA silencing pathways, which are mediated by distinct short RNAs.

1.3.1 RNA silencing in *Drosophila melanogaster*

1.3.1.1 RNA silencing by small interfering RNAs (siRNAs)

The trigger for RNAi is dsRNA, which is cleaved into short interfering RNAs (siRNAs) of 21-23 nt length (Elbashir et al., 2001a; Elbashir et al., 2001b; Elbashir et al., 2001c; Hammond, 2005). The source of the dsRNA can be endogenous, e. g. derived from heterochromatin, transposon repeats or it can be exogenous such as viral or experimentally introduced dsRNA. The dsRNA is processed by the multi- domain RNase III-like protein Dicer-2 (Dcr-2)

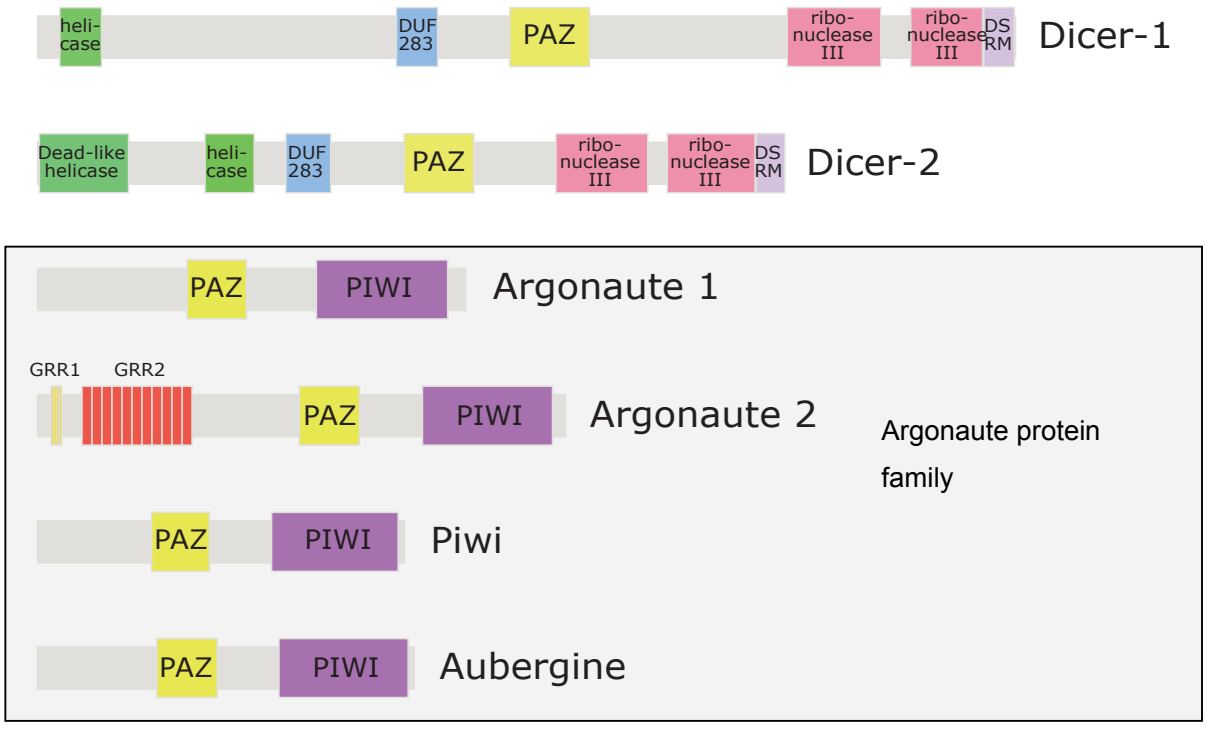

Figure 5: RNA silencing proteins

Protein structures of proteins that are involved in RNA silencing are shown. Except of R2D2 all contain a central PAZ domain. Dicer-1 consists of an amino-terminal helicase, a "domain of unknown function" DUF283, the PAZ domain, two ribonuclease III domains near the carboxy-terminus and a dsRNA binding motif. Dicer-2's structure is very similar to that of Dicer-1: it contains an additional Dead-like helicase at the amino-term. The Argonaute protein family consists of Argonaute 1, Argonaute 2, Ago3 (not shown) Piwi and Aubergine. All have in addition to the central PAZ domain a carboxy-terminal Piwi domain. Argonaute 2 contains two glutamine rich repeats of unknown function at its amino-terminus. DSRM: Double strand RNA binding motif, GRR: Glutamine-rich repeats.

(Figure 5) (Bernstein et al., 2001). Together with R2D2, Dcr-2 cleaves as a heterodimer dsRNA into siRNAs. One function of R2Ds is to facilitate incorporation of one strand of the siRNA duplex (the guide strand) into the RNA Induced Silencing Complex (RISC) (Figure 6) (Liu et al., 2003; Liu et al., 2006). The other siRNA strand, the passenger strand, is discarded. Depletion of Dcr-2 inhibits the production of siRNA and hence the entire RNAi machinery (Carmell and Hannon, 2004; Hammond, 2005). The effector complex RISC is a large multi-protein complex (Hammond et al., 2000; Tomari and Zamore, 2005). Surprisingly, however the biochemical activity of RISC only requires the small RNA and Ago2 (Rivas et al., 2005). RISC uses the guide strand to target complementary mRNAs. The target mRNA is degraded via a single endonucleolytic cleavage event known as slicing. Ago2 associates with the guide siRNA strand and provides the slicer catalytic activity (Figure 6). Cleavage of the mRNA occurs at a fixed position defined by the 5' end of the guide siRNA strand.

Ago2 protein belongs to the Argonaute protein family. The *Drosophila melanogaster* genome encodes four characterised Argonaute proteins: Ago1, Ago2, Piwi and Aubergine (Aub, also known as Sting) (Figure 5) (Carmell et al., 2002; Kataoka et al., 2001; Williams and Rubin, 2002). Another family member, Ago3 has been predicted from genomic DNA sequence by computer-based annotation. Proteins belonging to this family have a central PAZ (Piwi/Argonaute/Zwille) and a carboxy-terminal PIWI domain in common. PAZ forms a nucleic-acid binding pocket with a high affinity for binding single stranded 3' ends and duplex siRNA-like ends (Lingel et al., 2003; Ma et al., 2004; Song et al., 2003; Yan et al., 2003). PIWI is the slicing catalytic sub-domain that provides slicing activity and forms an RNase H-like fold (Liu et al., 2004; Meister et al., 2004; Rand et al., 2004; Rivas et al., 2005; Song et al., 2004). Additionally, Ago2 has two glutamine rich repeats (GRRs) at the amino-terminus of unknown function (Figure 5).

1.3.1.2 RNA silencing mediated by microRNAs (miRNAs)

RNA silencing by microRNAs (miRNAs) functions in a similar pathway. miRNAs differ from siRNAs in their biogenesis but not in their function (Tomari and Zamore, 2005). While siRNAs can be derived from any segment of the processed long dsRNA, miRNAs consist of a defined sequence and are encoded in the genome. miRNA genes are transcribed by RNA polymerase II into primary miRNAs (pri-miRNAs) (Lee et al., 2004a). The Drosha-Pasha/DGCR8 complex cleaves pri-miRNAs in the nucleus to release hairpin precursor miRNAs (pre-miRNAs) of 60-70 nt length (Figure 6) (Denli et al., 2004; Han et al., 2004; Lee et al., 2003; Lee et al., 2002; Yeom et al., 2006). pre-miRNAs are exported to the cytoplasm via Exportin-5. Together with the RNA binding protein Loquacious (Loqs) the RNase III enzyme Dicer-1 (Dcr-1) processes the pre-miRNAs to an imperfect

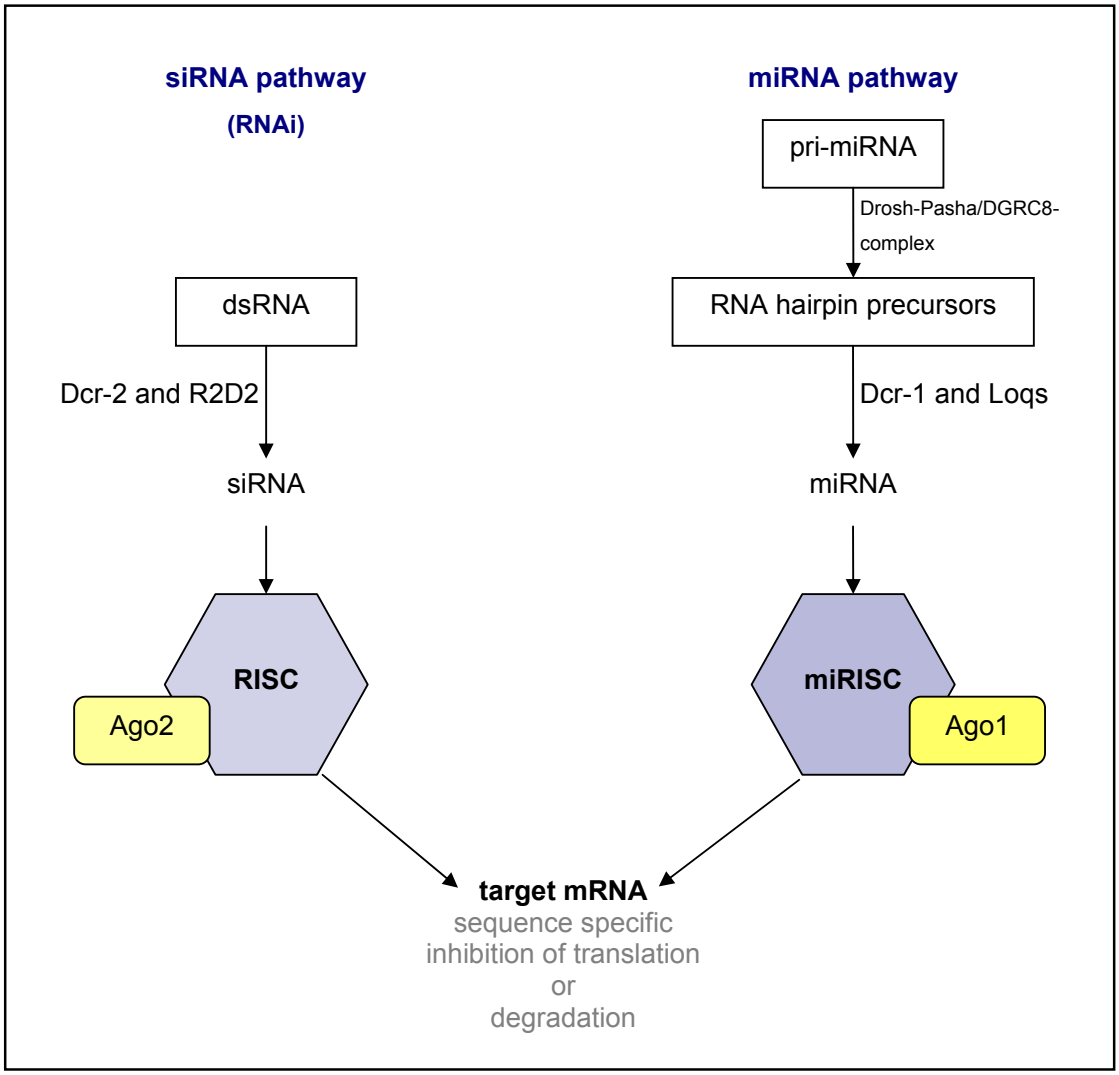

Figure 6: RNA silencing pathways in *Drosophila*

Two distinct RNAi pathways are suggested: dsRNA is cleaved by the heterodimer R2D2/Dcr-2 to short interfering RNA of 21-23 nt length. The antisense strand is incorporated into to the RNA Induced Silencing Complex (RISC), which guides the RISC to target mRNA. Ago2 is the core component of RISC. The target mRNA is then either not translated or degraded. The mRNA cleavage step is mediated by Ago2. On the other hand, endogenous encoded pri-miRNAs are processed to RNA hairpin precursors. Loqs associates with Dcr-1 to processes pre-miRNA into mature miRNA of 21-23 nt length. miRNAs are incorporated into RISC (also called miRNP) that guides the complex to target mRNAs and again translation is inhibited or the mRNA is degraded.

miRNA:miRNA* duplex of 21 to 23 nt length (Forstemann et al., 2005; Jiang et al., 2005; Saito et al., 2005). The strands are separated from each other and one strand is loaded into the miRNA-containing ribonucleoprotein (miRNP), which constitutes a RISC-like complex in the miRNA mediated silencing pathway. The core component of miRNP is Ago1 (Figure 5) (Okamura et al., 2004). miRNP complexes are frequently targeted to the 3' UTR of mRNAs (Ambros, 2001). Many animal miRNAs are not perfectly complementary to the target mRNA

and therefore fail to trigger slicing. Instead miRNP affects protein synthesis. However, when target mRNA show complete complementarity to the miRNA Ago1 is capable of slicing target mRNAs (Doench et al., 2003; Miyoshi et al., 2005; Okamura et al., 2004).
Mutations affecting genes of siRNA and miRNA mediated silencing have been reported. When components of the siRNA mediated silencing pathway are affected, flies develop grossly normal. Dcr-2 and Ago2 null mutants are reported to be viable and fertile (Lee et al., 2004b; Okamura et al., 2004; Xu et al., 2004). Recent publications have shown that RNAi is a major antiviral immune defence mechanism in *Drosophila*. dsRNAs produced during virus replication acts as the pathogen trigger whereas Dcr-2 and Ago2 act as host sensor and effector of the immunity. Consequently, Ago2 and Dcr-2 mutant flies do not survive virus infections (van Rij et al., 2006; Wang et al., 2006; Zambon et al., 2006). Mutations affecting components of the miRNA mediated silencing pathway as Dcr-1 and Ago1 are homozygous lethal (Kataoka et al., 2001; Lee et al., 2004b).

1.3.1.3 The role of Piwi and Aubergine in RNA mediated silencing

Ago1 and Ago2 play essential roles in RNA induced silencing. Both are expressed ubiquitously throughout development. In contrast, the Argonaute protein family members Piwi and Aub are only expressed in the germline (Williams and Rubin, 2002). It was shown that both proteins play important roles in germ cell formation. During oogenesis Aub is necessary for the activation of Oskar translation at the posterior pole. Translation of Oskar is an essential step in organising the pole plasm, which gives rise to the germline and contains abdominal body patterning determinants (Harris and Macdonald, 2001). Just like Ago1 and Ago2, Piwi and Aub play a role in RNA mediated gene silencing. Piwi has been implicated in post-transcriptional gene silencing in somatic cells (Pal-Bhadra et al., 2002). Piwi and Aub are involved in RNA silencing mediated by repeat-associated siRNAs (rasiRNAs), which are processed from long dsRNA precursors in a Dcr-1 and Dcr-2 independent manner (Vagin et al., 2006).
One example for this RNA trigger in *Drosophila* are the approx. 50 copies of the bidirectionally transcribed *Suppressor of Stellate* (*Su(Ste)*) locus on the Y-chromosome that in testes silence the ~200 copies of the protein-coding gene, *Stellate* (*Ste*), found on the X-chromosome, which ensures male fertility. rasiRNAs can be distinguished from siRNAs by their longer length of 24–29 nt (Aravin et al., 2001; Schmidt et al., 1999; Vagin et al., 2006). This silencing process is different from RNAi as Ago2 mutations have no influence on Stellate suppression (Vagin et al., 2006). Additionally, it has been reported that Aub is necessary for the establishment of RNAi in the oocyte during maturation (Kennerdell et al., 2002). Interestingly, during oocyte maturation only mRNAs that are translated become sensitive to RNAi while untranslated transcripts remain resistant. Recent studies report that

Piwi is not only essential for the self-renewal of adult germline stem cells in *Drosophila* (Cox et al., 1998; Cox et al., 2000; Megosh et al., 2006; Szakmary et al., 2005), but also connected to the miRNA mediated silencing pathway during germline fate determination in embryogenesis (Megosh et al., 2006). However, the mechanisms behind Piwi and Aub mediated silencing need to be investigated in the future.

1.3.2 RNA silencing in different model organisms

RNA silencing is a gene regulatory mechanism that is evolutionarily conserved. It has been shown that RNA silencing pathways in different model organisms share common features but do not follow completely identical pathways.

The human Argonaute family comprises eight members which were grouped into two subfamilies: the Piwi subfamily and the Ago subfamily (Sasaki et al., 2003). The Ago subfamily consists of Ago1, Ago2, Ago3 and Ago4. The multiple Argonaute proteins are biologically and biochemically distinct. Though all four Ago proteins can bind miRNAs indiscriminately of their sequence and can inhibit translation only Ago2-containing RISCs were able to guide cleavage of complementary target mRNAs (Meister et al., 2004). Furthermore Ago2 has been shown to be essential for mouse development (Liu et al., 2004). In vertebrate animals only a single gene encoding Dicer has been identified: vertebrate Dicer processes both miRNAs and siRNAs (Bernstein et al., 2003; Billy et al., 2001; Wienholds et al., 2003).

Also the nematode *C. elegans* contains only a single Dicer (Dcr-1) (Grishok, 2005). But in *C. elegans* 27 Argonaute genes were annotated (Grishok, 2005, Yigit et al., 2006). In *C. elegans*, distinct Ago proteins not only function in different RNA silencing pathways but also function incrementally during RNAi (Yigit et al., 2006). In contrast to *Drosophila*, RNAi acts in a systemic fashion in *C. elegans.* This means that the local application of dsRNA triggers silencing of homologous sequences throughout the organism and not only in the region exposed to the initial trigger (Roignant et al., 2003; Tijsterman et al., 2004). Remarkably, RNAi is heritable from one generation to the following in *C. elegans*. The effects can be maintained for three or more generations (Fire et al., 1998; Grishok et al., 2000). Essential for RNAi in *C. elegans* are RNA-dependent RNA polymerases (RDRs), which are also present in plants and fungi but neither exists in *Drosophila* nor in mammals. RDRs use primary siRNAs as primers and mature mRNAs as template and produce dsRNAs, which serve again as substrates for Dicer (Sijen et al., 2001; Smardon et al., 2000).

In fungi siRNA mediated silencing is known as quelling. So far no miRNA driven silencing could be identified (Nakayashiki, 2005). Using a comparative genomics approach, typical RNA silencing components such as Argonaute and Dicer-like proteins were identified in the

fungal genome databases (Nakayashiki, 2005). For example, the genome of the ascomycete *Neurospora crassa* encodes for two dicer-like proteins and two Argonaute proteins. The genome of *Schizosaccharomyces pombe* (fisson yeast) genome encodes for one Dicer-like and one Argonaute protein (Sigova et al., 2004). The baker's yeast *Saccharomyces cerevisiae* is an exception. No RNA silencing component could be determined (Nakayashiki, 2005).

In the plant kingdom three major classes of small RNAs exist: siRNAs, miRNAs and *trans*-acting siRNAs (ta-siRNAs). The *Arabidopsis* genome encodes four Dicer-like (DCL) proteins and ten Argonaute proteins (Chen, 2005; Herr, 2005; Qi and Hannon, 2005). Each of the DCL-proteins has a distinct function in different small RNA pathways though a possible partial redundancy cannot be excluded: DCL-1 produces miRNAs, DCL-2, DCL-3 and DCR-4 all produce siRNAs. siRNAs produced by DCL-2 are involved in silencing viral sequences. DCL-3 produced siRNAs play a role in DNA methylation and heterochromatin formation. In contrast, siRNA production by DCL-4 is triggered by transgenes containing inverted repeats. DCL-4 activity is also associated with the ta-siRNA pathway (Bonnet et al., 2006). DCL-1 is the only essential Dicer as DCL-1 null alleles are embryonic lethal (Chen, 2005). Many *Arabidopsis* siRNAs do not show a high degree of similarity to any *Arabidopsis* mRNA. Instead they show high complementarity to viral sequences. Therefore, researchers hypothesise that siRNAs could constitute a reservoir of defence molecules (Bonnet et al., 2006). A major difference between animal and plant miRNA mediated silencing should be outlined: Unlike their animal counterpart plant miRNAs often share perfect complementarity to their target mRNA and are more often located in the coding region than in the 3' UTR. Thus silencing is achieved by target mRNA degradation rather than translational inhibition (Baulcombe, 2004; Bonnet et al., 2006). An alignment of *Arabidopsis* Ago proteins with human Ago2 revealed that eight *Arabidopsis* AGOs contain slicer motifs: AGO1, AGO4, AGO5, AGO6, AGO7, AGO8 AGO9 and AGO10. This observation suggests that different AGOs might interact with different subsets of small RNAs to regulate genes in different tissues or at particular developmental stages. Supporting this idea, AGO7 is involved in the regulation of vegetative developmental timing while AGO10 (as well known as Zwille or Pinhead) has a role in the regulation of central shoot meristem cell fate during embryogenesis (Baulcombe, 2004; Carmell et al., 2002; Qi and Hannon, 2005).

1.4 Aim of work

dop has been characterised as a female sterile mutation. Embryos from homo- or hemizygous *dop* mutant mothers show severe defects in cellularisation (Galewsky and

Schulz, 1992; Schreiber, 2003). The aim of the work was to characterise the gene that is affected by the *dop* mutation. After identifying *dop* as an allele of *ago2* this work has been driven by the question how RNA silencing pathways function in the fly and how these pathways contribute to the control of early embryonic development. Several problems were set out at the beginning of this work. What is the function of *ago2* and how do $ago2^{dop}$ mutations affect Ago2's function? How do *ago2* and $ago2^{dop1}$ interact with other components of RNA silencing machineries? Moreover, what could be the targets of RNA silencing in the early embryo? The research presented in this thesis reveals novel functions of Argonaute proteins and unexpected links between components of the RNA silencing machinery in *Drosophila*.

2 Material and Methods

2.1 Materials

2.1.1 Chemicals

All chemicals were obtained in *pro analysis* quality by the following companies: *Acros* (Geel, Belgium), *Baker* (Deventer, Netherland), *Biomol* (Hamburg, Germany) *Bio-Rad* (München, Germany), *Difco* (Detroit, USA), *Fluka* (Buchs, Switzerland), *Gibco/BRL Life Technologies* (Karlsruhe Germany), *Merck* (Darmstadt, Germany), *Roth* (Karlsruhe, Germany), *Serva* (Heidelberg, Germany), *Sigma-Aldrich* (Steinheim, Germany).

All solutions were made with demineralised H_2O and autoclaved or sterile filtrated prior use.

Restriction enzymes were purchased from *MBI Fermentas* (St. Leon-Rot, Germany), *Boehringer/Roche Diagnostics* (Mannheim, Germany) or *Promega* (Madison, USA). The DNA polymerase was purchased from *Promega* (Madison, USA).

Reverse transcriptase polymerase chain reaction (RT-PCR) was performed using the OneStep RT-PCR kit from *Qiagen* (Hilden, Germany).

For plasmid DNA preparation and for DNA extraction from agarose gels kits from *Qiagen* (Hilden, Germany), *Macherey-Nagel* (Düren, Germany) or *Promega* (Madison, USA) were used.

2.1.2 General laboratory equipment

UV Spectrophotometer: Gene Quant II (*Pharmacia Biotech*, Cambridge, UK); SDS PAGE & Western Blotting : Miniprotean 3 (*Bio Rad*, Munich, Germany); Centrifuge (*Heraus* biofuge fresco and pico); PCR machine (MS Research MiniCycler); X ray film development: developer: Tenetal Roentogen (*Tenetal*, Norderstedt, Germany), fixation: Tenetal Roentogen Superfix, (*Tenetal*, Norderstadt; Germany); Confocal microscope: Leica TCS NT (*Leica,* Heidelberg Germany) and Zeiss 510Meta (*Zeiss*, Jena, Germany); Light microscopy: Zeiss Axiophot2 (*Zeiss*, Oberkochen, Germany), Scanning electron microscope: Leo Supra (*Leo Electrone Microscopy Ltd.*, Cambridge, UK); Pictures were edited with Adobe Photoshop CS and Macromedia FreeHand MX.

2.1.3 *Escherichia coli* and oligonucleotides

For cloning, *Escherichia coli* DH5α [F$^-$, *lacZ*ΔM15, *recA*1, π$^-$, *hsdR*17, *supE*44, Δ(*lacZYA, argF*)] was used.

The sequences for the different oligonucleotides that were used in this work for sequencing the *ago2* alleles and RT-PCRs are given in Table 1.

Table 1: Sequences of oligonucleotides used in this work

Oligonucleotide	Sequence (5' → 3')	Reference
Ago2for203	TTTGCCGGATACATGCTTTTCA	this work
Ago2rev816	TGTTCAATTTCGCTTCATCTTTCA	this work
D2 1afor	TAGCAAATTCAAATCAGCCAAGTG	(Schreiber, 2003)
D2 1bfor	CAGCAGGTACAAGGGTGGACTAAA	
D2 1brev	CTGGCTGAGGCGGTAATGGTAA	
D2 2for	GCCAGGCCAATACCAATCTCGT	
D2 2rev	AGGGCCTCGTATCCATCATCCAG	
D2 3for	GCAGTGCGTGGAGGTTGTTTTG	
D2 3rev	GCTTAGGACGCGGGTGCTTAC	
D2 4for	TCCGCATTGCCAACGATTTTATT	
D2 4rev	TAGGCGTTACGGTACTCTTTAT	
D2 5for	CCCTACGGAGCCAGTTAT	
D2 5rev	CCGGGGTCCACGTTGTTGAA	
D2 6for	ATTTGCTGCGTGATTGTGGTGAAG	
D2 6rev	GAAAAGCGCGAGGATAAACAGGAA	
E1 for (= Ago2 RB for)	AGAACAAGAAAGGAGGACAGGAT	this work
E3 for (= GM for)	AATTGGGCGGAGCAGTTCTTG	this work
E7 rev (= PIWI rev)	CGGAGCCGGATAAGAAACC	this work
E5 rev (= GM rev)	AGGGCCTCGTATCCATCATCCA	this work
halo for	CTCAGTAAACAGCAGCAGGTAGCCGATGGGTGGGC	pers. comm. with M. Welte, Brandeis, USA
halo rev	CGCAATGTGATTTCCACTGTAGATTGTTAGCTCCC	

2.2 Methods

2.2.1 Cultivation of *Drosophila melanogaster*

Flies were kept on standard medium (356 g corn grist, 47.5 g soy flour, 84 g dry yeast, 225 g malt extract, 75 ml 10 % Nipagin, 22.5 ml propionic acid, 28 g agar, 200 g sugar beet molasses, 4.9 l dH_2O) at 18°C, RT and 25°C. For egg collection, flies were kept on apple juice agar plates (40 g agar, 340 ml apple juice (100 %), 17 g sucrose, 30 ml Nipagin (10 %; 100 g Nipagin were dissolved in 1 l 70 % Ethanol) ad 1 l H_2O), which were supplied with yeast for stimulation.

A list of flies that were subject to this study is given in Table 2.

Table 2: List of fly stocks that were used in this work

When flies were ordered from stock centres the stock numbers are given. B stands for Bloomington *Drosophila* stock center at Indiana University, Bloomington, USA (http://flystocks.bio.indiana.edu/) and SZ stands for Szeged *Drosophila* stock centre, Szeged, Hungary (http://expbio.bio.u-szeged.hu/fly/index.php).

Name	Genotype	Reference
Or R	standard laboratory *wild-type* strain	(Lindsley and Zimm, 1992)
w^{1118}	w^- *wild-type*	(Lindsley and Zimm, 1992)
red e	red^1 e^1	B #1662
$ago2^{dop1}$/ *TM3*	w^-, $ago2^{dop1}$ *st/ TM3 [ftz::lacZ]*	(Schreiber, 2003)
Df(3L)XG9/ TM3	w^-; *Df(3L)XG9/ TM3*	(Grosshans et al., 2003)
EP(3)3417	*P[EP]*$Ago2^{EP3417}$	SZ
$ago2^{dop46}$/*TM3*	$ago2^{dop46}$/ *TM3 [ftz::lacZ]*	this work
$ago2^{51B}$	$ago2^{51B}$/ $ago2^{51B}$	(Xu et al., 2004)
$ago2^{414}$	$ago2^{414}$/ $ago2^{414}$	(Okamura et al., 2004)
mat::ago2	w^-; *mat::ago2/mat::ago2*	(Schreiber, 2003)
mat::ago2; $ago2^{dop1}$	w^-; *mat::ago2/mat::ago2;* $ago2^{dop1}$/*TM6*	this work
UAS::ago2	*w-; UAST::ago2/ UAST::ago2*	(Schreiber, 2003)
UAS::ago2; $ago2^{dop1}$	w^-; *UAST::ago2/ UAST::ago2;* $ago2^{dop1}$ *mat15/ TM6*	this work
UAS::ago1	w^-; *UAS::ago1/ UAS::ago1*	(Kataoka et al., 2001)
UAS::ago1; $ago2^{dop1}$	w^-; *UAS::ago1/ UAS::ago1;* $ago2^{dop1}$ *mat15/ TM6*	this work

Table 2 continued

Name	Genotype	Reference
mat15::GAL4	*w⁻; mat15::GAL4/ TM3*	(Dawes-Hoang et al., 2005)
ago2^{dop1}, mat15::GAL4	*w⁻; mat15::GAL4, ago2^{dop1}/ TM3*	this work
UAS-mir9a-6	*UAS-mir9a-6/ UAS-mir9a-6*	(Leaman et al., 2005)
UAS-mir9a-6; ago2^{dop1}	*UAS-mir9a-6/ CyO; ago2^{dop1}/ TM6*	this work
GMR::Gal4, DIAP1^{RNAi}	*GMR::Gal4, symDIAP1^{RNAi}/ CyO*	(Huh et al., 2004)
GMR::Gal4, DIAP1^{RNAi}; ago2^{dop1}	*GMR::Gal4, symDIAP1^{RNAi}/ CyO; ago2^{dop1}/ TM6*	this work
GMR::Gal4, DIAP1^{RNAi}; ago2^{51B}	*GMR::Gal4, symDIAP1^{RNAi}/ CyO; ago2^{51B}/ TM6*	this work
GMR::Gal4, DIAP1^{RNAi}; Df(3L)XG9	*GMR::Gal4, symDIAP1^{RNAi}/ CyO; Df(3L)XG9/ TM6*	this work
halo	*Δ(halo)/Δ(halo)*	(Gross et al., 2003)
ago1/CyO	*w⁻; ago1^{K08121} w⁺/ CyO*	(Kataoka et al., 2001)
dcr-1/TM3	*y⁻ w⁻ hs::Flp; FRT82B dcr-1^{Q1147X}/ TM3*	(Lee et al., 2004b)
dcr-2	*y⁻ w⁻ hs::Flp; FRT42D dcr-2^{L811fsX}/ FRT42D dcr-2^{L811fsX}*	(Lee et al., 2004b)
piwi/CyO	*P[ry$^{+t7.2}$=PZ] piwi^{06843} cn^{1}/ CyO; ry^{506}*	B #12225
aub/CyO	*y^{1}, w^{67c23}; P[y$^{+mDint2}$ w$^{BR.E.BR}$=SUP or-P] aub^{KG05389}*	B #14001
ago1/CyO; ago2^{dop1}/ TM3	*w⁻; ago1^{K08121} w⁺/CyO [hb::lacZ]; ago2^{dop1}/ TM3 [hb::lacZ]*	this work
ago1/CyO; dcr-1/TM6	*w⁻; ago1^{K08121} w⁺/Cyo; FRT82B dcr-1^{Q1147X} /TM6*	this work
ago1/CyO; dcr-1/TM3	*w⁻; ago1^{K08121} w⁺/ Cyo [hb::lacZ]; FRT82B dcr-1^{Q1147X} /TM3 [hb::lacZ]*	this work
ago1/CyO; ago2^{51B}/TM6	*w⁻; ago1^{K08121} w⁺/ CyO; ago2^{51B}/ TM6*	this work
ago1/CyO; ago2^{51B}/TM3	*w⁻; ago1^{K08121} w⁺/ CyO [hb::lacZ]; ago2^{51B}/ TM3 [hb::lacZ]*	this work
dcr-2; dcr-1/TM6	*w⁻; FRT42D dcr-2^{L811fsX}/ FRT42D dcr-2^{L811fsX}; FRT82B dcr-1^{Q1147X}/ TM6*	this work
piwi/CyO; ago2^{dop1}/ TM6	*P[ry$^{+t7.2}$=PZ] piwi^{06843} cn^{1}/ CyO [hb::lacZ] ; ago2^{dop1}/TM6*	this work

Table 2 continued

Name	Genotype	Reference
piwi/CyO; ago2^{51B}/ TM6	*P[ry$^{+t7.2}$=PZ] piwi^{06843} cn^{1}/ CyO [hb::lacZ]; ago2^{51B}/TM6*	this work
piwi/CyO; dcr-1/TM6	*P[ry$^{+t7.2}$=PZ] piwi^{06843} cn^{1}/ CyO[hb::lacZ]; FRT82B dcr-1^{Q1147X}/ TM6*	this work
aub/CyO; ago2^{dop1}/ TM6	*P[y$^{+mDint2}$ w$^{BR.E.BR}$=SUP or-P] aub^{KG05389}/ CyO [hb::lacZ]; ago2^{dop1}/TM6*	this work
aub/CyO; ago2^{51B}/ TM6	*P[y$^{+mDint2}$ w$^{BR.E.BR}$=SUP or-P] aub^{KG05389}/ CyO [hb::lacZ]/ ago2^{51B}/ TM6*	this work
aub/CyO; dcr-1/TM6	*P[y$^{+mDint2}$ w$^{BR.E.BR}$=SUP or-P] aubKG05389/ CyO [hb::lacZ] ; FRT82B dcr-1^{Q1147X} /TM6*	this work
GMR::GAL4	*P[GMR::GAL4.w^{-}]2*	B #9146
GMR::hid	*P[w^{+mC}=GMR::hid] G1/ CyO*	B #5771
EP(3)EP3622	*P[EP]CG17667^{EP3622} ban^{EP3622}*	SZ
EP(3)EP3622 h st cu	*EP(3)EP3622 h st cu/ TM3*	this work
GMR::hid; EP(3)3622	*GMR::hid/ CyO; EP(3)EP3622 h st cu/ TM6*	this work
GMR::GAL4/ EP(3)3622	*GMR::GAL4/ CyO; EP(3)EP3622 h st cu/ TM6*	this work
GMR::hid; EP(3)3622 ago2^{51B}	*GMR::hid/ CyO; EP(3)EP3622 ago2^{51B}/ TM6*	this work
GMR::GAL4/ EP(3)3622 ago2^{51B}	*GMR::GAL4/ CyO; EP(3)EP3622 ago2^{51B}/ TM6*	this work
GMR::hid; EP(3)3622 ago2^{dop1}	*GMR::hid/ CyO; EP(3)EP3622 st ago2^{dop1} cu e/ TM6*	this work
GMR::GAL4/ EP(3)3622 ago2^{dop1}	*GMR::GAL4/ CyO; EP(3)EP3622 st ago2^{dop1} cu e/ TM6*	this work
GMR::GAL4/ EP(3)3622 Df(3L)XG9	*GMR::GAL4/ CyO; EP(3)EP3622 Df(3L)XG9/ MKRS*	this work

2.2.2 Cultivation of *E. coli*

E. coli-strains were grown in Luria-Bertani medium (LB medium; 1 % Trypton, 0.5 % yeast extract, 1 % NaCl) at 37°C. For selective growth Ampicillin was added at a final concentration of 100 µg ml^{-1}. Solid medium contained 2 % Agar. SOB medium (2 % tryptone, 0,5 % yeast extract, 10 mM NaCl, 2,5 mM KCl, 10 mM $MgCl_2$, 10 mM $MgSO_4$) for preparation and transformation of competent *E. coli* cells were done as reported elsewhere (Inoue et al., 1990).

2.2.3 Isolation of Nucleic acids

2.2.3.1 Isolation of plasmid DNA from *E. coli*

E. coli was grown over night in 5 ml selective LB medium at 37°C. 1.5 ml of this over night culture was sedimented at 13000 rpm for 1 min. The pellet was resuspended in 150 µl P1 buffer (50mM Tris-HCl pH 8.0; 10 mM EDTA; 100 µg ml^{-1} RNaseA, stored at 4°C). To break open the cells, 150 µl of the buffer P2 (200 mM NaOH; 1 % SDS) were added, inverted and incubated for 5 min at RT. The reaction was stopped adding 150 µl of buffer P3 (3.0M KAcetate pH 5.5). The samples were centrifuged for 10 min at 13000 rpm. The supernatant was transferred into a fresh reaction tube. The DNA was precipitated with 300 µl isopropanol at 13000 rpm for 30 min. The pellet was washed with 70 % Ethanol at 13000 rpm for 5 min. The pellet was then air dried, resuspended in 30 µl H_2O and stored at -20°C until use.

For the purpose of cloning, sequencing and transformation of flies the plasmid DNA was obtained using the Plasmid Midi Kit Nucleobond AX (*Macherey-Nagel*, Düren, Germany). The preparation was done according to the manufacturer's protocol.

2.2.3.2 Preparation of genomic DNA from flies

This protocol was modified after E. J. Rehm from the Berkeley Drosophila Genome Project (BDGP): 30 flies were collected in a reaction tube and frozen in liquid nitrogen. 200 µl Buffer A (100 mM Tris-HCl, pH 7.5, 100 mM EDTA, 100 mM NaCl, 0.5 % SDS) were added. The flies were homogenised using the Bio-Vortexer (*Biospec Products*, Bartlesville, USA), additional 200 µl Buffer A were added and the homogenisation procedure was continued until cuticle remained. The solution was incubated at 65°C for 30 min. 800 µl of a LiCl/KAcetate-solution (1 part of 5 M KAcetate and 2.5 parts of 6 M LiCl) were added and incubated on ice for at least 10 min. Afterwards the samples were centrifuged at 13000 rpm for 15 min at RT. The supernatant was transferred into a fresh reaction tube. The DNA was

precipitated adding 600 µl Isopropanol and spinning for 15 min at 13000 rpm at RT. The pellet was washed with 70 % Ethanol and then air dried. The DNA was resuspended into 150 µl dH_2O.

2.2.3.3 Isolation of polyA$^+$-RNA from ovaries and embryos

Embryos of the desired age were collected from yeasted apple juice plates, dechorionated using 6.5 % NaOCl and shortly rinsed with dH_2O. They were transferred into reaction tubes and frozen in liquid nitrogen. For collecting ovaries, flies were fed with yeast for approx. 2 days. The flies were dissected in PBS (1.3 M NaCl; 70 mM $NaHPO_4$; 30 mM NaH_2PO_4) and the ovaries were collected on ice in a reaction tube containing PBS. Before freezing the ovaries in liquid nitrogen, the PBS was removed. For polyA$^+$-RNA isolation, the µMACS mRNA Isolation Kit from *Miltenyi Biotec* (Bergisch Gladbach, Germany) was used. polyA$^+$-RNA was isolated according to the protocol.

2.2.4 Cloning techniques

2.2.4.1 Polymerase chain reaction (PCR)

For molecular cloning, DNA fragments were amplified from plasmid DNA or genomic DNA by PCR (Saiki et al., 1985). A standard reaction contained 10 pmol oligonucleotides (Table 1) and 10 – 100 ng template DNA and was performed according to the protocol of the manufacturer. The reaction volume was set to 50 µl in all reactions. Annealing temperature and amplification time of a standard PCR protocol are indicated in Table 3 and were adjusted according to the needs of the particular experiment.

Table 3: Standard PCR programme

The duration of the synthesis step is variable depending on the length of the expected PCR product.

	Duration	Temperature
Initial denature	3 min	95 °C
Denature	50 sec	95 °C
Anneal	40 sec	55-60 °C
Extend	1 – 4 min	72 °C
Cycles	35	
Finale extension	10 min	72°C

2.2.4.2 RT-PCR

RT-PCR was carried out using the OneStep RT-PCR kit from *Qiagen* (Hilden, Germany) according to the manufacturer's instructions. A standard RT-PCR reaction contained 0.5 µg polyA$^+$-RNA and 0.60 µM oligonucleotides (Table 1). Annealing temperature and amplification time of a standard RT-PCR protocol are indicated in Table 4 and were adjusted according to the needs of the particular experiment.

Table 4: Standard RT-PCR programme

The duration of the synthesis step is variable depending on the length of the expected RT-PCR product.

	RT-PCR products < 2 kb		RT-PCR products 2 – 4 kb	
	Duration	Temperature	Duration	Temperature
Reverse Transcription	30 min	50°C	30 min	45°C
Initial denature	15 min	95°C	15 min	95°C
Denature	1 min	94°C	10 sec	94°C
Anneal	1 min	54°C	1 min	54°C
Extend	2 min	72°C	3 min 40 sec	68°C
Cycles	40		40	
Final extension	10 min	72°C	10 min	68°C

2.2.4.3 DNA restriction

For analytical restriction reactions, 0.5 µg DNA were digested with 1 – 2 units restriction enzymes in a total volume of 30 µl at 37°C for 2 h.

2.2.4.4 Agarose gel electrophoresis

0.2 volumes of DNA sample buffer (30 % Glycerol, 0.25 % Bromphenole blue, 0.25 % xylene cyanol) were added to the DNA solution. The DNA fragments were electrophoretically separated in a horizontal agarose gel (0.8 %) in TAE buffer (40 mM Tris-Acetate, 20 mM NaAcetate, 2 mM EDTA, pH 8.3) in the presence of 0.5 µg ml^{-1} Ethidiumbromide. DNA bands were detected with UV light (λ = 254 nm). The size of the DNA bands was estimated by comparing them with the standard Gene Ruler 1 kb ladder (*MBI Fermentas*).

2.2.4.5 Isolation of DNA fragments from agarose gels

The PCR product or DNA restriction samples were electrophoretically separated on an agarose gel. The corresponding band was excised. To isolate the DNA fragments the Wizard SV Gel and PCR Clean-Up System from *Promega* (Madison, USA) were used according to the manufacturer's protocol.

2.2.4.6 Ligation of DNA fragments

Linearised DNA fragments were ligated in a reaction mixture (total volume 20 µl) containing 5 units T4-DNA-Ligase (*Fermentas*) and 1 to 10 µg ml^{-1} DNA at 16°C over night. The molar Vector/Insert DNA ratio was between 1:5 und 1:10. After the ligation reaction the DNA was used immediately for transformation into *E. coli*.

2.2.4.7 Preparation of chemo-competent *E. coli* cells

The preparation of chemo-competent *E. coli* cells was done after Mandel and Higa (Mandel and Higa, 1970). A 2 l Erlenmeyer flask containing 250 ml SOB medium (2 % tryptone, 0.5 % yeast extract, 10 mM NaCl, 2.5 mM KCl, 10 mM $MgCl_2$, 10 mM $MgSO_4$) was inoculated with *E. coli* DH5α and incubated at 18°C and 200 rpm for at least 24 h until the culture has reached an OD_{600nm} = 0.6. To harvest the cells they were cooled for 10 min on ice. Afterwards the cells were sedimented at 7000 rpm for 10 min at 4°C. The pellet was resuspended in cold transformation buffer (TB buffer: 10 mM Pipes, 15 mM $CaCl_2 \cdot 2H_2O$, 250mM KCl, 55 mM $MnCl_2 \cdot 2H_2O$, pH 6.7), incubated on ice for 10 min and again centrifuged as described above. Then the cells were taken up in 20 ml TB buffer and resuspended carefully. 1.5 ml DMSO was added (final concentration 7 %). After mixing gently the solution was incubated for 10 min on ice. Finally, the solution was frozen in liquid nitrogen in 200 µl aliquots and stored at -70°C until use.

2.2.4.8 Transformation of *E. coli*

The competent *E. coli* cells were defrosted on ice. Per aliquot 1 – 5 µl DNA were added and incubated for 30 min on ice. After heat shock (45 s at 42°C) 800 µl LB medium were added und incubated at 120 rpm at 37°C for 1 h. Finally, 200 µl of the transformation reaction were plated on selective medium (LB^{Amp}) and incubated at 37°C over night.

2.2.4.9 DNA Analysis

DNA-Sequencing was done by *SeqLa*b (Göttingen, Germany). Sequence analysis was performed using Lasergene from *DNASTAR, Inc.* (Madison, USA).

2.2.5 Micromanipulation of *Drosophila melanogaster*

2.2.5.1 Germ band transformation

The germ band transformation of *Drosophila melanogaster* is a simple method for generating transgenic flies. For the gene transfer, transposable elements, so called P-elements are used. For the integration into the genome they require a transposase and their flanking recognition sites, the inverted repeats. For the germ band transformation technique these two components are located on two different plasmids. The transfer DNA is localised between the inverted repeats on a P-element transformation vector. The transposase is available on a helper plasmid (pUChsπΔ2-3), which in *trans* allows the integration of the P-element into the genome.

2.2.5.2 Injection solution and injection capillary

The injection solution consisted of 4 µg P-element transformation vector, 1 µg helper plasmid, 1 µl 10x injection buffer (5 mM KCl, 0.1 mM Na-phosphate buffer, pH 6.8) and 1 µl 2 % phenole red in a total volume of 10 µl. Before injection the solution was spinned down at 13000 rpm for 5 min to avoid that particles block the capillary.

Glass capillaries (GB120F-10, *Science Products GmbH*, Hofheim, Germany) were made with the Flaming/Brown Micropipette Puller (*Sutter Instrument Co.*, USA) in a two step programme 33 (First: Heat = 460, Pull = 0, V el. = 30, D el. = 50; Second: Heat = 460, Pull = 100, V el. = 60, D el. = 5). After pulling the capillaries were burnished for 5 min at an ankle of 30° (*Bachofer*, Reutlingen, Germany). The capillaries were filled from behind using a glass pipette. Some injection were performed by BestGene Inc, Chino Hills, USA or by VANEDIS *Drosophila* injection service, Oslo, Norway (former: EMBL injection service, Heidelberg, Germany).

2.2.5.3 Microinjection

For the injection, w^- embryos (w^{1118}) were used. Because all P-element transformation vectors carried a w^+ gene, which integrated as well into the genome, it was easy to identify transgenic flies by their eye colour. The injection occurred into the posterior region of the embryo before the pole cells, which will later differenciate into germ cells, were formed.

The *w*$^-$ flies were placed on yeasted apple juice agar plates for 20 min. The laid eggs were collected, shortly dechorionated in 6.5 % NaOCl and washed. The embryos were strung on a block of apple juice agar in the same orientation. The agar block was then glued on a coverslip. Under optical control the embryos are dried. The coverslip was then fixed on an object slide. The embryos were covered with 3S Voltalef oil (Atofina, Usine de Pierre Benite, France). The injection was done under a transmitting light microscope (Zeiss Axiovert 25) using compressed air (Pneumatic PicoPump PV 820, *World Precision Instruments Inc.*, Sarasota, USA) and the motor-operated micromanipulator (Piezo Manipulator PM 10). The injection was visualised by the phenole red which was present in the injection mix. The injected embryos were covered with 3S Voltalef oil and were kept in a wet chamber at 18°C until hatching. L1 larvae were transferred into a vial containing standard medium and kept on 18°C until flies hatched.

2.2.5.4 Isolation and Balancing of transgenic flies

The hatched flies (G_0) were crossed with balancer flies (*w*$^-$*; Gla/CyO* or *w*$^-$*; If/CyO; MKRS/TM6*). The red eyed flies of the F_1 generation were crossed again with the balancer flies in single fly crosses in order establish the line and to identify on which chromosome the insertion occurred.

2.2.6 Detection of RNA

2.2.6.1 Marked anti-sense RNA probe

Digoxigenin (DIG) - marked anti sense RNA probes were generated by *in vitro*-Transcription using the DIG RNA Labelling Mix (*Roche*) according to the manufacturerer's instructions. Quality and quantity of the RNA anti-sense probes were verified by a denatured RNA gel electrophoresis.

2.2.6.2 Denaturating RNA gel electrophoresis

For the electrophoretical separation of RNA molecules a denatured environment is essential to avoid secondary RNA structures. A denatured agarose gel consisted of 1.5 % agarose in 1x MOPS buffer (10x MOPS: 200mM -(N-Morphpolino)-propan-sulfonic acid; 50 mM NaAcetate; 10 mM EDTA; pH 7) and contained 1.9 % Formaldehyde. The RNA probes were treated as following prior loading on the gel: up to 9 µl RNA, 4 µl Formaldehyde (37 %), 3 µl 10x MOPS, 1 µl Ethidiumbromide (400 µg ml^{-1}) and 10 µl deionised Formamide. The samples were boiled for 5 min and the incubated on ice for 5 min. 3 µl RNA sample buffer (0.1 % Bromphenol blue; 0.1 % xylencyanol; 10 mM EDTA, pH 7.5; 70 % Glycerol)

was added. As a size marker the RNA High Range Ladder (*MBI Fermentas*) was used that was treated as the samples described above.

2.2.6.3 Northern Blotting

Northern Blotting is a method to transfer electrophoretic separated RNA (total RNA or polyA$^+$-RNA) onto a membrane, followed by the hybridisation with a marked anti-sense RNA probe that detects specific RNA fragments.

A photo of the RNA gel (see above) was taken with a ruler aside in order to be able to estimate the size of the RNA bands after hybridisation. The RNA gel was washed for 15 min with dH_2O and twice with 20x SSC (3 M NaCl; 300 mM NaCitrate, pH 7.0) for 15 min each. Then the Northern blot was built up as followed: The RNA gel was put on a Whatman paper (*Schleicher&Schuell*, Dassel, Germany). This was put on a supporting device over a container filled with 20x SSC allowing the ends of the Whatman paper to reach into the SSC. On top of the gel the Hybond N$^+$ nylon membrane (*Amersham Life Science*; Little Chalfont, UK) was placed in the size of the RNA gel. For a good transfer of the RNA onto the nylon membrane it was important that there were no air bubbles between gel and membrane. The gel was surrounded with Parafilm (*Brand*, Wertheim, Germany). On the membrane three layers of Whatman paper were placed followed by several layers of paper towels. On top of this gadget a glass plate was put which was weight down with approx. 500 g. The transfer was allowed for approx 18 – 20 h.

On the next day, the positions of the gel slots were marked to assure that the proper size of the band can be estimated after hybridisation. The RNA was attached to the membrane by UV light (120 mJ) using the Stratalinker 2400 from *Stratagene* (La Jolla, USA). The membrane was pre-hybridised for at least 1 h at 68°C in 25 ml hybridisation solution (5 x SSC, 50 % Formamide, 0.1 % N-lauroylsarcosine, 0.02 % SDS, 2 % Blocking reagent (*Roche*); in a plastic bag). The DIG labelled anti sense RNA probe was denatured for 5 min at 100°C in 100 µl hybridisation solution. The anti sense RNA probe was then cooled on ice. For hybridisation 1 ml hybridisation solution per 20 cm^2 was heated to 68°C and 100 ng ml^{-1} anti sense RNA probe was added. The membrane was incubated in this solution in a plastic bag at 68°C over night. On the following day the membrane was washed: twice with 50 ml 2x SSC and 0.1 % SDS at RT for 5 min and twice with 50 ml 0.1 x SSC and 0.1 % SDS at 68°C for 15 min. The detection of the DIG labelled anti sense RNA probe followed at RT. The membrane was equilibrated with washing buffer (100 mM Maleic acid, 150 mM NaCl, 0.3 % Tween-20, pH 7.5) and blocked in blocking solution (100 mM maleic acid, 150 mM NaCl, 1 % Blocking reagent (*Roche*), pH 7.5) for 1 h. The membrane was incubated for 1 h with a horseradish peroxidase coupled anti-DIG antibody (*Roche,* 1:10000 in blocking solution). The membrane was washed twice with washing buffer for 15 min and twice in

TBS-T (20 mM TrisCl pH 8, 150 mM NaCl, 0.2 % Tween-20) for 5 min. For the detection of the DIG labelled anti sense RNA probe the membrane was incubated with the BM Chemiluminescence Blotting Substrate (*Roche*) for 2 min and the exposed to a the Medical X-Ray Film100 NIF Super RX (*Fuji*, Tokyo, Japan) for some minutes to one hour.

2.2.7 Protein biochemical methods

2.2.7.1 Protein extraction from *Drosophila* tissue

For preparation of protein extracts, 0- to 12-h-old embryos were dechorionated and homogenised in CHAPS lysis buffer (20 mM Tris pH 8.0, 150 mM NaCl, 10 % Glycerol, 2 mM EDTA, 10 mM CHAPS). To prevent protein degradation during experimental procedure, protease inhibitors were added in 1:500 dilutions from original stock solutions: Aprotinin (10 mg ml^{-1}), Pepstatin (1mg ml^{-1}), Leupeptin (0.5 mg ml^{-1}) and Pefabloc (1 mg ml^{-1}) and the proteasome inhibitor Lactacystin (0.5 µg ml^{-1}). The solution was kept on ice for 10 min and then centrifuged for 15 min at 4°C at 13000 rpm. The supernatant was transferred into a new reaction tube and the protein concentration was measured using the Bradford assay (*Bio-Rad*, Hercules, USA).

2.2.7.2 SDS-PAGE and Western Botting

For SDS-PAGE and Western blotting, 30 µg of protein was boiled with 3 x SDS sample buffer (25 mM Tris HCl pH 6.8, 15 % Mercapto Ethanol, 30% Glycerol, 7 % SDS, 0.3% Bromphenole blue), and loaded onto a discontinuous, horizontal SDS-polyacrylamide gel (7.5 % or 12% AA/Bis stock solution (*Bio-Rad*), 0.1 % SDS 0.375 M TrisHCl pH 8.8, 0.3 % APS, 0.01 TEMED or 6 % AA/Bis stock solution (*Bio-Rad*), 7 % Glycerol, 1 % SDS, 0.15 % APS, 0.2 % TEMED). Ovaries were dissected in PBS, grinded and directly boiled in SDS-sample buffer. The separation of the proteins was performed in electrophoresis buffer (25mM TrisBase, 192 mM Glycerol, 0.1 % SDS (Laemmli, 1970) or 40 mM Tris, 20 mM NaAcetate, 2 mM EDTA, 1 % SDS, pH 7.4 (Bolt and Mahoney, 1997) at 90V or 55V. The proteins were blotted onto a Protan nitrocellulose membrane (*Schleicher&Schuell*) in transfer buffer (0.39 M Glycerol, 0.48 TrisBase, 0.37 % SDS, 20 % Methanol or 40 mM Tris, 20 mM NaAcetate, 2 mM EDTA, 0.05 % SDS, 20 % Methanol) at 30V or 10V at RT over night. The proteins were detected using the following antibodies (see as well Table 5: Antibodies used in this work): rabbit anti-Ago1 (1:250, *Abcam*, Cambridge, United Kingdom), rabbit anti-Dcr-1 (1:500, *Abcam*), rabbit anti-Loqs (1:2,000) (Forstemann et al., 2005)), rabbit anti-$Ago2_{Cterm}$ (1:5000, generated against the carboxylterminal peptide CIVPEFMKKNPMYFV), rabbit anti-Ago2 (1:300, gift of Q. Liu), rabbit anti-GFP antibody

(*Molecular Probes*, Carlsbad, USA) and mouse anti-αTubullin (1:1000, Sigma). As secondary antibodies, goat anti-rabbit antibodies conjugated with HRP were used at 1:10000 (*Jackson*, West Grove, USA). They were detected using the BM Chemiluminescence Blotting Substrate (*Roche*) for 2 min and then exposed to Medical X-Ray Film100 NIF Super RX (*Fuji*) for 2 min, 10 min or 60 min.

2.2.7.3 Co-immunoprecipitation

For immunoprecipitation, the rabbit anti-$Ago2_{Cterm}$ was covalently bound to the coupling gel using AminoLink Plus Immobilization Kit (*Pierce Biotechnology*, Rockford, USA). Protein extracts containing 500 µg of protein were used for each reaction. The extract was incubated with the covalently bound beads for 1.5 h at 4°C. The beads were washed, boiled in 3x SDS-sample buffer and subjected to SDS-PAGE and Western blotting.

2.2.8 Histological methods

2.2.8.1 Fixation of embryos

2.2.8.1.1 Heat fixation

Embryos were dechorionated using 6.5 % NaOCl and transferred to a scintillation vial containing boiling 2 ml Triton X Salt solution (3 ml Triton X-100, 40 g NaCl, ad 1l). The embryos were shortly incubated and then immediately cooled by adding 10 - 15 ml cold Triton X Salt solution. The scintillation vial was kept on ice for some minutes. The salt solution was discarded and replaced by heptane and methanol. By vigorous shaking the vitelline membrane of the embryos was removed. Embryos were transferred to a reaction tube and washed twice with methanol. The embryos were stored at -20°C in methanol.

2.2.8.1.2 Formaldehyde fixation

Embryos of the desired age were collected from yeasted apple juice plates and dechorionated using 6.5 % NaOCl. The embryos were rinsed and transferred to a scintillation vial containing 4 ml fixative (4 % formaldehyde in PBS) and 4 ml heptane. The embryos were incubated for 25 min under agitation. The lower phase was discarded and 4 ml methanol was added. By vigorous shaking the vitelline membrane of the embryos was removed. Embryos were transferred to a reaction tube and washed twice with methanol. The embryos were stored at -20°C in methanol.

Alternatively, Stefanini's solution (4 % formaldehyde, 75 mM PIPES, 15 % picric acid in dH_2O) was used as a fixative.

Table 5: Antibodies used in this work

Given are the dilutions and the purpose that the antibody was used for. Abbreviations used in this table: m: mouse, rb: rabbit, gt: goat, HF: Heatfix, FA: formaldehyde, IF: immuno staining, WB: Western blot, IP: immunoprecipitation. DSHB: Developmental Studies Hybridoma Bank, University of Iowa, Iowa City, USA.

antibody	dilution	purpose	reference
m-α-Neurotactin	1:10	IF, Stefanini, HF	DSHB
rb-α-Armadillo^{Central}	1:200	IF, Stefanini, HF	(Keßler, 2006)
m-α-KlarM	1:50	IF, HF	(Guo et al., 2005)
m-α-Wingless	1:50	IF, 4 % FA, Stefanini	DSHB
m-α-Engrailed	1:10	IF, 4 % FA, Stefanini	DSHB
m-α-Even-skipped	1:50	IF, 4 % FA	DSHB
rb-α-Fushi-tarazu	1:350	IF, 4 % FA	(Krause and Gehring, 1988)
rb-α-βGal	1:500	IF, 4 % FA, Stefanini	Cappel
rb-α-Ago2$_{Cterm}$	1:500	IF	this work
rb-α-Ago2$_{Nterm}$	1:100	IF	this work, generated against the peptide AGSIKRGTIGKPGQV),
gt-α-rabbit-biotin	1:200	IF	Jackson ImmunoResearch
gt-α-mouse-Cy2	1:200	IF	Jackson ImmunoResearch
gt-α-mouse-Cy3	1:200	IF	Jackson ImmunoResearch
gt-α-rabbit-Cy2	1:200	IF	Jackson ImmunoResearch
gt-α-rabbit-Cy3	1:200	IF	Jackson ImmunoResearch
rb-α-Ago1	1:250	WB, IP	Abcam
rb-α-Dcr-1	1:500	WB	Abcam
rb-α-Loqs	1:2000	WB	(Forstemann et al., 2005)
rb-α-Ago2$_{Cterm}$	1:5000	IP, WB	this work
rb-α-Ago2	1:300	WB	gift from Q. Liu*
rb-α-GFP		IP	Molecular Probes
m-α-Tubullin	1:1000	WB	Sigma
gt-α-rabbit-HRP	1:10000	WB	Jackson ImmunoResearch

*Q. Liu, University of Texas, Dallas, USA

2.2.8.2 Immunofluorescence

Indirect immunofluorescence was used exclusively for detection of proteins in fixed embryos. All steps were done under agitation. The fixed embryos were washed three times with PBT for 20 min each. Unspecific binding sites were saturated by blocking with blocking solution (10 % NHS in PBT) for 45 min at RT. The incubation with the primary antibody (Table 5) followed in blocking solution at 4°C over night. The following day, the embryos were washed three times with PBT for 20 min and incubated with a fluorescently labelled secondary antibody in blocking solution for 2 h at RT. In some cases DAPI (1:1000 from a 1 mg ml^{-1} stock solution) or YOYO-1 (1:7500) and RNaseA (final concentration 50 µg ml^{-1}) were added at this step. After three washings steps with PBT for 20 min each, embryos were embedded in Mowiol containing DABCO to prevent bleaching of fluorescence during confocal microscopy.

2.2.8.3 Nile Red staining

Embryos were collected from yeasted apple juice plates, dechorionated and transferred to a scintillation vial containing 2 ml PBS and 4 ml heptane. The embryos were incubated on the interface for 1 min. Then 2 ml Formaldehyde (37 %) was added. Embryos were left on fixative for 1 h without agitation. The embryos were recovered in wire-basket, shortly blotted on a paper towel and dropped into a small Petri dish containing PTX (1.3 M NaCl; 70 mM $NaHPO_4$; 30 mM NaH_2PO_4, 0.1 % Triton X 100). Embryos were transferred to an amber reaction tube. PTX was replaced by 1 ml 0.5 % BSA in PBS and 4 µl Nile Red stock solution (0.4 mg ml^{-1} in acetone) was added. Embryos were left on a nutator for 1 h at RT. The embryos were washed three times with PTX. The supernatant was replaced with mounting media (75 % Glycerol, 25 % PBS). The embryos were dispersed and the spinned down to remove them from the surface. They were kept on 4°C over night before they were mounted on a glass slide. Small cover slips were used as spacers.

2.2.8.4 *In situ* hybridisation

For *in situ* hybridisation embryos were fixed with 4 % formaldehyde as described above. The embryos were incubated in a mixture of xylene and ethanol (1:1) for 30 min. The embryos were rinsed shortly: five times with Ethanol, twice with Methanol and three times with PBT. A second fixation step followed for 25 min using 5 % Formaldehyde in PBS. The embryos were washed again five times with PBT for 5 min each. Optionally, the embryos were treated with 4 µg ml^{-1} Proteinase K in PBT for 8 min. Five short washing steps with PBT followed. The embryos were incubated in a 1:1 mixture of PBT and hybridisation solution (50 % deionised Formamide, 5 x SSC, 100 µg ml^{-1} denatured salmon sperm DNA,

100 µg ml^{-1} heparin, 0.1% Triton X-100) and washed three time in hybridisation solution. The embryos were pre-hybridised in hybridisation solution for at least 1 h at 63°C. The DIG labelled anti sense RNA probe was denatured for 5 min at 65°C in 100 µl hybridisation solution. The embryos were hybridised with the anti sense RNA containing hybridisation solution at 63°C over night.

On the following day, the embryos were washed four times for 15 min each with hybridisation solution and once with a 1:1 mixture hybridisation solution and PBT at 63°C. At RT the embryos were washed four times with PBT. The embryos were incubated with the pre-absorbed alkaline phosphatase coupled anti-DIG antibody (final concentration 1:2000 in PBT) at 4°C over night. Then they were washed four times with PBT and three times with NBT buffer (100 mM NaCl, 50 mM $MgCl_2$, 100 mM Tris-HCl pH 9.5, 0.1 % Triton X-100). The embryos were incubated in the staining solution (1 ml NBT buffer, 3 µl BCIP (50 mg ml^{-1} 5-Brom-4-Chlor-3-Indolylphosphate, Toluidin salt in DMF) and 3.4 µl NBT (75 mg ml^{-1} Nitroblue Tetrazolium salt in DMF)) until the desired intensity of the staining. The staining solution was discarded and the staining reaction was stopped with PBT.

If the embryos were carrying a lacZ marked balancer chromosome an anti-β-Gal staining was done. Therefore, the embryos were washed with PBT and blocked in blocking solution (10 % NHS in PBT) for 45 min at RT. The embryos were incubated with a biotin labelled rabbit anti-β-Gal antibody (1:200 in blocking solution) at 4°C over night. The embryos were washed with PBT for 15 min each. To boost the staining the intensifier kit Vectastain ABC kit (Vector Laboratories Inc., *Burlingame*, USA) was used. Therefore, 10 µl solution A was mixed with 1 ml PBT. Then 10 µl solution B was added and incubated for 30 min at RT prior use. The embryos were incubated with the AB solution for 45 min. Afterwards the embryos were washed three times with PBT for 15 min each. Then they were incubated in DAB staining solution (1 ml 1:3 DAB : PBS plus 0.2 µl H_2O_2) until the desired intensity of the staining was reached. The staining solution was discarded and the reaction was stopped by adding PBT.

For mounting, the embryos were dehydrated by incubation in successively higher alcohol concentration (30 % Ethanol, 50 % Ethanol, 70 % Ethanol, 80 % Ethanol, 96 % Ethanol and 100 % Ethanol) for 5 min each, followed by two washing steps with molecular sieve dried acetone for 5 min each. The embryos were left in an araldite-acetone (1:1) mixture at 4°C over night. The embryos were transferred to a microscope slide and oriented. The slides were placed at 65°C over night so that the acetone could evaporate. On the following day the embryos were embedded in 100 % araldite and were placed at 65°C over night to cure the araldite.

2.2.8.5 In vivo imaging of embryos

For in vivo observation, staged embryos were observed and staged on yeasted apple juice plates. They were mounted in halocarbon oil 27 (*Sigma-Aldrich*) on microscope slides. Videomicroscopy was performed on a Carl Zeiss (Jena) microscope equipped with Nomarski optics, and time-lapse videos were taken on conventional videotape.

2.2.8.6 Hatching rate determination and cuticle preparation

Flies were placed on yeasted apple juice plates for some hours or over night. The laid eggs were counted immediately. After 48 h the remaining embryos that did not hatch were counted again and the hatching rate was determined. The embryos that did not hatch were washed, dechorionated with 6.5 % NaOCl and embedded in Hoyer's Medium/Lactate (50 ml H_2O, 30 g gum arabic stirred over night, plus 200 g chloral hydrate, 16 ml Glycerol, centrifuged for 3 h at 12000 rpm; supernatant is mixed with lactate 1:1). The clearing of the embryos occurred at 65°C over night.

2.2.8.7 Preparation of eyes for scanning electron microscopy

The flies were decapitated and the heads were transferred into reaction tubes containing PBS. The heads were dehydrated by incubation in successively higher alcohol concentration (30 % ethanol, 50 % ethanol, 70 % ethanol, 80 % ethanol, 96 % ethanol and 100 % ethanol) for 5 - 10 min each followed by two washing steps 100 % acetone. The heads were incubated in acetone:tetramethylsilane (TMS, *Sigma-Aldrich*) (1:1), in acetone:TMS (1:2) and pure TMS for 30 min each. The TMS was replaced by fresh TMS and left to dry over night at RT. The heads were cut into halves, mounted on double stick tape, sputtered with gold (*Balzers Union*, Balzers, Lichtenstein; for 3 min at 25 mA, 0.1 Torr) and subjected to LEO scanning electron microscopy (*Carl Zeiss*, Jena, Germany)

3 Results

3.1 *dop*^{1} embryos show severe defects in polarised membrane formation

The female sterile mutation *drop out* (*dop*^{1}) was first identified in screen for maternal effect mutations by Galewsky and Schulz (Galewsky and Schulz, 1992). *dop*^{1} homo- and hemizygous flies are viable but embryos from *dop*^{1} homo- or hemizygous mutant mothers are embryonic lethal. They do not hatch and display defects in larval cuticle formation (Figure 10B-E) (Galewsky and Schulz, 1992; Schreiber, 2003). Hereafter, embryos from *dop*^{1} homo- or hemizygous mutant mothers are referred to as *dop*^{1} embryos.

Looking at early developing *dop*^{1} embryos, severe morphological defects can be observed about 3 h after fertilisation. At this time point the embryo enters cellularisation (Mazumdar and Mazumdar, 2002). As mentioned in the introduction, cellularisation can be divided into two phases: a slow and a fast phase. During the first 30 min membrane insertion occurs in a relatively slow speed. Then membrane insertion accelerates in the fast phase. By video microscopy the cellularisation can be observed and the progression of the cleavage furrow

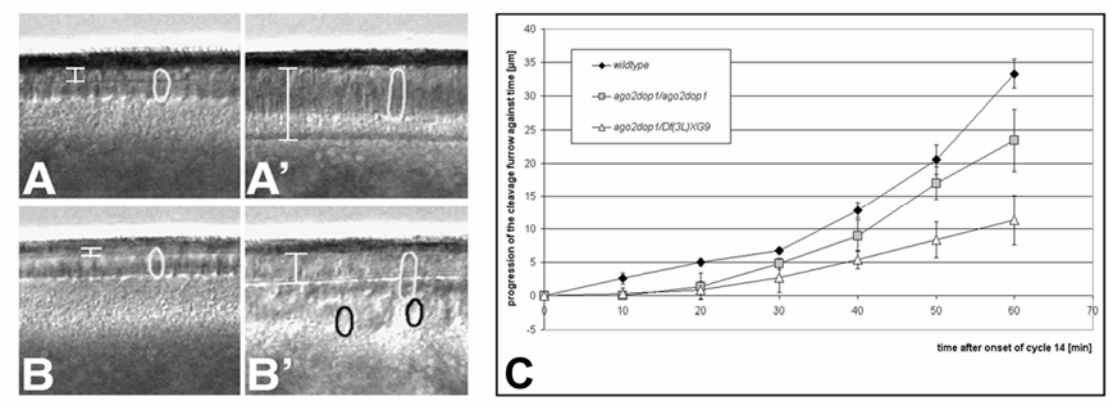

Figure 7: *dop*^{1} affects cell formation in the early embryo

The generation of the cleavage membrane was monitored by timelapse video recording of embryos during cellularisation (A, B,). In the *wild-type*, membranes grow slowly for the first 30 min of cycle 14 interphase (slow phase (A)), and then growth speeds up considerably (fast phase (A')). In embryos derived from homozygous *dop*^{1} mutant mothers membrane extension is strongly reduced (B and B' show *dop*^{1} embryos at corresponding time points). The shape of the nuclei (circles) and the extent of furrow progression are indicated (bars). The progression of the cleavage furrow was plotted against the time after the beginning of mitotic cycle 14 (C). Note that compared to the *wild-type* (C, black diamond) furrow progression is significantly slower in embryos derived from homozygous (*dop*^{1}*/dop*^{1}*,* grey casket) or hemizygous (*dop*^{1}*/Df(3L)XG9*; C, white triangle) *dop*^{1} females, within the first 30 min of cellularisation. In hemizygous *dop*^{1} embryos, membrane formation was even more severely impaired. It was slower during both slow and fast phase. Adopted from Schreiber (Schreiber, 2003).

can be measured (Figure 7A, A'). These data can be plotted against the time (Figure 7C). In *dop*^{1} embryos the first 13 mitotic divisions occurred as in *wild-type* embryos. But entering cycle 14 the initiation of membrane growth was significantly delayed (Figure 7A-C). During slow phase hardly any membrane insertion could be observed in *dop*^{1} homo- or hemizygous mutants (Figure 7C). Entering fast phase membrane insertion occurred relatively normal in homozygous *dop*^{1} embryos. In hemizygous *dop*^{1} embryos even fast phase was delayed (Schreiber, 2003). The defect in membrane growth was also visible when embryos where immunolabelled for endogenous membrane markers (Figure 11A-F). In *wild-type* embryos (Figure 11A-C) the membrane marker Neurotactin (Nrt) accumulates in the apical domain at the onset of cellularisation (Figure 11A) and is present at the cleavage membranes starting at mid cellularisation. Armadillo (Arm/ β-catenin) distribution marks the presence of basal junctions at the onset of cellularisation. At mid and late cellularisation, Arm protein is also found along the cleavage membrane with a bias to the apical domain, the future zonula adherens. In *dop*^{1} embryos, Arm and Nrt persist at the apical cytocortex during early and mid cellularisation (Figure 11D-F).

3.2 *dop*^{1} embryos display a disrupted polarised microtubule based transport of lipid droplet

When examined by videomicroscopy, *dop*^{1} embryos were abnormally transparent from gastrulation onwards (Figure 8B) in comparison to *wild-type* embryos (Figure 8A). Such altered transparency can be a signature of mislocalised lipid droplets, as cytoplasm filled with lipid droplets is opaque (Gross et al., 2000; Welte et al., 1998). Lipid droplets move bidirectional along microtubules. This movement is temporally coordinated with cellularisation. During syncytial stages the lipid droplets are evenly distributed around the embryo. No net transport of lipid droplet occurs. Entering cycle 14 lipid droplets are transported basally. As a result the periphery becomes clear (cytoplasmic clearing). During gastrulation lipid droplets are transported apical again. Therefore, lipid droplets are present throughout the embryo periphery after gastrulation, which turn the embryos opaque again (Welte et al., 1998). Because *wild-type* and *dop*^{1} embryos displayed very similar transparency up to the end of cycle 14, the initial basal droplet transport appeared normal. Embryos were stained with the droplet-specific fluorescent dye Nile Red (Figure 8C-D). While the lipid droplets are distributed evenly in *wild-type* embryos (Figure 8C), they have accumulated basally around the central yolk in the *dop*^{1} mutant embryos (Figure 8D).

To determine when the difference in droplet transport between these genotypes arises, embryos, in which expression of the directionality determinant Halo was reduced, were investigated. Under these conditions, basal transport is slower and less complete (Gross et

al., 2003). Embryos that expressed only a single copy of halo appeared similar early in cycle 14 independent of whether they were derived from *dop*^{1} homozygous or heterozygous mothers. Late in cycle 14, lipid droplets in embryos from *dop*^{1} homozygotes accumulated more basally (Figure 8E-H). This can be seen by higher embryo transparency (Figure 8E-F). Additionally Klar, a droplet associated regulator (Guo et al., 2005), has accumulated more basal (Figure 8H) in comparison to the control embryos (Figure 8G). Thus, droplet distribution in *dop*^{1} becomes abnormal late in cycle 14, and droplets fail to switch from basal to apical transport.

The abnormal lipid droplet distribution in *dop*^{1} embryos resembles the droplet-transport defects in *klar* mutant embryos (Welte et al., 1998). Klar was not affected in *dop*^{1} embryos as Klar expression and distribution was very much as in *wild-type* embryos (Figure 8I-K). As well Klar was physically associated with the lipid droplets (Figure 8L), as it is in *wild-type* embryos. Because Klar was not affected in *dop*^{1} mutant embryos, the distribution of the direction determinant Halo was checked. *halo* is not provided maternally but transcribed by

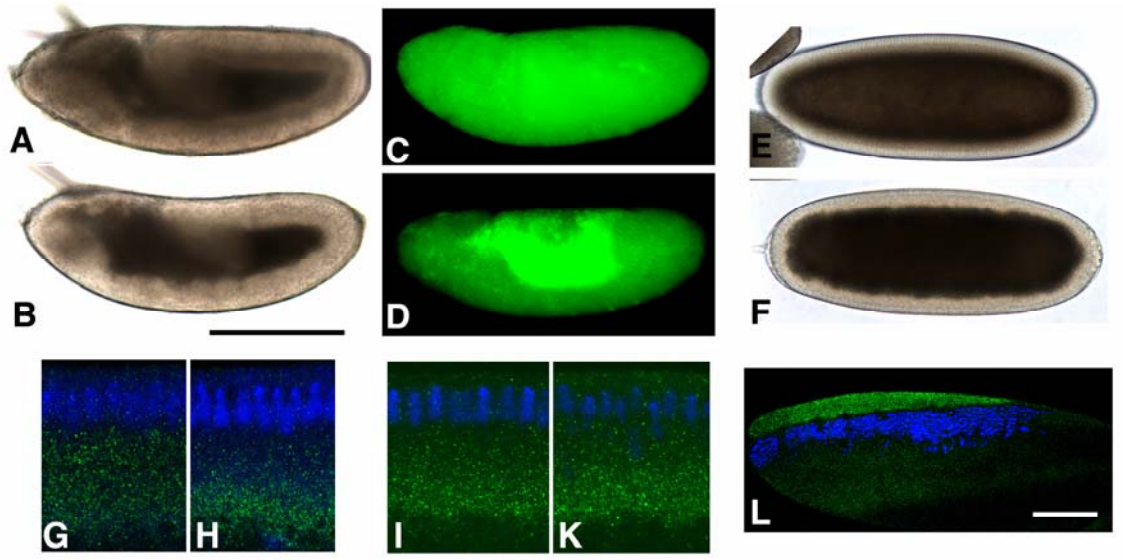

Figure 8: *ago2*^{dop1} comprises polarised microtubule-based transport

ago2^{dop1} mutant embryos (B) show a much more transparent periphery during germband extension than *wild-type* embryos (A). During early embryogenesis lipid droplets move bi-directionally along microtubules. Lipid droplets were stained with the droplet-specific fluorescent dye Nile Red and their distribution was recorded by epifluorescence microscopy (C, D). While lipid droplets were found throughout the periphery in the *wild-type* (C), they are accumulated around the central yolk in *ago2*^{dop1} mutant embryos. To generate embryos with reduced halo expression, males homozygously deleted for *halo* were crossed to *ago2*^{dop1} heterozygous (E, G) or homozygous (F, H) females. In these embryos, droplet distribution was assessed by overall transparency (E, F) or staining for the regulator Klar (green) (G, H). In late cycle 14, embryos from *ago2*^{dop1} homozygous mothers have a more transparent periphery and tighter basal accumulation of Klar puncta. The overall expression and distribution of Klar (green) is very similar in *wild-type* (I) and *ago2*^{dop1} embryos (K).
In centrifuged early embryos, lipid droplets accumulate in a distinct layer, just above nuclei (blue). In centrifuged *ago2*^{dop1} embryos, Klar (green) is highly enriched in the droplet layer, just as in the wild-type (Guo et al., 2005) indicating that it is physically associated with the droplets. (Courtesy of Michael Welte, Brandeis University, Waltham, USA)

the embryo itself. In *wild-type* embryos *halo* mRNA is highly upregulated entering cellularisation. After cellularisation *halo* mRNA levels dropped notable (Figure 9A, C, E, G). In *dop*^{1} embryos the *halo* mRNA expression is comparable to that of *wild-type* embryos (Figure 9B, D, F, H). Neither a delay in *halo* mRNA expression nor a delayed in *halo* mRNA degradation was observed.

Lipid droplets move bidirectionally along microtubules, and their apical-basal distribution results from the relative contribution of plus- and minus-end motion (Welte et al., 1998). Altered droplet distribution in *dop*^{1} embryos was not due to lack of droplet motion per se since droplets moved bidirectionally before, during, and after cellularisation This observation indicates that the motors driving droplet transport as well as the microtubule tracks are grossly intact. Therefore the basic machinery responsible for droplet motion must be intact. *dop*^{1} alters a specific aspect of transport resulting in faulty regulation of net transport direction.

Taken together, the *dop*^{1} mutation reveals the existence of a maternally established control mechanism to regulate specific events at the midblastula transition (MBT): formation and growth of membrane at the start and during cellularisation, and a developmentally regulated switch in organelle transport at the end of cellularisation.

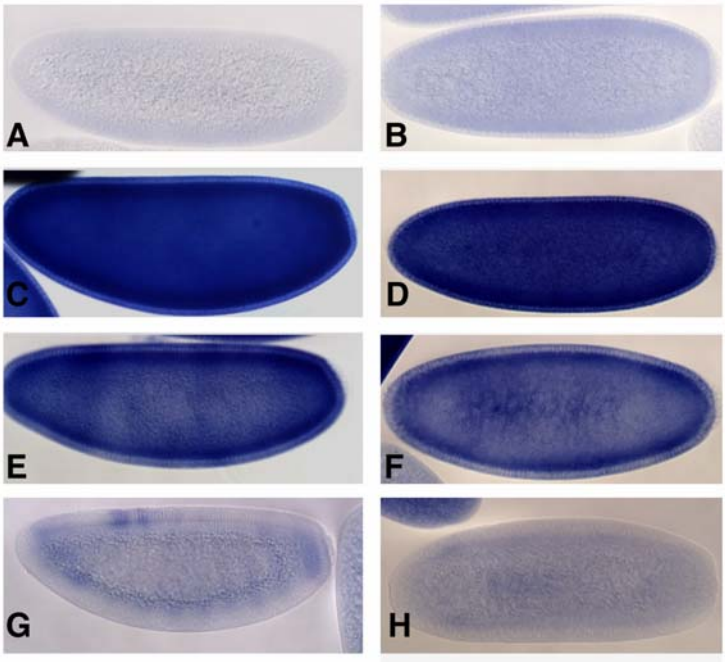

Figure 9: *halo* expression is normal in early *ago2*^{dop1} mutant embryos

The expression of the directionality determinant *halo* in *ago2*^{dop1} mutant embryos (B, D, E, H) occurs as in *wild-type* embryos (A, C, E, G). From top to bottom embryos in successive older stages are shown: syncytial blastoderm (A, B); early cycle 14 (C, D); mid-cellularisation stages (E, F); late cellularisation (fast phase; G, H). Please note that *halo* exhibits strictly zygotic expression, which is downregulated at the end of cellularisation (Gross et al., 2003).

3.3 *dop* is allelic to *ago2*

To identify the gene that is affected by the *dop*^{1} mutation chromosomal deletions we used that mapped *dop*^{1} to a 45-kb genomic region containing six predicted genes (Figure 4). Three P-element insertions were used for male recombination mapping (Preston and Engels, 1996) and revealed the genes *CG7739* and *ago2* (*CG7439*) as candidates for *dop*^{1} (Schreiber, 2003). Rescue constructs of both genes were cloned. The *dop*^{1} mutation is a maternal effect mutation as it only depends on the maternally encoded gene products, i.e. it depends on the genotype of the mother. Therefore the cDNAs of *CG7739* and *ago2* were cloned under the control of the maternal α4-tubulin67C promoter which allowed the maternal expression of the transgenes. Transgenic flies were established and crossed into *dop*^{1} mutant lines. The *mat::tub-ago2* transgene, but not *mat::tub-CG7739*, rescued embryos derived from *dop*^{1} mothers to viability (Figure 10A). *dop*^{1} embryos produce abnormal larval cuticles, which can be grouped into four classes. (Figure 10B-E): Class I embryos (continuous cuticle; Figure 10B, light green) form a continuous cuticle with more or less severely affected denticle belts. Class II embryos (shield; Figure 10C, yellow) produce a shield of continuous cuticle, reminiscent of neurogenic mutants. Class III embryos (*crumbs*-like: Figure 10D, orange) produce only small globular remnants of cuticle, reminiscent of mutations in genes required for epithelial polarity, such as *crumbs*. Class IV

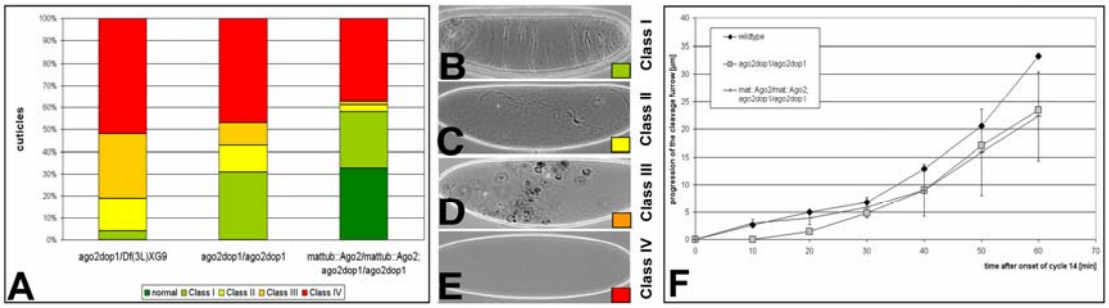

Figure 10: *dop*^{1} is rescued by *ago2* overexpression

Embryos derived from mothers homo- or hemizygous for *dop*^{1} do not hatch and produce abnormal larval cuticles, which can be grouped into four classes. Class I (continuous cuticle, B): such embryos form a continuous cuticle with more or less severely affected denticle belts. Class II (shield, C): such embryos produce a shield of continuous cuticle, reminiscent of neurogenic mutants. Class III (*crumbs*-like, D): such embryos produce only small globular remnants of cuticle, reminiscent of mutations in genes required for epithelial polarity, such as *crumbs*. Class IV (no cuticle, E): embryos in this class did not produce any cuticle at all. "Normal" represents hatching first instar larvae (A, dark green). The distribution of cuticle phenotypes of the different classes is shown in A; colour codes are given in B-E. The over expression of maternal *ago2* rescues embryos to hatching first instar larvae (A). The generation of the cleavage membrane was monitored by timelapse video recording of embryos during cellularisation. The progression of the cleavage furrow against time was measured and the data was plotted in the graph (F). The significant difference in membrane progression during slow phase that was observed between *wild-type* embryos (F, black diamond) and *dop*^{1} mutant embryos (F, grey casket), was rescued by the maternal over expression of *ago2* (F, black line). Please note: *dop*^{1} = *ago2*^{dop1}

embryos (no cuticle; Figure 10E, red) did not produce any cuticle at all. The distribution of cuticle phenotypes of the different classes is indicated in Figure 10D. “Normal” represents hatching 1st instar larvae (Figure 10A, dark green). The distribution of the cuticle phenotype of the different classes is shown in Figure 10A. By the maternal expression of *ago2* the embryos were rescued to hatching larvae and the fraction of embryos without cuticle was reduced by 10 % (Figure 10A). Moreover, the cellularisation defect of dop^{1} embryos was rescued by the maternal expression of *ago2* (Figure 10F). During slow phase membrane insertion took place at the same speed as in *wild-type* embryos. Another argument that dop^{1} is an allele of *ago2* is supported by examination of another, independently derived allele, called dop^{46}. This allele was created by a transposase induced imprecise excision of the P-element *EP(3L)3417* that is located in the 5’ UTR of *ago2*. Females homozygous or hemizygous for dop^{46} are sterile. Embryos from those mothers display very similar defects as dop^{1} embryos. As well dop^{46} embryos are rescued to viability by the expression of the *mat::tub-ago2* transgene dop^{46} did not complement the lethality neither the cellularisation defects of dop^{1} embryos.

In summary these data indicate that *dop* mutations are allelic to *ago2* and that maternal expression of a full-length *ago2* mRNA is capable to rescue the cellularisation defects of *dop* mutants. Therefore, dop^{1} and dop^{46} are referred to as $ago2^{dop1}$ and $ago2^{dop46}$ (embryos derived from homo- or hemizygous mutant mothers are named $ago2^{dop1}$ and $ago2^{dop46}$ embryos respectively).

3.4 $ago2^{dop1}$ does not represent a null allele of *ago2*

$ago2^{dop1}$ embryos show severe defects in morphological processes during MBT: The formation and growth of membranes and microtubule-based organelle transport are impaired during cellularisation. Surprisingly, the reported *ago2* null mutants $ago2^{51B}$ and $ago2^{414}$ were described to be viable and fertile (Okamura et al., 2004; Xu et al., 2004). A minor population of these *ago2* null mutant embryos showed weak defects in nuclear division cycles (Deshpande et al., 2005). Both alleles were derived from imprecise excisions of the P-element *EP(3L)3417*. The $ago2^{51B}$ allele leads to a 628 nucleotide deletion that eliminates the first two exons of *ago2* (Xu et al., 2004). In the $ago2^{414}$ mutant imprecise excision of the EP element generated a 2.3-kb deletion of genomic DNA, which included as well exons 1 and 2 of *ago2* (Okamura et al., 2004). In both cases the start codons for the two predicted Ago2 isoforms, Ago2-PB and Ago2-PC were eliminated. The severe defects that were observed for $ago2^{dop1}$ mutant embryos in MBT were not observed in any of these published *ago2* null mutant embryos. Immunolabelling of marker proteins

revealed that cellularisation in a*go2*^{51B} and *ago2*^{414} embryos occurred as in *wild-type* embryos (Figure 11).

The analysis of the *ago2*^{dop1} mutation suggested that *ago2* is an essential gene. The phenotype of *ago2*^{dop1} hemizygotes is stronger than that of *ago2*^{dop1} homozygotes. Therefore, *ago2*^{dop1} must either be a partial loss of function (hypomorph) mutation or *ago2*^{dop1} a dominant negative form of *ago2* (antimorph). Because the *ago2* transgene rescues the *ago2*^{dop1} mutation *ago2*^{dop1} must affect *ago2*'s function rather than an unrelated gene. The genetic behaviour of the *ago2* null allele *ago2*^{51B} in comparison to the *ago2*^{dop1} was evaluated in complementation tests (Table 6). Both *ago2*^{dop1} homo- and hemizygotes are female sterile. The same is observed for the *ago2*^{dop46} mutation: embryos from homo- or

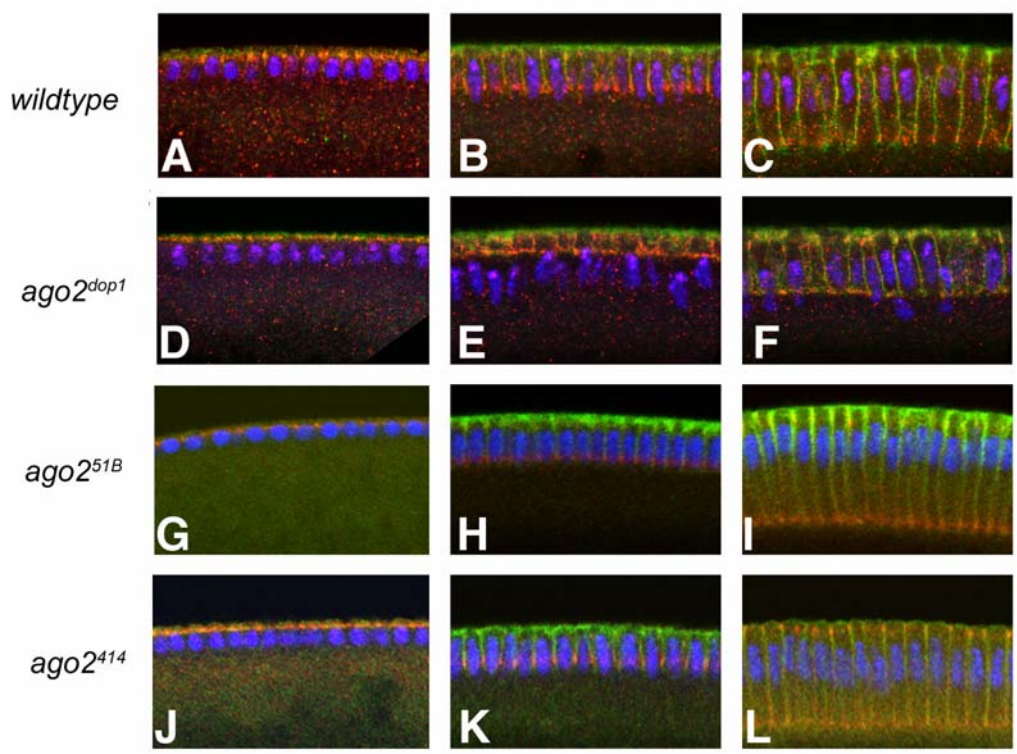

Figure 11: Defects in polarised membrane formation in *ago2*^{dop1} mutants

Immunostainings of embryos during cellularisation. The early *Drosophila* embryo undergoes 13 mitotic divisions. Entering cycle 14 a polarised epithelium is formed. From the left to the right a time series of embryos during cellularisation with successively older stages are shown. In the *wild-type* (A-C), the endogenous membrane protein Neurotactin (Nrt; green) first accumulates in the apical domain and is present in the cleavage membranes starting at mid cellularisation. Armadillo (Arm/ β-catenin; red; DNA stained blue) distribution marks the presence of basal junctions at the onset of cellularisation (A). At mid and late cellularisation, Arm protein is also found along the cleavage membrane with a bias to the apical domain, the future zonula adherens (B, C). In *ago2*^{dop1} mutant embryos (D-E), Arm and Nrt persist at the apical cytocortex until mid cellularisation. Nrt positive cleavage membranes are absent until fast phase. The ago2 null mutants *ago2*^{51B} (G-I, (Xu et al., 2004)) and *ago2*^{414} (J-K,(Okamura et al., 2004)) do not display such defects. Cellularisation occurs as in *wild-type* embryos.
Fixed embryos were staged by the extent of nuclear elongation, as described by (Lecuit et al., 2002)

hemizygous mothers fail to hatch. Moreover embryos from transheterozygous mothers *ago2*^{dop1}/*ago2*^{dop46} do not hatch and exhibit cellularisation defects. In contrast, embryos from *ago2*^{51B} hemi- or homozygous mothers hatch and develop into adult flies. Similarly, embryos from transheterozygous *ago2*^{dop1}/*ago2*^{51B} mothers hatch. If *ago2*^{51B} would represent a true null allele of *ago2* one would expect that it phenocopies hemizygous *ago2*^{dop1} embryos, i.e. that it behaves genetically like a complete depletion of the gene like in a chromosomal deletion of that locus.

To confirm the published molecular lesions within the *ago2* locus of *ago2*^{51B} and *ago2*^{414}, PCR (not shown) and RT-PCR (Figure 12D) analysis was performed. The molecular analysis of these alleles was consistent with the published data. Another possibility to explain the genetics of these alleles was that there was still another mRNA produced from the *ago2* gene. A computational approach was first employed to predict the position of potential alternative transcriptional start sites within the *ago2* locus. An analysis using McPromotor software (version3, McPromotor site at Duke: http://tools.genome.duke.edu/generegulation/McPromoter/) of 7835 nt (position 64.000 to 71835 of genomic contig AE003530) including the entire *ago2* gene identified an additional transcriptional start site (TSS) 40 nt before the third exon (Figure 12A and see page 95: Appendix Genomic Sequence of *ago2*).

The prediction of an alternative TSS suggested that the *ago2* locus might produce an alternative transcript from that promoter. To test this possibility, a Northern blot

Table 6: Complementation test between *ago2* alleles

The table shows the results of the complementation test of *ago2* mutant females. Homozygous, hemizygous and transheterozygous mothers were analysed for their fertility. Female sterile means that no embryos hatched, fertile means hatching first instar larvae.

genotype of mothers	phenotype
ago2^{dop1}/*ago2*^{dop1}	female sterile
ago2^{dop1}/*Df(3L)XG9*	female sterile
ago2^{dop46}/*ago2*^{dop46}	female sterile
ago2^{dop46}/*Df(3L)XG9*	female sterile
ago2^{dop1}/*ago2*^{dop46}	female sterile
ago2^{dop1}/*ago2*^{51B}	fertile
ago2^{51B}/*ago2*^{51B}	fertile
ago2^{51B}/*Df(3L)XG9*	fertile

analysis of mRNA from *wild-type* (w^{1118}), $ago2^{dop1}$ and $ago2^{51B}$ ovaries was carried out using a full length *ago2* anti-sense RNA probe. However this approach failed to visualise a short version of *ago2* (predicted transcript size of $ago2^{short}$ was 3801 bp). Only *ago2* full length was detected in RNA from *wild-type* (w^{1118}) and $ago2^{dop1}$ ovaries (Figure 12C). The expression levels of *ago2*, as measured by Northern blotting were the same in *wild-type* and $ago2^{dop1}$ ovaries. Interestingly, the $ago2^{dop1}$ transcript runs slightly faster than the *wild-type* transcript. It remains however possible, that the putative alternative *ago2* transcript might only be weakly expressed in ovaries and thus might be underrepresented and not

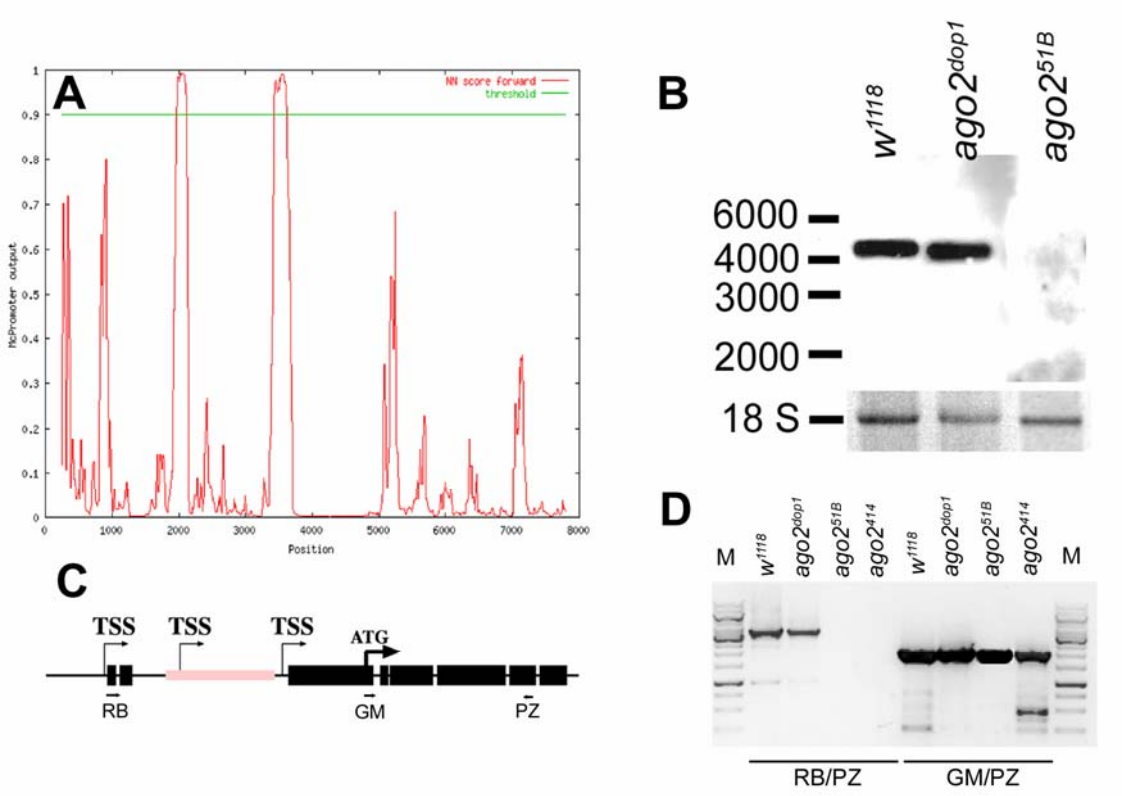

Figure 12: $ago2^{51B}$ and $ago2^{414}$ are not null alleles of *ago2*

The *ago2* locus contains 8 exons that are predicted to produce two differentially spliced isoforms encoded by the *ago2-RB* and *ago2-RC* transcripts. Using McPromoter (Version3) software to predict RNA polymerase II transcription start sites two high fidelity promoter were predicted in addition to the low fidelity promoter 10 nt and 58 nt respectively upstream of the first exon of RB and RC isoform: One localised to a natural S-element transposon (TE20119) and the other one mapped 40 nt upstream of the start of exon 3 (A). Northern blot analyses of $polyA^+$ RNA prepared from w^{1118}, $ago2^{dop1}$ and $ago2^{51B}$ using a full length anti-sense RNA probe ovaries showed a transcript of about 4 kb for *wild-type* and $ago2^{dop1}$ (B). Please note that the $ago2^{dop1}$ transcript runs slightly faster on the gel. *ago2* levels were very similar in *wild-type* and $ago2^{dop1}$. The 18S rRNA band served as a loading control. Using the predicted TSS in front of exon 3 would produce an expected transcript of 3801 bp which is not detectable in any of the lanes of the Northern analysis. RT-PCR analysis (D) using a forward primer (E1) in the first and a reverse primer (E7) in the seventh exon (C) indicates a transcript of 3488 nt for the *wild-type* and $ago2^{dop1}$ but not for $ago2^{51B}$ or $ago2^{414}$. However, using a forward primer located at the end of the third exon (E3) and the E7 primer transcripts of 2200 nt length were detected in all cases.

be detected by Northern blot using a DIG labelled anti sense RNA probe. Therefore a RT-PCR analysis was performed using primer pairs that were located at the end of the third and seventh exons (Figure 12B), which would allow amplification of a short *ago2* message. In RNA samples from *wild-type* and all *ago2* mutant ovaries a transcript of 3488 bp was detected using RT-PCR. *ago2* transcripts comprising the second until the seventh exon, which only allowed amplification of a long *ago2* transcript, were only detected in *wild-type* and $ago2^{dop1}$ mutant tissue but not in $ago2^{51B}$ nor in $ago2^{414}$ mutant ovary tissue.

These data suggest that the *ago2* locus contains two TSS, which are used to produce at least three different transcripts: two mRNAs, RB and RC encode very similar long isoforms and a novel mRNA encoding a short isoform. The transcript of *ago2-RB* is 4031 bp and of *ago2-RC* 4040 bp long and result in a protein of 1214 aa and 1217 aa of approx. 130 kDa.

The short *ago2* transcript is 3801 bp long. The translational start is located at the end of exon 3 and would result in a protein of 787 aa length. On a Western blot the short isoform was expected to appear as a band of approx. 90 kDa. Western blot experiments using different Ago2 antibodies were performed to examine, whether short protein isoforms can be detected (Suppl. Figure 28E, F). Using total *wild-type* ovary tissue preparations the $Ago2_{Cterm}$ antibody detected three bands in Western blot experiments (Suppl. Figure 28E): one band at 130 kDa which would correspond to Ago2 full length, the short Ago2 isoform of about 100 kDa and a band at approx. 70 kDa, which could be an Ago2 degradation product or a non-specific band. In preparations from $ago2^{dop1}$ ovary tissue all three bands were detected, too. Additionally, two more bands appeared: one slightly smaller than 100 kDa and one slightly smaller than 70 kDa. Neither the nature nor the origin of the second smaller bands is clear. In ovary tissue from $ago2^{51B}$ the 100 kDa band was detected. Using an Ago2 antibody from Q. Liu, PhD, University of Texas, Dallas, USA, Ago2 was detected in a slightly different pattern (Suppl. Figure 28F): In *wild-type* Ago2 full length at 130 kDa and Ago2 short at 100 kDa were detected. In $ago2^{dop1}$ protein extracts only full length Ago2 was detected. In $ago2^{51B}$ protein extracts a short Ago2 protein of about 80 – 90 kDa was detected. The Western blot results indicate that there might be protein made from the short transcript. But none of the antibodies could clearly show the presence of the different Ago2 isoforms as predicted from the transcript analysis. In summary, the genetic and RT-PCR results allow the statement that neither $ago2^{51B}$ nor $ago2^{414}$ are true null alleles of *ago2*.

3.5 $ago2^{dop}$ mutation affects Glutamine Rich Repeats (GRR)

To summarise the last paragraph neither $ago2^{dop1}$ nor $ago2^{51B}$ nor $ago2^{414}$ represent null alleles of *ago2*. The genomic DNA from homozygous $ago2^{dop1}$ flies was sequenced and compared it to the sequence from *red e* flies, which constitute the genetic background in

which the original *ago2*^{dop1} allele was induced. In order to analyse the nature of the mutation in *ago2*^{dop1}, genomic DNA was prepared from homozygous flies. Primer pairs were designed to amplify overlapping party of the genomic DNA of the *ago2* locus (Table 1, Suppl. Figure 27). The PCR products were then sequenced and analysed for mutation when compared to the DNA sequence of the original *red e* chromosome. The *ago2*^{dop1} allele contains a 69 nt in frame deletion in the third exon. This deletion leads to the loss of one Glutamine Rich Repeat (GRR) at the amino-terminus of the Ago2 protein (Figure 13, Suppl. Figure 27). The Ago2 protein has two GRRs at the amino-terminus, a central PAZ

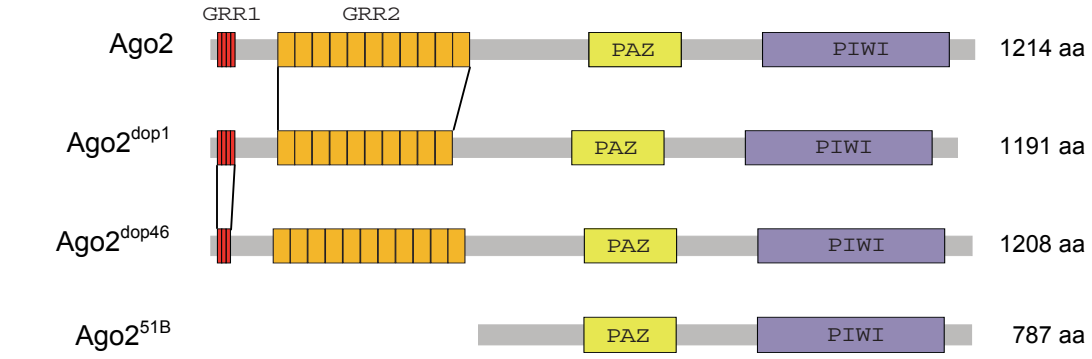

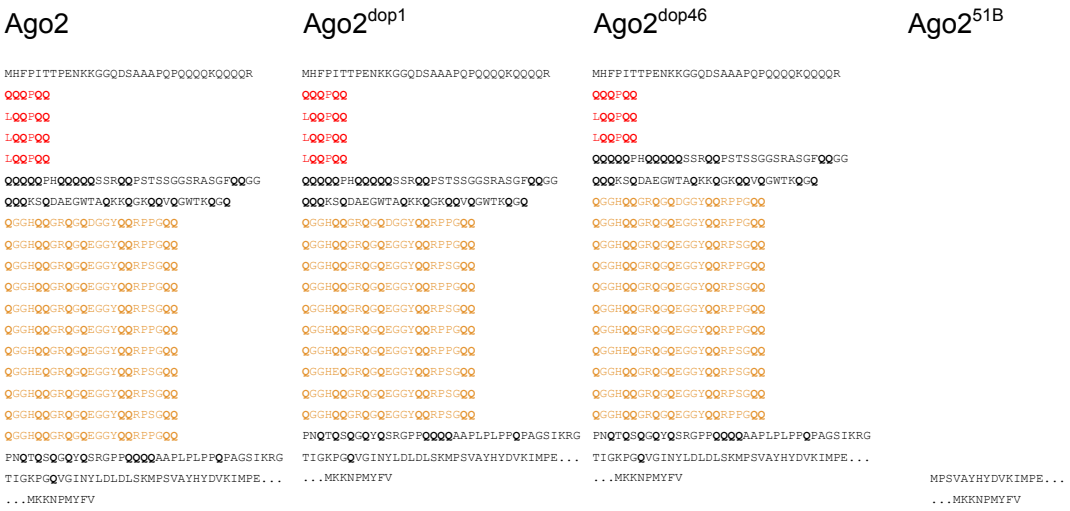

Figure 13: The mutation in *ago2*^{dop} affects the amino-terminal Glutamine Rich Repeats (GRR)

The cartoon of the Ago2 protein indicates the positions of the GRR region at the amino-terminus, a central PAZ domain, and a carboxyl-terminal PIWI domain. The amino-terminus of Ago2 contains four imperfect GRR1 (LQQPQQ) repeats and 11 imperfect GRR2 (QGGHQQGRQGQEGGYQQRPPGQQ) repeats. The RB transcript codes for a protein of 1214 aa. The protein encoded by the *ago2*^{dop1} allele contains only 1191 aa and lacks one of the GRR2 repeats (repeat number 9 or 10). The *ago2*^{dop46} mutation represents an 18-nucleotide deletion, leading to the loss of one GRR1 and a predicted protein of 1208 aa. The short version of Ago2, represented here by Ago2^{51B} completely lacks the GRR1 and GRR2 and results in a protein of 787 aa.

and a carboxy- terminal PIWI domain. The function of the PAZ and the PIWI domains are known. PAZ forms a nucleic acid-binding pocket that can bind small RNAs (Lingel et al., 2003; Song et al., 2003). The PIWI domain is a ribonuclease domain and can degrade cognate RNAs (Liu et al., 2004; Meister et al., 2004; Rand et al., 2004; Rivas et al., 2005; Song et al., 2004). The function of GRRs has not yet been characterised. GRR1 is made up of four imperfect repeats of 6 aa length (LQQPQQ) and GRR2 consists of eleven imperfect repeats of 23 aa length (QGGHQQGRQGQEGGYQQRPPGQQ). The *ago2*^{dop1} mutation leads to the loss of exactly one repeat in GRR2, which by nature of its imperfect sequence must be either the 9th or the 10th repeat (Figure 13, Suppl. Figure 27). The presence of the deletion is also consistent with the slightly faster motility of the *ago2*^{dop1} transcript in the Northern blot (Figure 12B). Sequencing of the *ago2*^{dop46} allele revealed an in frame deletion of 18 nt which leads to the loss of one LQQPQQ repeat in GRR1.

It is very striking, that a mutation that alters the copy number inside one GRR of Ago2 has such dramatic effects on embryonic development. Embryos with a reduced number of GRRs show dramatic defects at MBT whereas embryos completely lacking the GRR domain develop grossly normal. These observations demonstrate that the GRRs of Ago2 are essential for the function of the protein and that Ago2 might play an important role in *Drosophila* development. But so far it cannot be defined how the GRRs contribute to Ago2's function. One possibility could be that Ago2^{dop1} negatively interferes with Ago2^{short} or with other proteins, which will be discussed later.

The GRRs of Ago2 are essential for the correct function of the protein in *Drosophila melanogaster*. Nothing has been reported so far about Ago2's GRRs. Are the GRRs special for *Drosophila melanogaster* Ago2 protein or are the GRRs conserved in other species as well? An evolutionary analysis of sequences of Ago2 proteins revealed that the GRRs are present not only in *Drosophila* but as well among insect species (Figure 14). In each *Drosophila* species one or several imperfect GRRs are evident in the third exon (yellow, blue or green in Figure 14). Like in *Drosophila melanogaster* the GRRs are followed by a conserved sequence at the 3' end of the third exon (purple Figure 14).

Though the sequences between species are highly variable, the glutamine-rich character of this region is preserved. The GRRs might regulate Ago2's function not only in *Drosophila* but also in other insect species. Therefore the GRRs might be of general importance for Ago2 function.

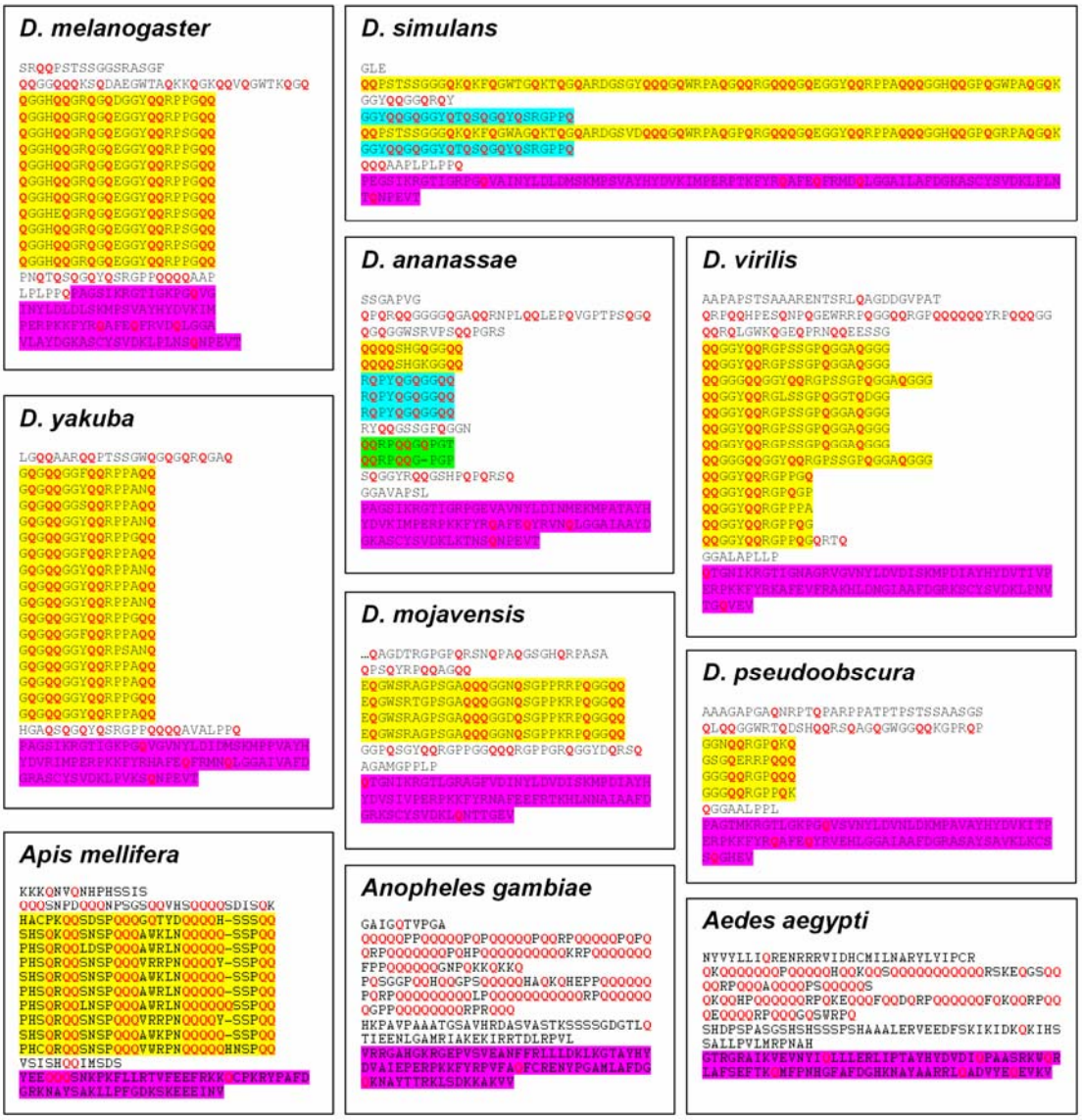

Figure 14: Amino-terminal glutamine-rich repeats in Ago2 proteins from different insects

The protein sequence encoded in *ago2* exon 3 of *D. melanogaster* is listed at the top. The corresponding region of Ago2 predicted from genomic sequences are shown for six additional *Drosophila* species, the malaria mosquito *A. gambiae*, the yellow fever mosquito *A. aegypti* and the honeybee *A. mellifera*. In each case, a bi-partite structure is apparent: an amino-terminal glutamine-rich region (glutamines indicated in red and bold) of variable sequence followed by a conserved stretch at the 3' end of exon 3 (purple). In many instances, the glutamine-rich regions contain multiple imperfect copies of distinct repeats (yellow, blue, or green).

3.6 *ago2^{dop}* impairs RNAi

Ago2 is known to be essential for siRNA mediated RNA silencing, called RNA interference (RNAi) (Hammond et al., 2001; Okamura et al., 2004). If the *ago2^{dop1}* mutation affects *ago2* function one would predict RNAi to be compromised in these mutants. Effects of *ago2* mutations on siRNA triggered RNAi were assayed using an UAS construct that reduces the function of the cell death inhibitor DIAP1 by expression of dsRNA complementary to the DIAP1 mRNA (*GMR::Gal4, UAS::DIAP1^{RNAi}*) (Huh et al., 2004). When this construct is expressed in the developing eye, DIAP1 levels are reduced. As a result the cells die by

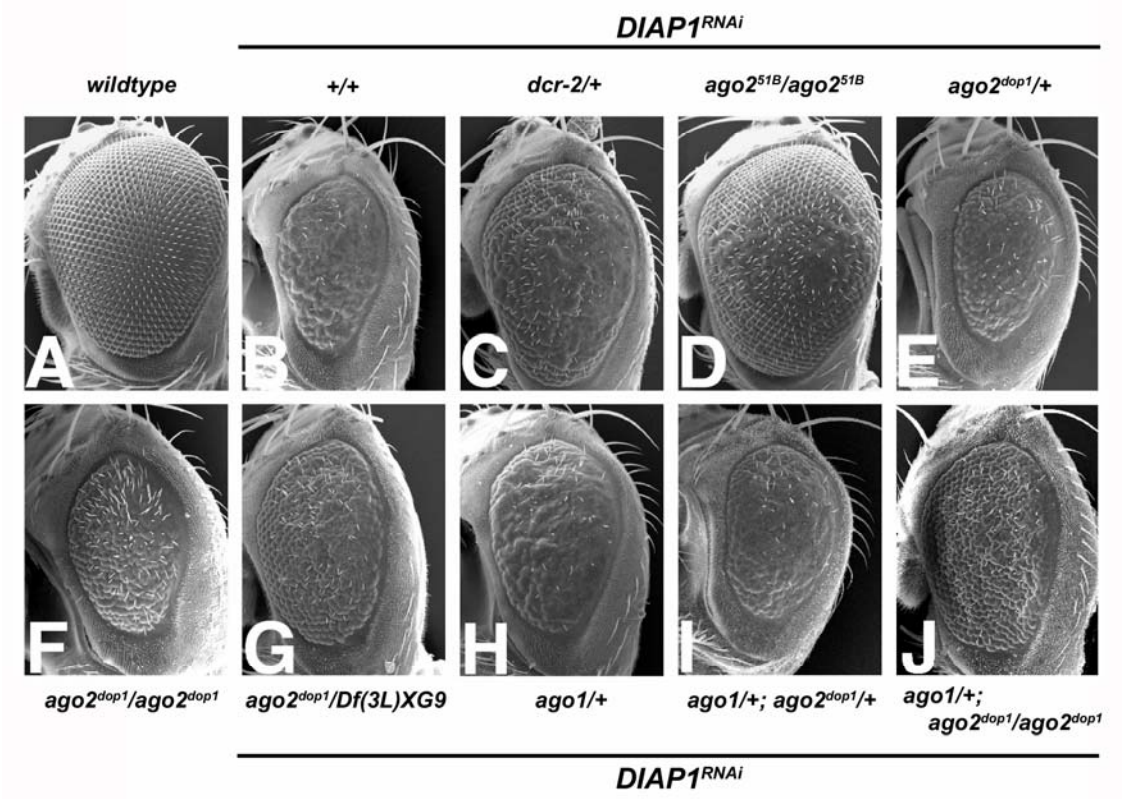

Figure 15: The requirement of *ago2* and *ago1* for siRNA-mediated RNAi

Effects of *ago2* mutations on the siRNA-mediated RNAi were assayed using a *UAS* construct that reduces the function of the cell death inhibitor DIAP1 by dsRNA expression (*GMR::Gal4, UAS::DIAP1^{RNAi}*; (Huh et al., 2004). Scanning EM micrographs of compound eyes of 2- to 4-d-old females are displayed. A *wild-type* compound eye is shown in A. The expression of *GMR::DIAP1^{RNAi}* reduces the normal size of the eye (B). In flies with only a single copy of the *dicer2* gene, this phenotype was partially suppressed (C; *GMR::DIAP1^{RNAi}/dcr-2^{L811fsX}*). Complete suppression is observed by the *ago2^{51B}* allele (D; *GMR::DIAP1^{RNAi}/CyO*; *ago2^{51B}/ago2^{51B}*). In heterozygous *ago2^{dop1}* flies no suppression of the phenotype could be observed (E; *GMR::DIAP1^{RNAi}/CyO*; *ago2^{dop1}/TM6*). Only a mild suppression of the reduced eye phenotype was visible in flies homozygous (F; *GMR::DIAP1^{RNAi}/CyO*; *ago2^{dop1}/ago2^{dop1}*) or hemizygous (G; *GMR::DIAP1^{RNAi}/CyO; ago2^{dop1}/Df(3L)XG9)* for *ago2^{dop1}*) for *ago2^{dop1}*. Mutations in *ago1* only mildly suppresses the siRNA-mediated RNAi (H; *GMR::DIAP1^{RNAi}/ago1^{K08121}*). Reducing the level of Ago1 in an *ago2^{dop1}* heterozygous (I; *GMR::DIAP1^{RNAi}/ago1^{K08121}; ago2^{dop1}/TM6*) or homozygous background (J; *GMR::DIAP1^{RNAi}/ago1^{K08121}; ago2^{dop1}/TM6*) shows a stronger repression than *ago2^{dop1}* alone.

apoptosis and therefore the eyes are significantly smaller (Figure 15A, B). In this experimental design, the efficiency of RNAi induced by long dsRNA can be simply observed by the size of the eye: when RNAi is working efficiently the eyes are much reduced in size. When RNAi is disrupted, the reduced eye phenotype is repressed and results in a normal-sized eye. In flies with only a single functional copy of the *dcr-2* gene, this phenotype was partially suppressed (Figure 15C). Thus, the activity of the *DIAP1*^{RNAi} depends on siRNA production through Dcr-2. The *ago2*^{51B} allele which completely lacks Ago2^{long} suppressed the phenotype completely (Figure 15D). Together these results are consistent with the requirements of Dcr-2 and Ago2 for RNAi in biochemical assays (Lee et al., 2004b; Okamura et al., 2004; Xu et al., 2004). In contrast, alteration in the GRRs shows only a mild suppression of the phenotype. In heterozygous *ago2*^{dop1} flies no suppression of the phenotype could be observed (Figure 15E). Only a mild suppression of the reduced eye phenotype was visible in *ago2*^{dop1} homozygous flies (Figure 15F). The suppression was slightly stronger in *ago2*^{dop1} hemizygous flies (Figure 15G*)*. But compared to the level of suppression achieved by *ago2*^{51B} the effect of *ago2*^{dop1} was much less pronounced (Figure 15D, F, G). Thus, the *ago2*^{dop1} mutation affects but does not eliminate *ago2*'s function in the siRNA- triggered RNAi. In agreement with Williams and Rubin (2002), mutations in *ago1* also mildly affected siRNA-triggered RNAi (Figure 15H). Reducing the level of Ago1 in an *ago2*^{dop1} heterozygous (Figure 15I) or homozygous background (Figure 15J) showed a stronger suppression than *ago2*^{dop1} alone. This observation suggests that Ago1 is also required for RNAi. The effect of Ago1 in RNAi is more pronounced when Ago2 function is reduced. This result suggests that Ago1 and Ago2 at least in the compound eye are acting together in RNAi.

3.7 *ago2* interacts with *ago1*

As shown in the last chapter, Ago1 and Ago2 exhibit both requirements for siRNA-triggered RNAi in the eye. The result raises the possibility that Ago1 and Ago2 might be acting together in RNAi or other biological processes. It was therefore interesting to examine if an interaction between Ago1 and Ago2 could be observed in the embryo and in particular at the MBT.

Genetic interactions were investigated in two ways: (1) by generation of double mutants and (2) by misexpression of *ago1* in an *ago2* mutant background. The double mutants show that cellularisation of *ago2*^{dop1} homozygous embryos is significantly enhanced by a reduction in *ago1* activity (Figure 16A). In homozygous *ago2*^{dop1} embryos membrane insertion during slow phase is significantly slower than in *wild-type*. Reducing the level of

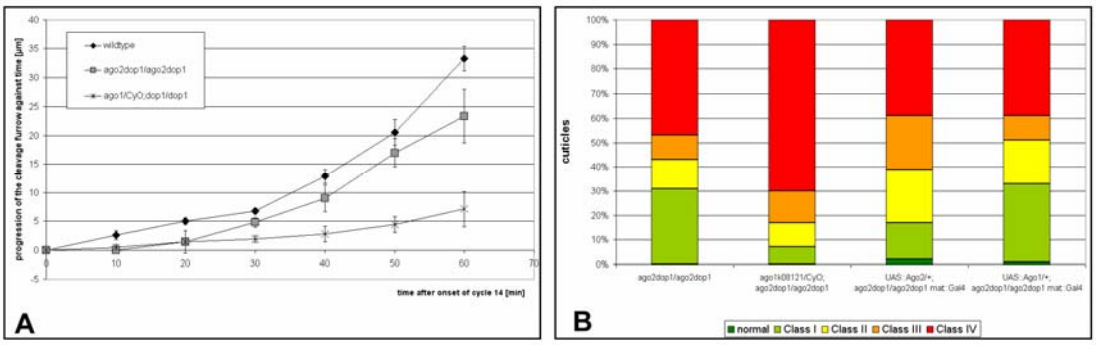

Figure 16: Genetic interaction of *ago1* and *ago2^{dop1}*

The reduction of *ago1* gene doses enhances the *ago2^{dop1}* cellularisation phenotype (A). The progression of the cleavage furrow during cellularisation is reduced in embryos from *ago2^{dop1}* mutant mothers (grey casket, A) in comparison to *wild-type* (black diamonds, A). Embryos from *ago1^{K08121}/CyO ; ago2^{dop1}/ago2^{dop1}* mutants (black cross, A) show a strongly reduced furrow progression even during fast phase.
The enhancement of the *ago2^{dop1}* phenotype in embryos with reduced *ago1* gene doses can be observed as well in cuticle formation (B). The *ago2^{dop1}* phenotype can be rescued not only by the zygotic overexpression of *ago2* but also by the zygotic overexpression of *ago1* (B).
Normal (hatching first instar larvae), Class I (continuous cuticle), Class II (shield), Class III (crumbs-like), Class IV (no cuticle).

ago1 in an *ago2^{dop1}* homozygous background not only membrane insertion during slow phase but also during fast phase is strongly affected. Hardly any membrane extension was observed. This phenotype goes along with a stronger disruption of larval cuticle in *ago1 ago2^{dop1}* double mutants than in *ago2^{dop1}* single mutants (Figure 16B). In the second approach *ago1* and *ago2* were overexpressed using the *GAL4/UAS* system. The experimental design allowed maternal expression of *GAL4*, which then becomes active in transcription in the zygote. Intriguingly, not only zygotic expression of *UAS::ago2* but also *UAS::ago1* improved larval cuticle formation of *ago2^{dop1}* mutant embryos considerably; in some of them rescue allowed for hatching first instar larvae (Figure 16B). In conclusion, these experiments show that the severity of the *ago2^{dop1}* phenotype is sensitive to the level of *ago1* expression.

As shown in earlier paragraphs, *ago2^{dop1}* is a specific mutation that alters the number of Ago2's aminoterminal GRRs. The mutation leads to specific disruptions at MBT. The complete loss of Ago2's GRRs (like in *ago2^{51B}* flies) does not have an impact on embryonic development as the altered number of GRRs has. As the interaction between *ago1* and *ago2^{dop1}* was observed the question arose whether the genetic interaction between *ago1* and *ago2* is exclusive for the *ago2^{dop1}* allele and therefore represents a novel function for *ago2^{dop1}* or whether this is true for *ago2* in general. To answer this, one observation in larval cuticle formation was very instructive. Some of the *ago1 ago2^{dop1}* double mutant embryos that formed Class I cuticles displayed a novel phenotype with significant patterning defects

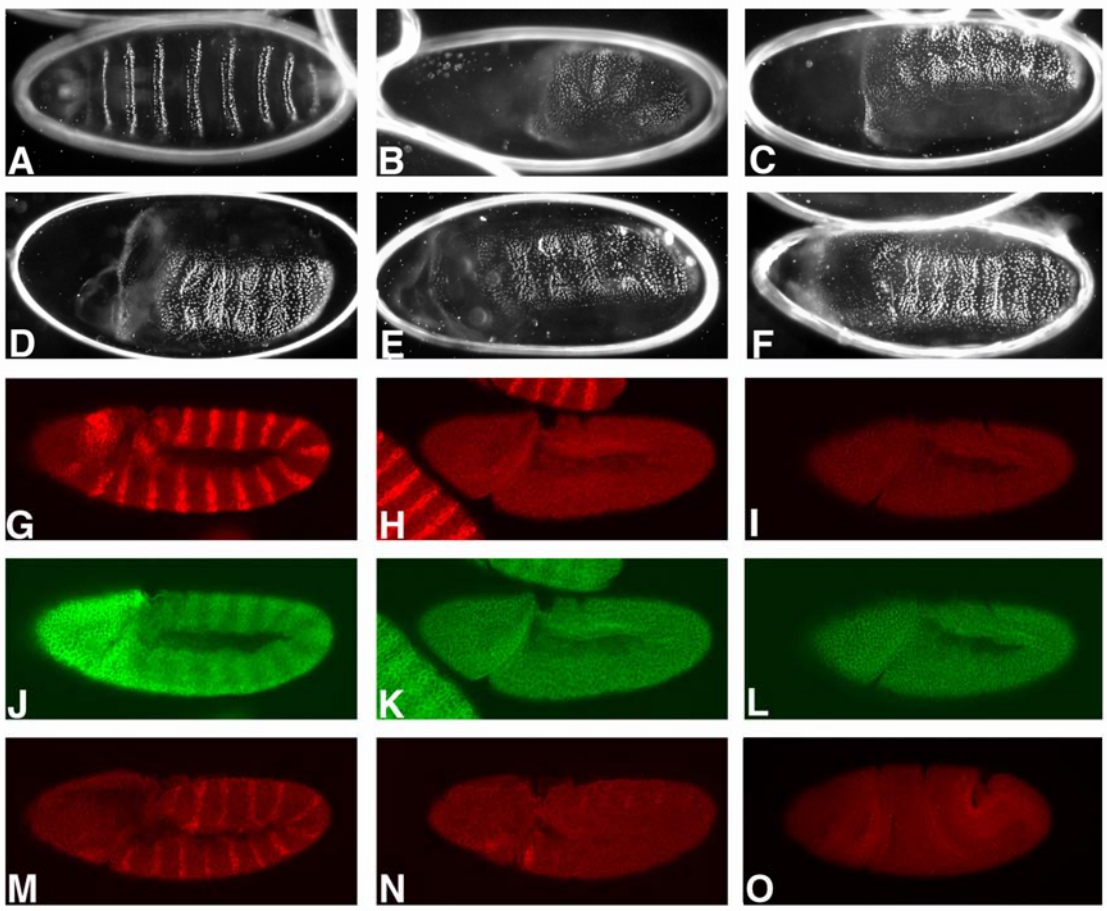

Figure 17: Requirements of *ago1*, *ago2* and *dcr-1* for Segmentation

Segment-polarity defects in *ago1*^{K08121} *ago2*^{dop1}, *ago1*^{K08121} *ago2*^{51B} or *ago1*^{K08121} *dcr-1*^{Q1147X} double mutant embryos are evident from alterations of the larval cuticle (A–F) or the pattern of immunolabelling of Wg, Arm or En (G–O). All embryos are oriented with their anterior to the left. Larval cuticles of those embryos that failed to hatch were examined (A–F). Embryos from *dcr-2*^{L811fsX}*/dcr-2*^{L811fsX}*; dcr-1*^{Q1147X}*/TM6* parents exhibit normal cuticle differentiation (A). Class I cuticles from *ago1*^{K08121}*/CyO; ago2*^{dop1}*/ago2*^{dop1} mutants exhibit a lawn of denticles, indicative of a defect in establishing segment polarity (B). Embryos from *ago1*^{K08121}/CyO; *ago2*^{dop1}*/TM6* mutant parents develop a segment polarity defect with an anterior hole (C). Embryos from *ago1*^{K08121}*/CyO; ago2*^{51B}*/TM6* mutant parents (E) or from *ago1*^{K08121}*/CyO; ago2*^{51B}*/ago2*^{51B} parents show similar segment polarity defects (D). Embryos obtained from *ago1*^{K08121}*/CyO; dcr-1*^{Q1147X}*/TM6* parents also exhibit a typical segment polarity defect (F). Immunolabelling of Wg (G–I), Arm (J–L) or En (M, N) proteins in extended germband embryos (stage 9). To identify homozygous embryos, *CyO[hb::lacZ]* and *TM3[hb::lacZ]* balancer chromosomes were used for the *ago1*^{K08121}/CyO; *ago2*^{dop1}*/TM3* stock (G, J, M). The presence of the *[hb::lacZ]* transgene on the balancers results in β-galactosidase expression in the anterior part of the embryo (J). In embryos that are heterozygous for *ago1*^{K08121} and *ago2*^{dop1} Wg and En proteins are expressed in 14 stripes (G, M); cytoplasmic Arm protein is elevated in 14 stripes (J). In embryos from parents of the genotype *ago1*^{K08121}*/CyO; ago2*^{51B}*/TM6*, Wg protein expression is completely abolished (H). Cytoplasmic levels of Arm (K) are equally low in all cells of the embryo and expression of En (N) is not maintained and fades from stage 9 onward. The same is observed in embryos from *ago1*^{K08121}*/CyO; dcr-1*^{Q1147X}*/TM6* parents. Those embryos also lack Wg (I) and hence also fail to accumulate Arm (L) stripes. In earlier stages (Stage 7), embryos from *ago1*^{K08121}*/CyO; dcr-1*^{Q1147X}*/TM6* parents already lack detectable Wg protein (O).

(Figure 17B). The embryos displayed cuticle phenotypes that had been reported for the segment polarity mutants *wingless* (*wg*) or *armadillo* (*arm*). This phenotype had never been observed in *ago1* or *ago2*^{dop1} single mutant embryos. Cuticles showing the same patterning defects where also observed in embryos from the heterozygous stock (*ago1*^{k08121}*/CyO, ago2*^{dop1}*/TM3,* Figure 17C). Interestingly, the same patterning defects displayed embryos from heterozygous and homozygous *ago1*^{k08121} *ago2*^{51B} double mutant parents (*ago1*^{k08121}*/CyO, ago2*^{51B}*/TM6,* Figure 17D and *ago1*^{k08121}*/CyO, ago2*^{51B}*/ ago2*^{51B}, Figure 17E). This indicates that the interaction between *ago1* and *ago2* is not specific for the *ago2*^{dop1} allele but is more general.

The double mutants of *ago1* and *ago2* alleles affect a specific patterning process, segment polarity, raising the question whether small RNAs are involved in segmental patterning. siRNA triggered RNAi is impaired in *ago2*^{dop1} mutants but not abolished. Therefore, it is unlikely that the interaction of *ago1* and *ago2* depends on siRNA mediated silencing. Another possibility would be that this interaction is based on miRNA triggered RNAi as Ago1 is essential for miRNA mediated RNAi (Okamura et al., 2004). In order to test this hypothesis *dcr-1* and *ago1* double mutants were investigated. *dcr-1* is essential for processing miRNA from double stranded pre-miRNAs (Lee et al., 2004b). Cuticles from the non-hatched embryos derived from *ago1*^{K08121}*/CyO; dcr-1*^{Q1147X}*/TM6* parents exhibited the same type of strong patterning defects as observed in *ago1 ago2* double mutants (Figure 17F). This observation indicates that the segment polarity defects are a result of a defective miRNA mediated silencing pathway. This observation was verified by investigating cuticles from *dcr-1 dcr-2* double mutants. *dcr-2* is essential for processing long double stranded RNAs into siRNAs (Lee et al., 2004b). Embryos from *dcr-2 dcr-1* double mutant parents displayed mostly normal cuticles. Less than 1 % of these embryos displayed segment polarity defects which is negligible few in comparison to approximately 20 % in *ago1 ago2* and *ago1 dcr-1* double mutants (Table 7). This 1 % might reflect a maternal contribution of *dcr-1* to segment polarity. In summary, these results show that segment polarity defects might be consequence of a defective miRNA silencing pathway.

In the *Drosophila* embryo, *armadillo* (*arm*), *wingless* (*wg*) and *engrailed* (*en*) are segment polarity genes that are required for normal patterning. Mutations in those genes lead to segmentation defects similar to the ones that were observed here. Wg and En are initially expressed in 14 non-overlapping segmental stripes. In response to Wg signalling, levels of cytoplasmic Arm increase and En expression is maintained in the receiving cells (Riggleman et al., 1990). The embryos from *ago1 ago2* and *ago1 dcr-1* double mutant parents were stained for Arm, En and Wg. protein (Figure 17G-O). In heterozygous *ago1 ago2*^{dop1} mutants the proteins are expressed in a *wild-type* pattern (Figure 17G, J, M). In embryos obtained from *ago1*^{k08121}*/CyO, ago2*^{51B}*/TM6* parents no Wg protein could be

detected (Figure 17H). The lack of Wg protein expression in these embryos is sufficient to result in the observed patterning defects. As a consequence of the lack of Wg protein expression, cytoplasmic Arm stripes are not present and En expression is not maintained in these embryos (Figure 17K, N). The same observation was made in embryos from *ago1*^{K08121}*/CyO; dcr-1*^{Q1147X}*/TM6* parents (Figure 17I, L). Even in gastrula stages Wg protein was absent (Figure 17O) which indicates that Wg protein expression is not established in the first place.

The reduction of the zygotic expression of *ago1* and *dcr-1* as two major components of the miRNA mediated silencing pathway resulted in similarly strong patterning defects as the reduction of the zygotic expression of *ago1* and *ago2*. It is therefore likely that *ago2* might also function in a miRNA dependant manner. In summary, if two major components of the miRNA silencing pathway are reduced in their function, segment polarity defects are observed. Furthermore, this analysis strongly suggests the requirement for miRNAs in *wg* expression and segmentation.

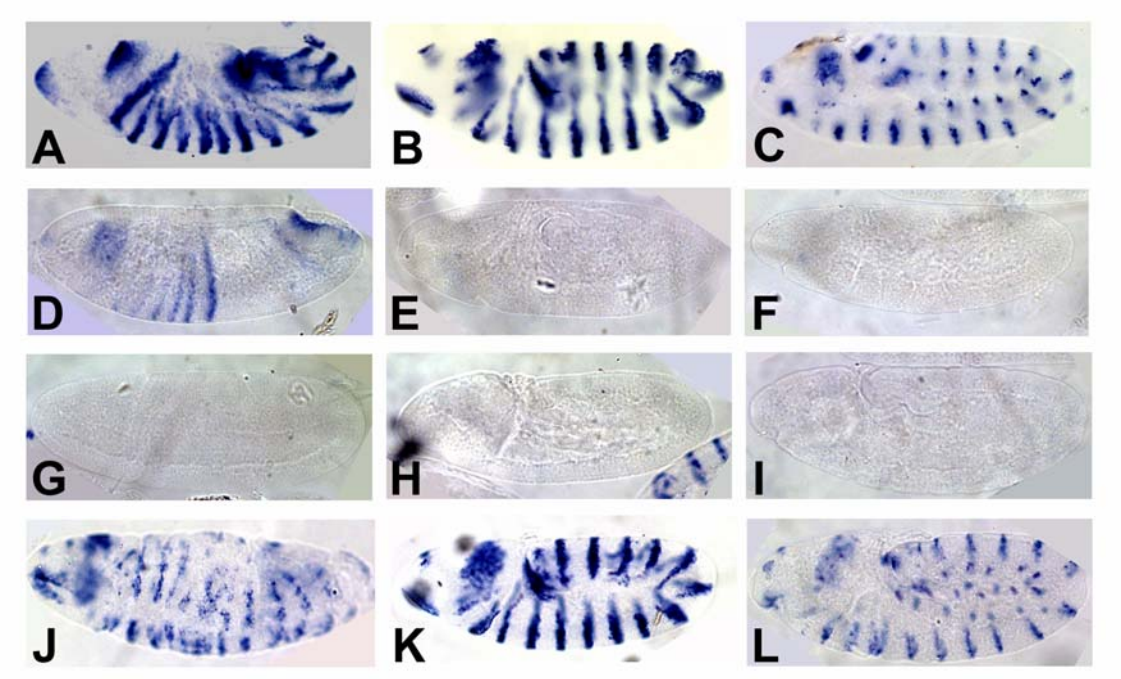

Figure 18: *wingless* is not expressed in zygotic *ago1 ago2* double mutants and miss-expressed in zygotic *ago1 dcr-1* double mutants

The expression of the segment polarity gene *wingless* (wg) in embryos derived from heterozygote parents was examined. All embryos are oriented with their anterior to the left. Embryos from successively older stages are shown: stage 6-7 (A, D, G, J), stage 9 (B, E, H, K) and stage 11 (C, F, I, L). Embryos from *ago1*^{K08121}*/CyO; ago2*^{dop1}*/TM3* parents either show a *wild-type wg* expression (A-C) or do not express *wg* correctly (D). *wg* expression is not maintained in older stages (E, F). Most of the embryos from *ago1*^{K08121}*/CyO; ago2*^{51B}*/TM6* do not show any *wg* expression (G-I). *wg* expression was impaired in stage 6 embryos (J) from *ago1*^{K08121}*/CyO; dcr-1*^{Q1147X}*/TM3* parents but was mainly normal in older embryos (K, L).

No Wg protein could be detected in *ago1 ago2* and *ago1 dcr-1* double mutant embryos. Several mechanisms how Wg protein expression might be regulated are possible: (1) *wg* mRNA might not be expressed in the first place. (2) *wg* might be transcribed but not be translated. (3) *wg* mRNA might be instable and therefore insufficient amounts of protein would be made. (4) *wg* mRNA could not be correctly localised; apical localisation of *wg* mRNA is required for correct intracellular Wg signalling activity (Simmonds et al., 2001; Wilkie and Davis, 2001). To discriminate between some of these possibilities, the expression of *wg* mRNA was investigated by in situ hybridisation (Figure 18A-L). In embryos derived from $ago1^{k08121}/CyO$, $ago2^{dop1}/TM3$ heterozygotes *wg* transcripts were detected either in 14 stripes as in *wild-type* embryos (Figure 18A-C) or *wg* transcripts were not correctly localised or maintained (Figure 18D). The maintenance of *wg* expression depends on an intercellular signalling circuit. This circuit involves the interaction of the segment polarity genes *en*, *wg* and *hh*. If one of these genes is absent or not correctly expressed the feedback loop is not maintained. In the absence of *wg* activity the pattern is disturbed. Consistent with the immunostaining for Wg protein, *wg* mRNA expression is absent in many of the embryos derived from $ago1^{k08121}/CyO$, $ago2^{51B}/TM6$ parents (Figure 18G-I). Embryos derived from $ago1^{K08121}/CyO$; $dcr\text{-}1^{Q1147X}/TM6$ parents did not express *wg* mRNA correctly in early gastrula stage embryos. In embryos that displayed a normal gross morphology after gastrulation (stage 9 to stage 11) *wg* mRNA was localised correctly (Figure 18K-L).

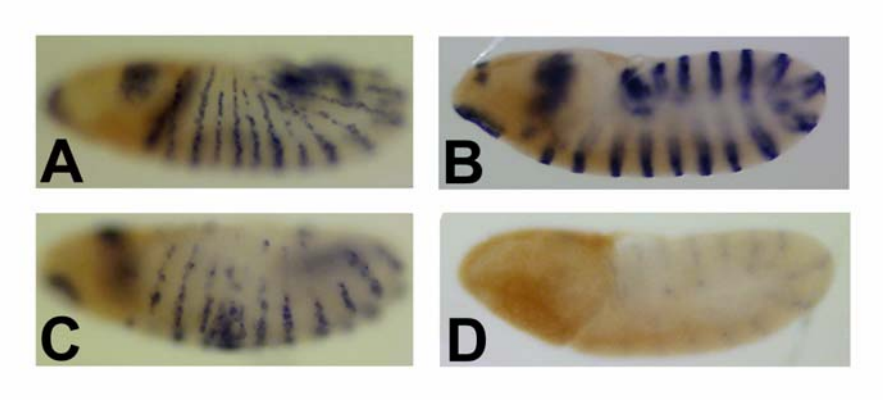

Figure 19: *wg* expression in embryos of $ago1^{K08121}/CyO[hb::lacZ]$; $ago2^{dop1}/TM3[hb::lacZ]$ parents and the presence of balancers

To determine the genotype of the embryos that showed defects in *wg* expression CyO[hb::lacZ] and TM3[hb::lacZ] balancer chromosomes were used. The presence of the [hb::lacZ] transgene on the balancers results in ß-galactosidase expression in the anterior of the embryo (brown staining). Not only embryos showing *wild-type wg* expression showed a brown staining (A, B) but also those embryos where *wg* expression was impaired showed the presence of at least one balancer (C, D).

While the phenotype of the double mutants is very clear, it genotype of the embryos that display segment polarity defects is unclear. One could assume that the embryos were zygotically homozygous mutant for both mutations. To answer this question fly strains were established that contain balancer chromosomes with marked *lacZ* transgenes. Marked balancers have the advantage that they can be visualised by immunocytochemistry and thus embryos carrying one or more balancers can be readily distinguished from the homozygous mutant embryos. In this case embryos carried a balancer that expressed lacZ in the anterior of the embryo under the control of the *hunchback* (*hb*) promoter. In situ hybridisation with anti-sense *wg* RNA probe was repeated and the balancers were visualised by staining with an anti-β-Gal antibody (Figure 19). Both balancer chromosomes, *CyO* and *TM3*, expressed lacZ under the same promoter. Therefore, an identification of the genotype would be possible only if the embryos with abnormal *wg* expression or localisation would be homozygous mutant for both $ago1^{k08121}$ and $ago2^{dop1}$ and therefore the β-Gal staining would be negative. Unexpectedly however, a balancer chromosome was detected in embryos with normal *wg* expression (Figure 19A-B) as well as in embryos were *wg* mRNA localisation was impaired (Figure 19C-D). These results indicate that the phenotype is not only produced by embryos that are zygotically homozygously mutant for both genes. This result suggests that the phenotype might be dependent on the maternal doses of the genes under examination.

Another approach that helps to determine the possible genotype is to examine the ratio of the phenotypic classes of crosses and compare this to the expected Mendelian segregation of the chromosomes. The number of embryos that hatched or displayed cuticles of cuticle classes I-IV were determined (Table 7 and see Figure 10B for cuticle class determination).

Summarising the results for embryos from $ago1^{K08121}$ and *ago2* or $dcr\text{-}1^{Q1147X}$ double mutants, when females were crossed to males of the same genotype, 19 to 27 % of the embryos hatched (Table 7). This result corresponds to the expectations as 25 % of the embryos will have the same genotypes as the parents and therefore should be viable. More than 50 % of the embryos displayed class I cuticles. Within the class I cuticle population most embryos displayed *wild-type* looking cuticles and a little less than the half showed segment polarity defects. All other cuticle classes were represented only by a minor fraction

Table 7: Requirements of *ago1*, *ago2* and *dcr-1* for Segmentation: Distribution of larval cuticle phenotypes

Numbers represent percentages of observed phenotypes; for classification of cuticle phenotypes see Figure 10 and Figure 17. ‘‘normal’’ represents hatching first instar larvae. “variable” means that embryos displayed cuticle phenotypes that were not like *wild-type* but neither belonging to any other class. Embryos are derived from mothers of the indicated genotypes crossed to fathers of the same genotype or to *wild-type*. *ago1* = ago^{K08121}, *dcr-1* = $dcr\text{-}1^{Q1147X}$; *dcr-2* = $dcr\text{-}2^{L811fsX}$

	normal	**Class I**				**Σ Class I**	**Class II**	**Class III**	**Class IV**
	hatched	wt	pair-rule	segment polarity	variable		shield	crumbs	no cuticle
ago1/CyO; ago2^{dop1}/TM3	18,60	24,79	0,00	23,35	7,84	55,97	5,92	4,96	14,55
ago1/CyO; ago2^{51B}/TM6	23,80	31,25	0,00	19,49	5,96	56,71	6,12	5,32	8,05
ago1/CyO; dcr-1/TM6	26,80	26,31	0,41	20,02	6,54	53,27	4,98	3,19	11,76
dcr-2/CyO; dcr-1/TM6	85,80	6,70	0,03	0,40	4,14	11,27	0,97	0,00	1,96
ago1/CyO; ago2^{dop1}/TM3 x w^{1118}	56,75	8,67	2,57	0,00	2,32	13,56	8,15	0,00	21,54
ago1/CyO; ago2^{51B}/TM6 x w^{1118}	49,25	26,54	0,58	0,00	8,42	35,55	3,63	0,00	11,58
ago1/CyO; dcr-1/TM6 x w^{1118}	46,10	27,20	0,83	0,08	9,54	37,65	6,22	0,17	9,87
dcr-2/CyO; dcr-1/TM6 x w^{1118}	80,75	8,09	0,00	0,00	2,43	10,51	0,49	0,00	8,25

of embryos. More than 85 % of the embryos from *dcr-2*^{L811fsX} *dcr-1*^{Q1147X} double mutant parents hatched. As the *dcr-2*^{L811fsX} mutation is homozygous viable this result was expected as well. To find out whether the segment polarity defects are based upon maternal or zygotic effects, mothers were crossed to *wild-type* males (*w*^{1118}). If the segment polarity defect was a maternal effect the phenotype would depend only on the maternally-encoded gene products, i. e. the phenotype depends on the genotype of the mother. The phenotype would arise even if the embryo is heterozygous for the mutation. In contrast, in zygotic mutations the phenotype that arises in the embryo is the result of the embryo's genotype and not the mother's. If segment polarity defects were still observed when mothers were crossed to *wild-type* males, this would mean that segment polarity defects are solely maternal effects. If they are not observed any more demonstrates that segment polarity defects are zygotic or a mixture of both maternal and zygotic defects.

When heterozygous a*go1*^{K08121} and *ago2* or *dcr-1*^{Q1147X} double mutant females were crossed with *wild-type* males only approximately half of the embryos hatched (Table 7). No cuticles showing segment polarity defects were observed from *ago1*^{K08121} and *ago2* double mutant females when crossed to *wild-type* males. Only 13.5 % Embryos from *ago1*^{K08121} and *ago2*^{dop1} females showed Class I cuticles. Most of Class I cuticles displayed a *wild-type* cuticle pattern. Interestingly, a few embryos showed cuticles as they are characteristic for embryos mutant for pair-rule genes. A minor fraction of embryos (0.08 %) from *ago1*^{K08121} and *dcr-1*^{Q1147X} mutant females still displayed segment polarity defects when crossed to *wild-type* males. Cuticle differentiation was hardly altered when *dcr-2*^{L811fsX} *dcr-1*^{Q1147X} double mutant females were crossed with *wild-type* males. In summary, the segment polarity defects do not depend solely on maternal gene products. Taken together, the segment polarity phenotype is a result of maternal and zygotical gene expression defects of the genes under examination.

ago1 and *ago2* interact genetically with each other. The next step was to investigate whether there is biochemical evidence that Ago1 and Ago2 proteins interact with each other. To examine this, a co-immunoprecipitation experiment was performed using *wild-type* embryo protein extracts. Ago2 protein complexes were precipitated with the Ago2$_{Cterm}$ antibody and probed for the presence of Ago1. And indeed, Ago1 could be co-immunoprecipitated with Ago2 protein complexes. Therefore, at least in some cases Ago2 and Ago1 must be present in the same protein complex (Figure 20D). This result supports the result that Ago1 and Ago2 share overlapping functions.

In the last paragraph I presented evidence that the *ago2*^{dop} phenotype results from an impairment of the miRNA mediated RNA silencing pathway rather then from RNAi. To ensure that other components of the miRNA silencing machinery like Ago1, Dcr-1 and

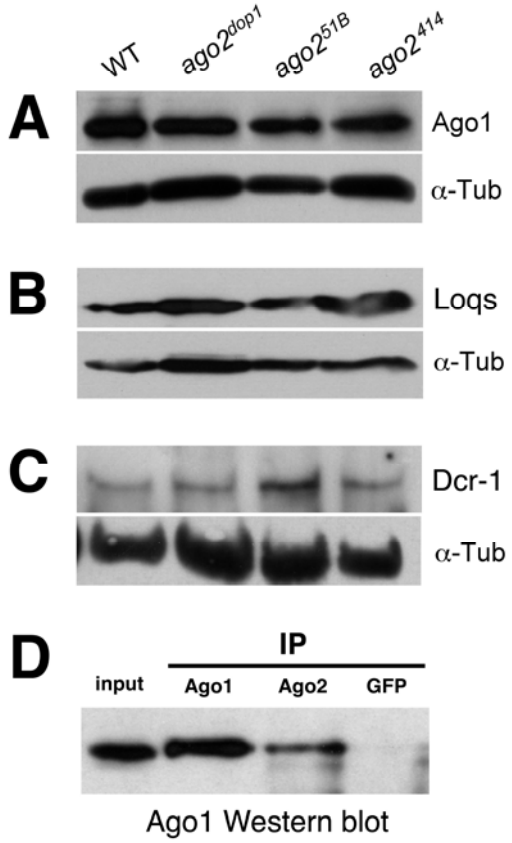

Figure 20: Analysis of protein levels of Ago1, Loqs and Dcr-1 in *ago2* mutants and co-immuno precipitation of Ago1 and Ago2

Western blot using anti Ago1 antibody shows that Ago1 protein level in embryo extracts was very similar in the *wild-type* (w^{1118}), $ago2^{dop1}$, $ago2^{51B}$, and $ago2^{414}$ mutants (A); α-tubulin was used as a loading control. Likewise, the protein levels of Loqs (B) and Dcr-1 (C) are largely unimpaired in extracts from $ago2^{dop1}$, $ago2^{51B}$, and $ago2^{414}$ mutants when compared to the *wild-type* (w^{1118}). In (C) ovary extracts were used instead of embryo extracts. Co-immunoprecipitation experiments of Ago1 with Ago2 showed that Ago1 and Ago2 are present in the same protein complex (D). Ago1 protein in extracts from *wild-type* embryos is shown in the left lane (input). Immunoprecipitations (IP) were performed using anti Ago1 and $Ago2^{Cterm}$ antibodies or with an antibody against GFP as a control; immunoprecipitates were analysed by Western blotting with Ago1 antibodies.

Loquacious (Loqs) were not co-depleted by the *ago2* mutations protein levels of Ago1, Dcr-1 and Loqs were assessed by Western blotting (Figure 20A-C). Loqs is an RNA binding protein and important for Dcr-1 function to process pre-miRNAs and can form a complex with Ago1 and Dcr-1 (Forstemann et al., 2005; Saito et al., 2005). Ago1 protein levels from *wild-type* embryo extracts are very similar to those from $ago2^{dop1}$, $ago2^{51B}$ *and* $ago2^{414}$ mutants (Figure 20). The same is observed for Dcr-1 and Loqs levels. Protein levels were mainly unaffected in *ago2* mutants (Figure 20B, C). Taken together, mutations in *ago2* did not result in an overall change of protein expression of components of the RNAi machinery. It was shown before that $ago2^{dop1}$ does not inhibit the siRNA mediated RNAi but overlaps with *ago1* functions in many aspects. *ago1* has been shown to be essential for miRNA mediated silencing (Okamura et al., 2004). To test whether *ago2* or $ago2^{dop1}$ is involved

directly in miRNA function an eye reporter assay was applied that allows to test the interference of mutations in *ago2* with the function of the *bantam* (*ban*) miRNA. *ban* negatively regulates the expression of the pro-apoptotic regulator Hid by binding to *hid* mRNA 3' UTR and inhibiting its translation (Brennecke et al., 2003). If *hid* is ectopically

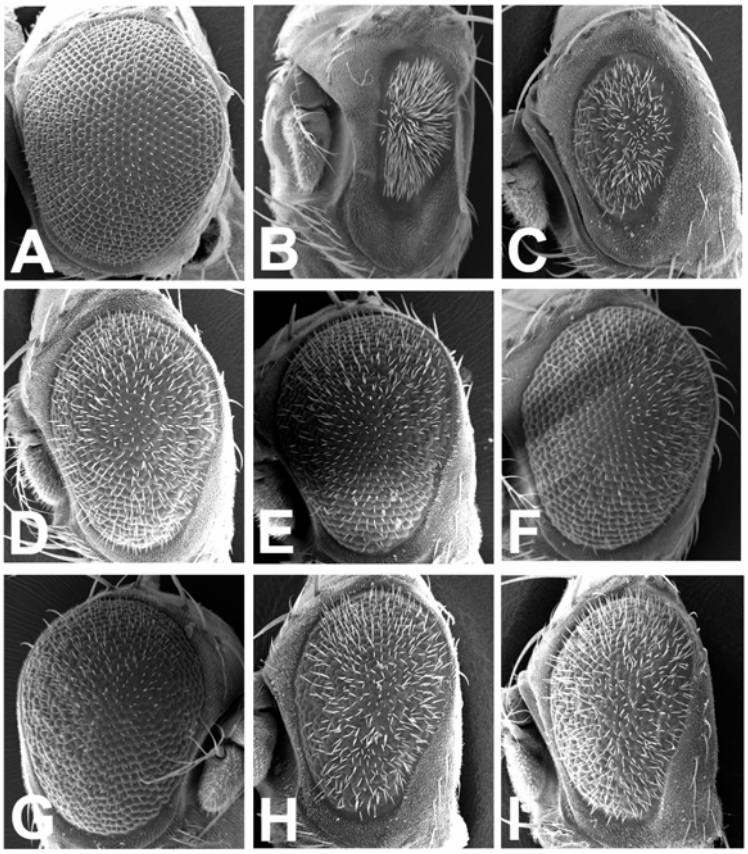

Figure 21: The *ago2^{dop1}* mutation does not interfere with the activity of the miRNA *bantam* (*ban*)

An eye-based reporter assay for the function of *ban* was performed. *ban* negatively regulates the expression of the pro-apoptotic regulator Hid (Brennecke et al., 2003). Expression of *ban* in the eye using *GMR::Gal4* does not grossly affect eye development (A, *GMR::GAL4/+; ban^{EP3622}ago2^{dop1}/ ban^{EP3622}ago2^{dop1}*). Expression of *GMR::hid* induces cell death in the retina and thus results in a strongly reduced eye size (B, *GMR::GAL4/GMR::hid; ago2^{dop1}/TM6*). This phenotype is only slightly suppressed by the EP insertion *ban^{EP3266}* alone (C, *GMR::hid/+; ban^{EP3622}ago2^{dop1}/ ban^{EP3622}ago2^{dop1}*) but strongly suppressed by overexpression of *ban^{EP3266}* using *GMR::Gal4* (D, *GMR::GAL4/GMR::hid; ban^{EP3622}/ MKRS*). To test interference of *ago2^{dop1}* with *ban* activity, the same experiment in *ago2^{dop1}* heterozygous (E; *GMR::GAL4/GMR::hid; ban^{EP3622}ago2^{dop1}/TM6*), *ago2^{dop1}* homozygous (F, *GMR::GAL4/GMR::hid; ban^{EP3622}ago2^{dop1}/ ban^{EP3622}ago2^{dop1}*) or *ago2^{dop1}* hemizygous (G, *GMR::GAL4/GMR::hid; ban^{EP3622}ago2^{dop1}/ ban^{EP3622}Df(3L)XG9*) genetic backgrounds was done. In neither case a suppression of *ban* activity could be detected, which should result in a reversion to the *GMR::hid* phenotype and produce a strong reduction of the size of the eye. In an *ago2^{51B}* homozygous background (I, *GMR::GAL4/GMR::hid; ban^{EP3622}ago2^{51B}/ ban^{EP3622}ago2^{51B}*), activity of *ban* seems to be slightly reduced: in the presence of two copies of *ban^{EP3266}* the size of the eye is considerably smaller as compared to *ago2^{51B}* heterozygotes (H, *GMR::GAL4/GMR::hid; ban^{EP3622}ago2^{51B}/MKRS*), which contain only one copy of *ban^{EP3266}*. *TM6* and *MKRS* correspond to balancer chromosomes.

expressed in the eye, it will induce cell death and the size of the eye will be strongly reduced (Figure 21B). When *ban* is expressed together with *hid* in the eye, the reduced eye phenotype was strongly suppressed (Figure 21D). If *ago2^{dop1}* would interfere with *ban* miRNA function, the described suppression of the Hid phenotype is reverted to the reduced eye phenotype. However, in heterozygous, homozygous or hemizygous *ago2^{dop1}* mutants *ban* function was not reduced, if an effect was observed at all, *ban* function appeared to be slightly enhanced (Figure 21E-G). In contrast, in an *ago2^{51B}* homozygous background (Figure 21I) activity of *ban* seems to be slightly reduced: in the presence of two copies of overexpressed *ban* the size of the eye is considerably smaller than compared to *ago2^{51B}* heterozygotes with only one copy of overexpressed bantam (Figure 21H).
In summary this assay did not reveal an involvement of *ago2* for miRNA function. One reason for the outcome of this experiment could be the redundancy of Ago1 and Ago2.

3.8 The microRNA *miR-9a*

Using the *bantam* miRNA eye based reporter assay it was not possible to show a direct involvement of *ago2* in miRNA mediated silencing. It was recently reported that embryos depleted for the miRNA *miR-9a* rarely form any cuticle and do not show much internal differentiation. Furthermore, those embryos show defects in pole cell formation, cellularisation and basal movement of lipid droplets (Leaman et al., 2005). These data suggest that embryos depleted for *miR-9a* might display a very similar phenotype as *ago2^{dop1}* mutant embryos. It might therefore be possible that *miR-9a* is necessary for morphogenetic processes at MBT and that the function of *miR-9a* is impaired or reduced in *ago2^{dop1}* mutant embryos. To test this hypothesis it was examined whether *miR-9a* overexpression could rescue the *ago2^{dop1}* phenotype. *miR-9a* was overexpressed using the *GAL4/UAS* system. The experimental design allowed maternal expression of *GAL4*, which then becomes active in transcription in the zygote. Both cellularisation and lethality of *ago2^{dop1}* embryos were rescued by the zygotic overexpression of *miR-9a* (Figure 22). Cellularisation occurred as in *wild-type* embryos (Figure 22A). About 15 % of *ago2^{dop1}* embryos were rescued to hatching first instar larvae (Figure 22B). This is a much better rescue compared to the zygotic rescue overexpressing *ago1* or *ago2* (Figure 16B). Most of the embryos that did not hatch failed to form any cuticle (more then 75 % were class I cuticle, Figure 22B). This result indicates that *miR-9a* levels might be critical for embryonic

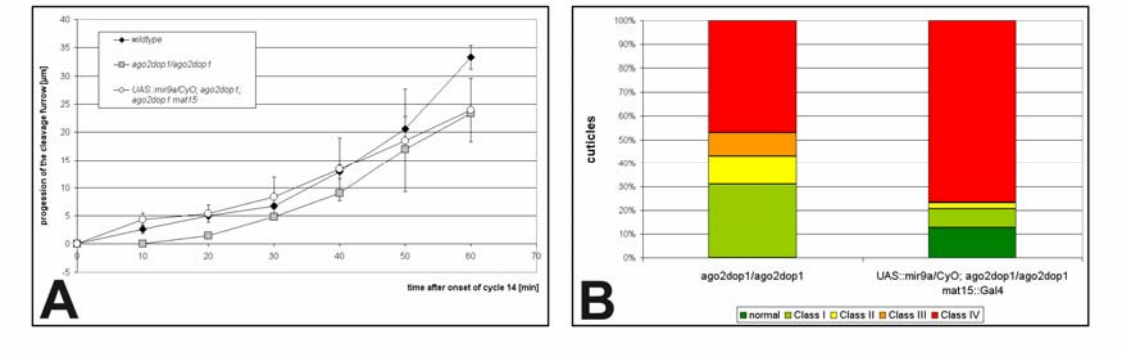

Figure 22: Overexpression of the miRNA *miR-9a* rescues the *ago2^{dop1}* mutation phenotype

The zygotic overexpression of the miRNA *miR-9a* (Leaman et al., 2005) rescues the *ago2^{dop1}* cellularisation phenotype (A). *miR-9a* was overexpressed using the *GAL4/UAS* system. The experimental design allowed maternal expression of *GAL4*, which then becomes active in transcription in the zygote. The progression of the cleavage furrow during slow phase of cellularisation is reduced in embryos from *ago2^{dop1}* mutant mothers (grey casket, A) in comparison to *wild-type* (black diamonds, A). Embryos overexpressing *mir9a* zygotically in an *ago2^{dop1}* mutant background (white circle, A) show a strong rescue of this phenotype. 15 % of these embryos are rescued to hatching first instar larvae ("normal", A). Class I (continuous cuticle), Class II (shield), Class III (crumbs-like), Class IV (no cuticle).

development, e.g. timing of *miR-9a* expression and/or *miR-9a* expression levels might be important for development.

These results allow the conclusion that *ago2* might be required for the function of *miR-9a*. Whether and to what extend *ago2* is involved in general in miRNA function needs to determined in the future.

3.9 Novel functions for *piwi* and *aub* during embryogenesis

The *Drosophila* genome encodes five Argonaute family proteins four of which have been characterised: Ago1, Ago2, Piwi and Aubergine (Aub). Piwi is required for the maintenance of germ-line stem cells and for post-transcriptional silencing within somatic cells (Cox et al., 1998; Pal-Bhadra et al., 2002). Aub is required for the RNAi-like silencing of the *Stellate* locus in testes which is essential for male fertility. As well, Aub is necessary for activation of *oskar* translation, a process that is essential for the organisation of the pole plasm (Aravin et al., 2001). Aub is required for germ-line RNAi (Kennerdell et al., 2002). So except for Ago3, which has not been characterised yet, all *Drosophila* Argonaute family members have been shown to function in RNA silencing. In the last section the novel interaction between *ago2* and *ago1* was shown. In *Drosophila ago1* and *ago2* have been assigned strictly to miRNA and siRNA mediated silencing, respectively. The finding that *ago1* and

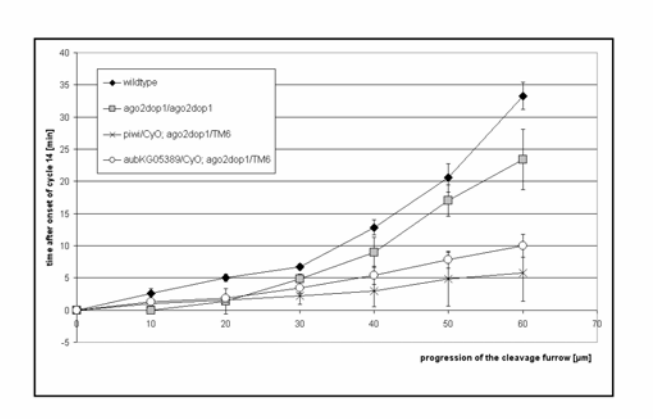

Figure 23: Genetic interaction of *piwi* and *aub* with *ago2^{dop1}*

The reduction of *piwi* or *aub* gene doses enhances the *ago2^{dop1}* cellularisation phenotype. The progression of the cleavage furrow during cellularisation is reduced in embryos from *ago2^{dop1}* mutant mothers (grey casket) in comparison to *wild-type* (black diamonds). Embryos from *P(PZ)piwi^{06843}/CyO; ago2^{dop1}/ago2^{dop1}* mutants (black crosses) or from *P(SUPor-P)aub^{KG05389}/CyO; ago2^{dop1}/ago2^{dop1}* mutants (white circles) show a strongly reduced furrow progression even during fast phase. The phenotype is more severe in *piwi ago2^{dop1}* than in *aub ago2^{dop1}* double mutants.

ago2 do interact with each other shows that miRNA mediated silencing pathway might be more complicated and divergent as previously believed.

Thus, a remodelling of the miRNA and siRNA silencing pathways is required. Also the observation raises the question whether other Argonaute proteins interact with Ago2. Is the interaction between the Argonaute protein family members *ago1* and *ago2* restricted to these two genes or do the genes of this family interact with each other more generally?

To investigate to what extend *ago2* interacts with *piwi* and *aub*, double mutants were created. *piwi ago2^{dop1}* and *aub ago2^{dop1}* were examined for their impact on cellularisation. In *ago2^{dop1}* homozygous embryos with a reduced *piwi* or *aub* activity the cellularisation phenotype was enhanced significantly (Figure 23). The progression of the cleavage furrow was strongly reduced during slow phase as it was already observed for *ago2^{dop1}* embryos with reduced *ago1* activity. But the effects of reduced *piwi* or *aub* activity on cellularisation are not identical and can be distinguished. In *ago2^{dop1}* embryos with reduced *piwi* activity cellularisation occurred very similar to *ago2^{dop1}* embryos with a reduced *ago1* activity (Figure 16A). *ago2^{dop1}* embryos with reduced *aub* activity showed an enhanced cellularisation defect but the enhancement was milder than that of *ago2^{dop1}* embryos with reduced *piwi* activity. Summarising the observations not only *ago1* but also *piwi* and *aub* are required for MBT.

Again, the question arose whether the interaction between *ago2^{dop1}* and *piwi* and *aub* respectively is specific to the *ago2^{dop1}* allele. Do *piwi* and *aub* as well have a function in

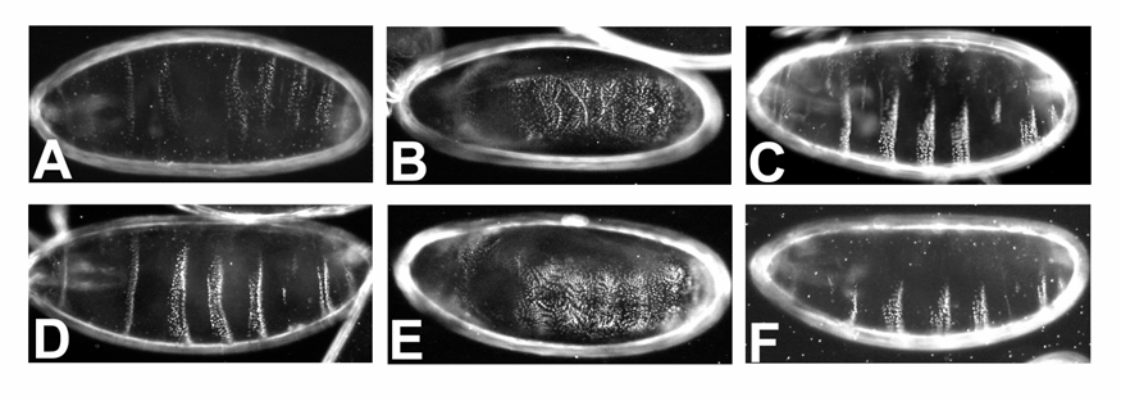

Figure 24: Requirements of *piwi*, *aub*, *ago2* and *dcr-1* for Segmentation

Segmentation defects in double mutant embryos of the following genotypes are evident in alterations of the larval cuticle (A–F). Parents of the indicated genotypes were mated and the cuticles of those embryos that failed to hatch were examined. All embryos are oriented with their anterior to the left. Embryos from *P(PZ)piwi*^{06843}*/CyO; ago2*^{51B}*/TM6* (B) and *P(SUPor-P)aub*^{KG05389}*/CyO; ago2*^{51B}*/TM6* (E) parents exhibit a lawn of denticles indicative of a defect in establishing segment polarity. Embryos from parents *P(PZ)piwi*^{06843}*/CyO; ago2*^{dop1}*/TM6* show cuticles of an irregular pattern (A). Embryos from *P(PZ)piwi*^{06843}*/CyO; dcr-1*^{Q1147X} */TM6* (C), *P(SUPor-P)aub*^{KG05389}*/CyO; ago2*^{dop1}*/TM6* (D) or *P(SUPor-P)aub*^{KG05389}*/CyO; dcr-1*^{Q1147X}*/TM6* (F) parents developed a continuous cuticle with posterior stripes missing. Normal cuticle differentiation is shown in Figure 17A: embryos from *dcr-2*^{L811fsX}*/dcr-2*^{L811fsX}*; dcr-1*^{Q1147X}*/TM6* parents.

miRNA mediated RNA silencing? Such a model was recently proposed for Piwi by Megosh and colleagues who could show that Piwi interacts with Dcr-1 but not with Dcr-2 (Megosh et al., 2006). Because the interaction between *ago1*, *ago2*^{dop1}, *ago2*^{51B} and *dcr-1* exhibited a requirement of Argonaute proteins for segment polarity, cuticle differentiation was analysed from embryos of double mutant heterozygous parents (*P(PZ)piwi*^{06843} or *P(SUPor-P)aub*^{KG05389} in combination with *ago2*^{dop1}, *ago2*^{51B} or *dcr-1*^{Q1147X}. Though *piwi* and *aub* levels had a significant impact on cellularisation in *ago2*^{dop1} mutants cuticle formation was only mildly affected in *piwi ago2*^{dop1} or in *aub ago2*^{dop1} zygotic double mutants (Figure 24A, D). None of these embryos exhibited the strong segment polarity defects as they were observed in *ago1 ago2* or *ago1 dcr-1* double mutants. The denticle bands were present in an irregular pattern in embryos derived from *P(PZ)piwi*^{06843}*/CyO; ago2*^{dop1}*/TM6* parents (Figure 24A).The sixth thoracic denticle band was often missing in embryos from *P(SUPor-P)aub*^{KG05389}*/CyO; ago2*^{dop1}*/TM6* parents (Figure 24D). A very similar cuticle pattern

Table 8: Requirements of *piwi*, *aub*, *ago2* and *dcr-1* for Segmentation: Distribution of larval cuticle phenotypes

Numbers represent percentages of observed phenotypes; for classification of cuticle phenotypes see Figure 10 and Figure 17. ‘‘normal’’ represents hatching first instar larvae. Embryos are derived from mothers of the indicated genotypes crossed to fathers of the same genotype. *piwi* = *P(PZ)piwi*^{06843}, *aub* = *P(SUPor-P)aub*^{KG05389}, *dcr-1* = *dcr-1*^{Q1147X}

	normal	**Class I**				**Σ Class I**	**Class II**	**Class III**	**Class IV**
	hatched	wt	pair-rule	segment pol	n.d.		shield	crumbs	no
piwi/CyO; ago2^{dop1}/TM6	14,25	37,97	0,43	0,00	5,97	44,37	8,96	0,00	5,97
piwi/CyO; ago2^{51B}/TM6	28,50	21,96	1,17	17,99	6,08	47,20	5,61	0,00	6,08
piwi/CyO; dcr-1/TM6	17,75	50,90	0,16	0,00	12,12	63,18	3,88	0,16	12,12
aub/CyO; ago2^{dop1}/TM6	31,25	22,39	0,00	0,00	19,02	41,41	6,54	0,00	19,02
aub/CyO; ago2^{51B}/TM6	27,50	22,90	0,87	23,01	9,88	56,65	5,54	0,33	9,88
aub/CyO; dcr-1/TM6	31,00	33,31	0,00	0,00	15,78	49,09	4,90	0,00	15,78

exhibited cuticles derived from*P(PZ)piwi*^{06843}*/CyO; dcr-1*^{Q1147X} */TM6* or*P(PZ)piwi*^{06843}*/CyO; dcr-1*^{Q1147X} */TM6* parents (Figure 24C, F).

In contrast, *piwi ago2*^{51B} and *aub ago2*^{51B} double mutant embryos did show segment polarity defects. 18 % of the embryos derived from *P(PZ)piwi*^{06843}*/CyO; ago2*^{51B}*/TM6* as well as 23 % from *P(SUPor-P)aub*^{KG05389}*/CyO; ago2*^{51B}*/TM6* parents exhibited a lawn of denticle bands as observed in *ago1 ago2* or *ago1 dcr-1* double mutants (Figure 24B, E; Table 8). A minor fraction of these embryos exhibited a pair-rule cuticle phenotype (Table 8).

To find out the molecular bases for the segmentation defects, the distribution of En and Wg protein was investigated in zygotic *piwi ago2*^{51B} and *aub ago2*^{51B} double mutants (Figure 25A-F). In both cases Wg was either not expressed (Figure 25B, C') or in embryos from *aub ago2*^{51B} heterozygous parents the 14 Wg stripes were not evenly arranged. Instead

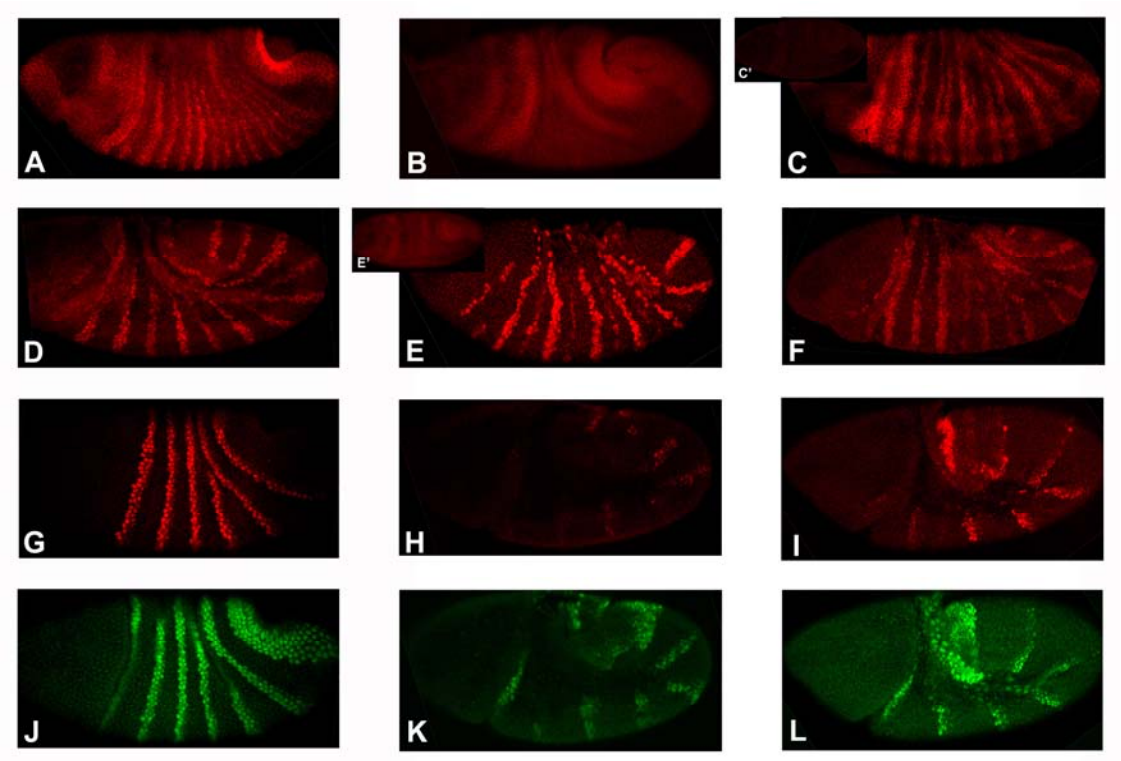

Figure 25: Requirements of *piwi*, *aub* and *ago2*^{short} for segmentation

Immunolabelling of Wg (A-C), En (D-F), Eve (G-I) and Ftz (J-L) proteins in stage 7 (A-G, J) or stage 9 embryos (H, I, K, L). All embryos are orientated with the anterior to the left. Embryos from *P(SUPor-P)aub*^{KG05389}*/CyO; ago2*^{51B}*/TM6* parents either showed a *wild-type* expression of the proteins (A, D, G, J) or showed different defects (C, F, I, L). Very similar defects were observed in embryos from *P(PZ)piwi*^{06843}*/CyO; ago2*^{dop1}*/TM6* parents (B, E, H, K). In both *ago2*^{51B} double mutant cases Wg was either not established (B, C') or the 14 stripes were not evenly arranged in *aub ago2*^{51B} double mutants (C). In *piwi ago2*^{51B} double mutants En is either completely absent (E') or not maintained (E). Every second (even) of the 14 En stripes is disappearing. In embryos from *P(SUPor-P)aub*^{KG05389}*/CyO; ago2*^{51B}*/TM6* parents En stripes are not evenly expressed (F). The pair-rule proteins Eve and Ftz are still present in stage 9 embryos from *P(PZ)piwi*^{06843}*/CyO; ago2*^{dop1}*/TM6* (H, K). Even more Eve and Ftz protein is present in stage 9 embryos from *P(SUPor-P)aub*^{KG05389}*/CyO; ago2*^{51B}*/TM6* parents (K, L).

they were rather grouped into pairs (Figure 25C). In mutant embryos from *piwi ago2*^{51B} heterozygous parents En was either not expressed at all (Figure 25E') or not maintained in the even stripes (Figure 25E). The En protein expression pattern was disturbed in mutant embryos from *aub ago2*^{51B} parents (Figure 25F). The embryos exhibited different phenotypic classes: not only the complete loss of Wg and En protein expression but also an irregular arrangement of the 14 Wg or En stripes was observed. The *en* gene is only expressed in those cells that express high levels of the pair-rule genes *even-skipped* (eve) or *fushi-tarazu* (*ftz*). Because an irregular arrangement of the En pattern was observed it was likely that pair-rule gene expression was already impaired. Therefore protein expression of the pair-rule genes *eve* and *ftz* were investigated by immunocytochemistry. In late stage 6 embryos Eve and Ftz proteins are expressed in seven alternating stripes (Frasch et al., 1987). In embryos that have completed germ band elongation Eve is only expressed near the posterior end of the germ band and the original pair-rule expression pattern is no longer seen (Frasch et al., 1987). *ftz* was also expressed only until stage 9 (http://www.flyexpress.net/). In embryos from *piwi ago2*^{51B} and *aub ago2*^{51B} heterozygous mutant parents Eve and Ftz were correctly localised in stage 6 and 7 embryos (Figure 25G, J). But looking at stage 9 embryos, where Eve and Ftz expression are not detectable in *wild-type*, some Eve and more clearly Ftz protein expression remained (Figure 25H, I, K, L). Summarising the results, the pair-rule proteins Eve and Ftz were initially expressed and localised normally in stage 6 and 7 embryos from heterozygous *piwi ago2*^{51B} or *aub ago2*^{51B} zygotic double mutants. Later Eve and Ftz failed to be degraded and expression remained beyond stage 9 embryos. Consequently, the segment polarity proteins En and Wg were not correctly localised.

These observations suggest that *piwi* and *aub* interfere with *ago2*'s function in segment polarity. Interestingly, the observations indicate that *ago2*^{long} is required for segment polarity as only *piwi ago2*^{51B} and *aub ago2*^{51B} double mutants displayed segment polarity defects but not *piwi ago2*^{dop1} and *aub ago2*^{dop1} double mutant embryos. This observation resumes the discussion about how the GRRs contribute to Ago2's function. Furthermore it might indicate that different Ago2 isoforms contribute to different functions of Ago2 at distinct developmental stages. This hypothesis will be addressed in the discussion.

4 Discussion

In *Drosophila* different RNA silencing pathways have been identified. RNA silencing is triggered by small RNAs. They are named siRNAs, miRNAs or rasiRNA and are processed from distinct dsRNAs precursors. In contrast to other model organisms, there has been some evidence that siRNA and miRNA mediated silencing pathways are two biochemically distinct pathways in *Drosophila.* Different Dicer and Argonaute proteins function in distinct pathways. Dcr-1 is required for miRNA processing while Dcr-2 is necessary for processing siRNAs from long dsRNAs (Lee et al., 2004b). The same was reported for Argonaute proteins: Ago1 but not Ago2 is required for miRNA accumulation. Ago2 is required for siRNA triggered RNA silencing while Ago1 is dispensable (Okamura et al., 2004). A possible redundancy between different Argonaute or Dicer proteins has not been addressed. Furthermore, the mutations in the respective genes exhibit distinct features. Dcr-2 and Ago2 null mutants were reported to be viable and fertile, while homozygous Dcr-1 and Ago1 mutations cause embryonic lethality (Kataoka et al., 2001; Lee et al., 2004b; Okamura et al., 2004; Xu et al., 2004). On the other hand it was shown that siRNA and miRNA differ only from the origin, that they are processed from, but that they do not differ in their function (Tomari and Zamore, 2005). There is also evidence that components from the miRNA silencing pathways co-precipitated with components of the siRNA mediated silencing pathway (Caudy et al., 2002). Furthermore, *ago1* mutants show a reduced response to siRNA mediated silencing (Williams and Rubin, 2002). And very recent data from Rehwinkel and colleagues showed that some miRNA targets are also regulated by Ago2. In addition this group could show that both Ago1 and Ago2 silence expression of a common set of mobile genetic elements (Rehwinkel et al., 2006). These studies raise the question, whether miRNA and siRNA silencing pathways are really as distinct as previously thought (see Figure 6). To what extend do the components of these two pathways interact with each other and with other members of the Argonaute protein family? The analysis of the *ago2*^{dop1} allele revealed new interactions not only between miRNA and siRNA mediated silencing but also between Ago2 and Piwi and Aub respectively. In the following the functional implication of these novel interactions of *ago2*^{dop1} is discussed with respect to a novel function of *ago2* as a key regulator of *Drosophila* development.

4.1 *ago2* and its GRRs

4.1.1 The *ago2^{dop1}* mutation

This work identified the maternal effect mutation *dop* as a novel allele of the *Drosophila argonaute2* gene (*ago2*). *ago2^{dop1}* mutant embryos show distinct phenotypes during early embryogenesis affecting cellularisation, lipid droplet transport and establishment of tissue polarity as shown in this thesis. Membrane insertion during slow phase of cellularisation is strongly reduced in *ago2^{dop1}* mutant embryos. Maternally provided *ago2* in *ago2^{dop1}* embryos not only accelerated membrane formation to a normal speed during slow phase but also rescued embryos to hatching larvae and even to adult flies. This shows unequivocally that *ago2* function is impaired in *ago2^{dop1}* mutants. The *Drosophila* Ago2 protein contains a PAZ and a PIWI domain that are conserved in Argonaute family members. In addition *Drosophila* Ago2 contains two glutamine rich repeats (GRRs) of unknown function at its amino-terminus. This work shows that GRRs in Ago2 are conserved not only among *Drosophila* species but also in other insects like the malaria mosquito *Anopheles gambia*, honey bee *Apis melifera* and yellow fever mosquito *Aedes aegypti*. The number of GRR within *Drosophila* Ago2 seems to be of high relevance for its function during embryogenesis. This view is supported by the finding that two individual *ago2* mutants identified in this work, namely *ago2^{dop1}* and *ago2^{dop46},* show an altered number of GRR, resulting in a strikingly similar phenotype. Both, *ago2^{dop1}* and *ago2^{dop46}* homozygous individuals show defects at MBT as well as female sterility but hardly impair Ago2's function in siRNA triggered silencing. Sequencing of the mutant ago2^{dop} alleles revealed that a 69 nt deletion in *ago2^{dop1}* leads to a loss of exactly one repeat in the amino-terminal GRR2 domain. The *ago2^{dop46}* mutation contains an 18 nt deletion that leads to the loss of exactly one repeat in GRR1. These observations allow the conclusion that a minimum number of GRR is essential for Ago2's function at the MBT. The functional importance of GRRs with respect to Ago2 function is discussed in the following paragraph.

4.1.2 Identification of a novel *ago2* isoform: *ago2^{short}*

The *ago2^{dop}* mutations analysed in this thesis lead to striking defects at MBT and female sterility. These results clearly show that Ago2 function is essential for embryonic development. In contrast, the development was normal in reported *ago2* null mutants *ago2^{51B}* and *ago2^{414}* was observed as undistinguishable from *wild-type*. However, *ago2^{51B}* and *ago2^{414}* are not functional in RNAi and lack the antiviral immune defence mechanism (Okamura et al., 2004; van Rij et al., 2006; Wang et al., 2006; Xu et al., 2004; Zambon et al., 2006). One explanation for these obviously contradicting observations might be the

presence of multiple Ago2 isoforms. The *ago2*^{dop} mutations might only affect one isoform while it might not affect the other. One would then predict that different Ago2 isoforms have mutually exclusive functions in RNAi on the one hand and MBT and fertility on the other hand.

The hypothesis that *ago2* is transcribed in multiple isoforms is supported by this work suggesting that *ago2*^{51B} and *ago2*^{414} indeed do not represent *ago2* null alleles: (1) Transheterozygous *ago2*^{dop1}/*ago2*^{51B} embryos do not show the same defects as *ago2*^{dop1} homo- or hemizygous embryos and hatch without cellularisation defects. Thus *ago2*^{51B} fully complements *ago2*^{dop1}. (2) Semi-quantitative RT-PCR experiments confirmed that *ago2* mRNA is transcribed in the *ago2*^{51B} and *ago2*^{414} homozygous mutant situation. Interestingly, a promoter prediction analysis reveals an alternate promoter 40 bp 5' of the third exon that might give rise to the short new *ago2* isoform additional to the *ago2-RB* or *ago2-RC* isoforms known so far. This *ago2* isoform will be referred to as *ago2*^{short}. To confirm the existence of the short *ago2* transcript an RT-PCR analysis should be performed using a forward primer that is located on the TSS. As the TSS is 40 bp upstream of the third exon outside the *ago2-RB* or *ago2-RC* transcript it would amplify only the *ago2*^{short} transcript. This would demonstrate that there would be transcript synthesised from the *ago2* locus by this promoter.

However, northern blot results are not consistent with the RT-PCR results. Surprisingly, Northern blot analysis did not confirm the existence of the *ago2*^{short} transcript neither in *wild-type* nor in *ago2*^{dop1} or in *ago2*^{51B}. Two possibilities could explain the absence of *ago2*^{short} on Northern blot analysis: The *ago2*^{short} transcript could be either very instable or is only produced in a low ratio. To test which of the two possibilities might result in the low expression of *ago2*^{short} I suggest two experiments: To quantify *ago2* transcription levels quantitative real time PCR could be performed. qRT-PCR is a very efficient and reliable method to detect transcripts even in a low abundance. On the other hand, if the mechanisms of *ago2*^{short} transcript degradation were known, one cold achieve stabilisation by introducing a genetic mutation that abolishes transcript degradation. Furthermore, Ago2 antibodies did detect protein in *ago2*^{51B} and *ago2*^{414} (Figure 28). Additionally it would be worthwhile to check, whether different *ago2* isoforms are expressed in different tissues or at different developmental stages only. However, a reliable, functional, good Ago2 antibody would finally clarify the existence of the Ago2^{short} protein.

4.1.3 Genetics of *ago2*^{long}, *ago2*^{short} and *ago2*^{dop1}

This work presents the observation that *ago2* is transcribed in multiple isoforms and that individual transcripts are affected by *ago2*^{dop} mutations. One observation is difficult to interpret: Why do small alterations in Ago2's GRRs have such a strong impact on

embryonic development, if the complete loss of Ago2^{long} allows embryos to develop normal? These findings lead to the hypothesis that the *ago2* isoforms, either with and without GRRs, have mutually exclusive functions in RNAi and MBT. One obvious question that arises from this hypothesis is: What could be the function of the GRRs?

It was reported that glutamine rich domains of proteins exhibit prion behaviour in yeast. These regions do not share sequence homologies to each other (Tuite, 2000). Characteristic is that these regions often do not form any secondary structure which is an indication of conformational flexibility that probably relates to their ability to switch states from a cellular to prion form. The loss-of-function phenotypes caused by yeast prions are dominant rather than recessive. Furthermore prions can form aggregates and can be inherited in a non-Mendelian manner. Prion-like properties were as well reported for the translational factor CPEB in *Aplysia*. Interestingly, the aggregated CPEB form induces translation more efficiently (Si et al., 2003; Tuite, 2000). Taken together the GRR could be responsible for keeping regulatory proteins in a certain state and/or regulate their binding affinity. This would allow the conclusion that the reduced GRR number in Ago2^{dop1} could negatively interfere with Ago2's binding ability or activity, both of which would compromise Ago2's function. This work provides genetic evidence that loss of one GRR in Ago2^{dop1} leads to a dominant Ago2 form that seems to interfere with the function of Ago2^{short}. Correct

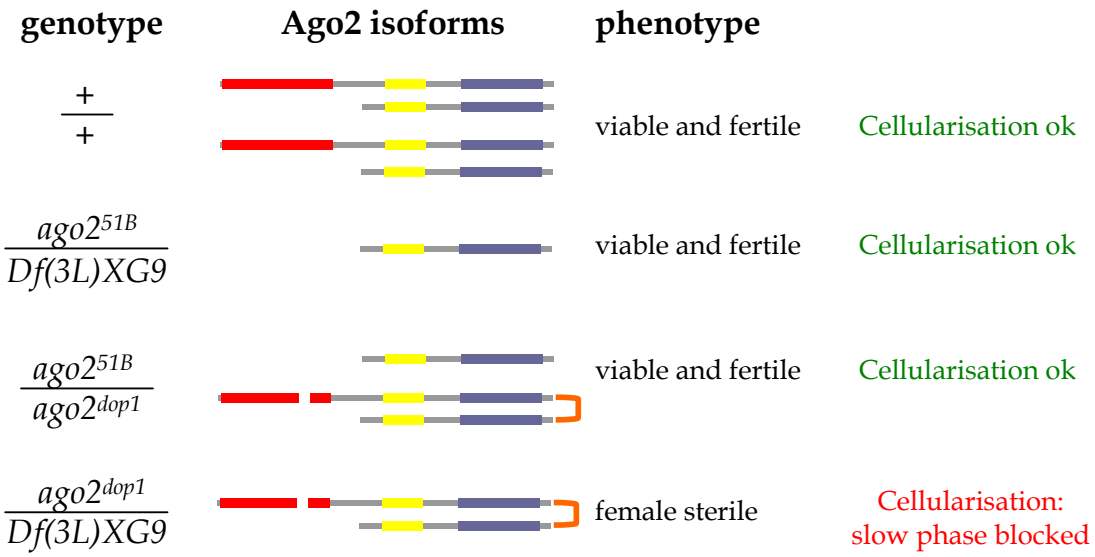

Figure 26: Model for *ago2^{dop1}* as an antimorphic mutation

The female sterility and cellularisation phenotype could result from a negative interference between Ago2^{dop1} and Ago2^{short}. The *ago2^{dop1}* phenotype would be a consequence of the availability of *ago2^{short}*. This model explains why *ago2^{dop1}/ago2^{51B}* transheterozygous and *ago2^{51B}* hemizygous flies are fertile and why their embryos develop normally.

cellularisation seems to be dependent on the availability of Ago2^{short} as proposed by the following model (Figure 26): In a *wild-type* situation the cell produces two copies Ago2^{full} as well as two copies of Ago2^{short} and therefore does not exhibit any phenotype. In hemizygous *ago2^{51B}* flies Ago2^{long} is absent but one copy of Ago2^{short} is available which is sufficient for fly development. The same applies to transheterozygous *ago2^{dop1}/ago2^{51B}* flies. In contrast neither in *ago2^{dop1}* homozygous (not shown) nor *ago2^{dop1}* hemizygous flies free Ago2^{short} is available (Figure 26). Here all available Ago2^{short} might be titrated out by Ago2^{dop1} and therefore Ago2^{short} cannot function. This results in cellularisation defects and female sterility.

4.1.4 Functions of GRRs for miRNA mediated silencing

In the last paragraph I discussed the importance of GRRs for Ago2's function by the means of the correct number of GRRs. The question that I would like to discuss now is whether GRRs are of general importance for Ago2's function. Several possibilities how GRR contribute to Ago2's function are likely: as mentioned in the last paragraph the GRRs could keep Ago2 at a certain activity state. On the other hand GRRs could be important for subcellular localisation of Ago2. A combination of both functions is possible as well. The immunolabelling of Ago2 using two different Ago2 antibodies (Ago2$_{Cterm}$ and Ago2$_{Nterm}$) in early embryos showed a dotty staining pattern (Suppl. Figure 28). This indicates that Ago2^{long} might form aggregates or might be recruited to distinct subcellular compartments. It seems that some of the dots are slightly bigger in *ago2^{dop1}* embryos than in *wild-type*. Those dots are located more in the yolk than at the cortex of the embryo. These observations indicate either that the modified GRR in *ago2^{dop1}* embryos enhances its ability to form aggregates or that Ago2^{dop1} has a higher ability to be localised to a subcellular compartment. As the Ago2$_{Nterm}$ antibody would only recognise Ago2^{long} but not Ago2^{short} (the peptides that the antibodies were raised against are indicated in Figure 27) it would be a worthwhile experiment to repeat these stainings with *ago2^{51B}* and *ago2^{414}* embryos.

A different approach to study the behaviour of Ago2^{long}, Ago2^{dop1} and Ago2^{short} would be to work with tagged transgenes. If tagged transgenes would be expressed maternally one could study the localisation in the early embryo. Additionally, working with tagged Ago2 would allow biochemical approaches like Western blots and co-immunoprecipitations. This could eventually clarify which of the bands that were detected by different Ago2 antibodies corresponds to which isoform. Additionally, co-immunoprecipitations could show biochemically whether Ago2^{dop1} and Ago2^{short} bind to each other.

This work presents the possibility that Ago2 forms aggregates or is located in subcellular compartments. It was published recently that mammalian Argonaute proteins (Ago1 and Ago2) localise in GW bodies (Liu et al., 2005). GW bodies are cytoplasmic processing bodies, also known as P-bodies that concentrate enzymes involved in mRNA turnover. It

was shown that endogenous or exogenous miRNAs became concentrated in GW bodies in a miRNA dependent manner (Rehwinkel et al., 2005). Furthermore, central components of GW bodies like GW182 and decapping enzymes DCP1:DCP2, have been shown to be involved in miRNA-mediated gene silencing in *Drosophila* cultured cells (Rehwinkel et al., 2005). It might be possible that *Drosophila* Ago2 localises to GW bodies as well, as Ago2 immunolabelling showed a dot-like pattern. To test whether Ago2 localises in GW bodies an antibody staining using Ago2 and GW182 antibodies should be done. If both proteins would overlay it would show that Ago2 is present in GW bodies. One could also use immunoprecipitation of tagged Ago2 isoforms to test for binding of Ago2 to GW body components, too. To reveal the molecular function of Ago2's GRR domain it will be necessary to determine whether the *ago2*^{dop} alleles alter the recruitment of Ago2 to particular cytoplasmic mRNA degradation complexes and whether Ago2^{short} is recruited there at all. However, these data clearly point out that Ago2's GRRs of great importance for Ago2's function.

4.2 *ago2* and RNA mediated silencing

4.2.1 Ago2 functions in miRNA mediated RNAi

To date it is not clear how GRRs contribute to *ago2*'s function during development. However, this work shows that GRRs are essential for its function in siRNA mediated silencing in the compound eye. Consistent with earlier results, *ago2* completely lacking the GRR domain does not respond to siRNA triggers any more and therefore the target gene is not silenced (Okamura et al., 2004). Alterations in GRR cause cellularisation defects and female sterility but only mildly impair Ago2's function in siRNA mediated silencing. Therefore the cellularisation phenotype and female sterility are very unlikely to be a consequence of siRNA mediated silencing. What might then be the cause of the observed phenotype? Interestingly, mild interactions between Ago1 and Ago2 have been reported earlier (Kataoka et al., 2001; Williams and Rubin, 2002). This work strengthens the idea that Ago1 and Ago2 interact with each other by various genetic, molecular and biochemical data: (1) Ago1 and Ago2^{dop1} genetically interact during siRNA mediated gene silencing. (2) *ago1* and *ago2*^{dop1} interact with each other at MBT and consequently during later embryogenesis as judged by the enhanced cuticle phenotypes in *ago1 ago2*^{dop1} double mutants. (3) Zygotic over-expression of *ago2* but also *ago1* could improve and even rescue the *ago2*^{dop1} phenotype. (4) Ago1 and Ago2 can be co-immunoprecipitated. These observations allow the assumption that Ago2 might be present in an Ago1 containing miRISC. Consequently, Ago2 itself might have a novel role in miRNA mediated silencing. The first evidence for this novel role is presented in this work. Therefore the *ago2*^{dop1}

phenotype could be a consequence of an impaired or misfunctional miRNA silencing pathway.

Ago1 and Ago2 might share overlapping functions in miRNA mediated silencing. This is indicated by the *ago1* rescue experiment. But the function of Ago1 and Ago2 are probably not fully redundant as *ago1* null mutants for example do not show cellularisation defects. Therefore, Ago1 and Ago2 containing RISC might incorporate different miRNAs and consequently might regulate different target mRNAs. This hypothesis is consistent with the results from Rehwinkel and colleagues (Rehwinkel et al., 2006). They investigated the regulation of transcripts by RNA silencing pathways at the genomic level in *Drosophila* S2 cells. They found out that some miRNAs are regulated by Ago2 containing RISC. Taken together, this thesis indicates that Ago1 and Ago2 not only interact with each other but also that the interaction is of more importance than previously thought.

4.2.2 *ago2* and *miR-9a*

This thesis presents evidence for a novel function of Ago2 in miRNA mediated silencing. The function of Ago2 containing miRISC might be the regulation of distinct miRNAs during several developmental processes like MBT. At the early stage of development where MBT occurs, it is very important for further development that zygotic transcription is initiated and maternal mRNAs are degraded (Bashirullah et al., 1999; Mazumdar and Mazumdar, 2002). If miRNA mediated gene silencing is necessary for MBT it might be very likely that a misregulation of mRNA targets would result in a cellularisation and lipid droplet phenotype similar to that *ago2*^{dop1} mutant situation. Thus, the observed phenotype in *ago2*^{dop1} mutants might be a direct consequence from a disruption of miRNA mediated silencing. This raises the question which miRNA could be involved in regulating developmental processes at MBT.

One good candidate miRNA that might be guided to targets by an Ago2 containing RISC is the miRNA *miR-9a*. It was reported that *miR-9a* depleted embryos show cellularisation defects (Leaman et al., 2005). Indeed, this thesis could demonstrate that zygotic over-expression of *miR-9a* repressed cellularisation defects of *ago2*^{dop1} embryos very efficiently and even rescued a significant amount of embryos to viable animals. This shows that at least some target mRNAs are not correctly regulated by *miR-9a* – Ago2^{dop1} containing RISC. However, it needs to be identified in the future, whether other and if so which miRNAs are involved in transcript regulation at MBT. Furthermore it would be essential to identify the target mRNAs that are misregulated at this stage.

4.2.3 Transcript regulation at MBT

It is likely that the *ago2*^{dop1} cellularisation and lipid droplet phenotype might result from a disruption of miRNA mediated silencing as discussed in the previous paragraphs. To address this question, microarray experiments were preformed recently in our laboratory comparing mRNA expression levels of *ago2*^{dop1} mutant to those of *wild-type* embryos at different time points during early embryogenesis. These comparative genomic studies showed that 6.8 % of 13900 transcripts were significantly up-regulated and 4.6 % were down-regulated at MBT (Gehlen, Westwood, Smibert, Müller, unpublished results). Among those were also predicted *miR-9* targets.

ago2^{dop1} mutants show defects at MBT. The MBT is marked by the switch from maternal to zygotic control of embryogenesis. Thereby maternal gene products are downregulated while zygotic transcription is initiated. In invertebrates as well as in vertebrates it is crucial for development that maternal RNAs are downregulated at this time point. As the results of the microarray experiments demonstrate many mRNAs fail to be downregulated at MBT in *ago2*^{dop1} mutant embryos. The timing of maternal transcript elimination in *Drosophila* at MBT has been investigated earlier (Bashirullah et al., 1999). Two degradation pathways for maternal mRNA degradation were suggested: a maternal and a zygotic pathway. Either pathway acting alone was sufficient to eliminate maternal transcripts but only both pathways working in concert allowed elimination of maternal transcripts prior MBT. Furthermore it was shown that the maternal degradation pathway depends on *cis*-acting elements target 3' UTRs of maternal mRNA for degradation. The zygotic pathway functions independently of *cis*-acting elements and becomes active 1.5 – 2 h after fertilisation. The data presented in this work suggests a third degradation pathway for maternal RNAs which depends on Ago2 function and miRNA mediated silencing.

The observations presented here correspond to recently published data about maternal transcript regulation in zebrafish (Giraldez et al., 2006). Interestingly, maternal and zygotic *dicer* mutants showed severe morphogenetic defects during zebrafish development. Some of these defects could be rescued by *miR-430* overexpression (Giraldez et al., 2005). Giraldez and colleagues found out that zebrafish *miR-430* is expressed at the onset of zygotic transcription and directly regulates several hundred targets of which most are maternally expressed mRNAs. In the absence of *miR-430* these maternal mRNAs accumulate. This shows that a specific phenotype is caused by loss of a specific miRNA. Though *miR-430* is not conserved in evolution and no fly homologue has been identified to date, these results emphasise the outcome of the work presented here. Taken together, the genetic analysis of this work showed that although *ago2*^{dop} alleles represent maternal-effect mutations, they specifically perturb processes shortly after the onset of zygotic transcription at the MBT. Therefore it is likely that Ago1 and Ago2 are key mediators of the zygotic

pathway of maternal transcript degradation. Furthermore the data suggest that *miR-9a* might fulfil a similar function in *Drosophila* as *miR-430* in zebrafish.

4.2.4 Possible targets that are regulated by Ago2-miRISC that cause *ago2^{dop1}* phenotype at MBT

The data presents evidence that Ago1 and Ago2 are involved in maternal transcript degradation at MBT in a miRNA dependent manner. As cellularisation and lipid droplet transport both require the microtubule network it is possible that the transport machinery itself is targeted by the *ago2^{dop1}* mutation. The investigation of the lipid droplet movement revealed that droplet motion was not inhibited in general. Rather net transport direction was misregulated. During cellularisation, membrane insertion was only blocked during slow phase in *ago2^{dop1}* mutant embryos. Therefore, the transport machinery including microtubule tracks must be mainly intact.

Interestingly, the above mentioned microarray experiment identified that *jaguar* (*jar)* was significantly downregulated in *ago2^{dop1}* mutant embryos three to five hours after egg laying (Gehlen, Westwood, Smibert, Müller, unpublished). Jar belongs to the class VI myosins. Class VI myosins are unconventional myosins as they are able to move towards the minus end of actin filaments which is in the opposite direction to all other myosins (Wells et al., 1999). Jar is important for the formation of the pseudocleavage furrow in the embryo (Mermall and Miller, 1995). Inhibition of Jar function leads to dramatic defects in syncytial blastoderm organisation (Mermall and Miller, 1995). Jar has been implicated in the movement of vesicles and particles, for instance during cellularisation (Mermall et al., 1994; Mermall and Miller, 1995). Its role as a vesicle transporter on actin filaments maybe linked with microtubules since it was shown to coimmunoprecipitate with CLIP-190, which is a microtubule binding protein (Lantz and Miller, 1998). However, the precise mechanism for membrane delivery to specific sites of plasma membrane and membrane targeting for cellularising embryos in *Drosophila* is not clear yet. The observation that *jar* is downregulated three hours after egg laying in an Ago2^{dop1} dependent manner might indicate that Jar might play an important role in moving vesicles to the membrane during slow phase. To investigate Jar's role during cellularisation it could be tested in the future whether the maternal overexpression of *jar* would be able to rescue *ago2^{dop1}* cellularisation defects.

4.3 *ago2* is required for establishment of segment polarity

ago1 and *ago2* double mutants display severe segment polarity defects. Interestingly, *ago1* was identified in a genetic screen for regulators of Wg signalling pathway (Kataoka et al., 2001). *ago1* acts as a positive regulator at the level of Arm.

Arm accumulates in Wg signal receiving cells, where it is translocated to the nucleus and activates the expression of Wg target genes with the help of the transcription factor TCF (reviewed in Jones and Bejsovec, 2003). Thus, Arm is essential for the feed back loop that maintains Wg signalling and helps to define segment polarity in the early *Drosophila* embryo (Figure 3). Depletion of cytoplasmic Arm in wing imaginal discs result in a defect in Wg signalling that can be rescued by *ago1* over-expression (Kataoka et al., 2001). To the authors' surprise however, *ago1* null alleles did not exhibit segment polarity defects in the embryo, suggesting that either *ago1* does not regulate Arm in the embryo or that an additional factor acts redundantly to *ago1*. The results of this present work support the model that in the embryo Ago2 acts redundantly to Ago1 as only *ago1 ago2* double mutants but neither mutant alone displayed segment polarity defects. This clearly shows that *ago1* and *ago2* do have overlapping functions. They work in concert to maintain Wg signalling. Like at MBT, the segment polarity phenotype might result through a disrupted miRNA silencing pathway and is siRNA independent: Only *ago1 ago2* and *ago1 dcr-1* double mutants display segment polarity defects but not *dcr-2 dcr-1* double mutants. If the segment polarity defects are a result of a disrupted miRNA silencing pathway, several ways are possible how miRNAs might interfere with *wg*. miRNAs might affect: (1) *wg* transcription, (2) *wg* transcript stability, (3) *wg* translation. Another possibility would be that (4) miRNAs might target directly or indirectly microtubule based transport that localise *wg* mRNA apical. The correct apical localisation of *wg* mRNA is required for correct intracellular Wg translation and signalling activity (Simmonds et al., 2001; Wilkie and Davis, 2001).

The analysis of *wg* mRNA expression pattern showed that *wg* transcription or *wg* transcript stability is effected in *ago1 dcr-1* or *ago1 ago2* double mutants. Whether *wg* was localised apically cannot be answered by this in situ experiment. This requires a high resolution and sensitivity in situ. However, a more detailed analysis with respect to age and genotype of the analysed embryos would be needed to further determine the role of Ago1 and Ago2 for the regulation of segment polarity. As well it might be possible that segment polarity is dependent on the gene doses of *ago1* and *ago2*.

4.3.1 The requirement of *piwi* and *aubergine* for segment polarity

ago2^{dop1} homozygous mutant embryos that are reduced in *piwi* or *aub* showed as well an enhancement of the cellularisation phenotype. This observation suggests that both *aub* and

piwi could interfere with miRNA meditated silencing at MBT. Indeed, Megosh and colleagues observed a crucial role for Piwi in miRNA mediated silencing (Megosh et al., 2006). As Aub is a close homologue of Piwi it could be possible that Aub interferes with miRNA mediated silencing as well. Interestingly, segment polarity defects were as well observed in *piwi ago2*^{51B} and *aub ago2*^{51B} double mutant embryos as described in this work. However, neither *dcr-1*^{Q1147X} nor *ago2*^{dop1} in combination with *piwi* or *aub* mutations did exhibit segment polarity defects. These observations indicate that *piwi* and *aub* might interact with Ago2^{long} in the regulation of segment polarity. These data show that Aub and Piwi interact in a redundant fashion with miRNA mediated silencing at the level of Ago1 and Ago2 respectively. Furthermore, the results reveal that full length Ago2 (Ago2^{full}) but not Ago2^{short} is essential for segment polarity establishment. When Ago2^{full} is completely absent (e. g. in *ago2*^{51B} mutants) and any other member of the Argonaute family is absent as well (Ago1, Piwi, Aub) segment polarity defects are observed. In contrast *ago2*^{dop1} mutants display only segment polarity defects in combination with the *ago1* mutation but not with *piwi* and *aub* mutations. Therefore, Ago2^{dop1} must be able to fulfil at least some of its normal function while Ago2^{short} is not. This would mean that the GRRs are important for Ago2 function in segment polarity. One possibility would be that Ago2's GRR guide Ago2 to the site of function for establishing segment polarity. As Ago2^{short} lacks the GRRs it might not be localised in the subcellular compartment where its activity would be required. Probably, *ago2*^{dop1}-GRRs are still capable of allowing Ago2 to reach the site of function. Ago2^{dop1}'s disrupted GRR might be compensated by Ago1 in a *piwi* or *aub* mutant background. Explained in a different way neither Piwi nor Aub can compensate the *ago1* mutation in *ago1 ago2*^{dop1} double mutants. The hypothesis that Ago2's GRRs are important for Ago2's subcellular localisation should be tested in the future when good Ago2 antibodies are available which would allow to distinguish between Ago2^{long} and Ago2^{short} or when different tagged *ago2* constructs are available.

Taken together, the observations suggest that Piwi and Aub might interfere with miRNA mediated silencing but might play a less important role as Ago1 or Ago2 in establishing segment polarity. This is consistent with the observations by Rehwinkel and co-workers that only a minority of transcripts are regulated by Piwi and Aub (Rehwinkel et al., 2006).

4.3.2 *piwi* and *aub* interfere with the expression of pair-rule genes

Double mutant analysis of *piwi* and *aub* with *ago2* exhibited a redundant requirement of these genes for segmentation on the level of pair rule genes. *piwi ago2*^{51B} and *aub ago2*^{51B} double mutants showed patterning defects that are characteristic for pair-rule mutants. When embryos were stained for the pair-rule gene products Ftz and Eve it was observed that both proteins were still present in extended germband stage embryos (stage 9).

Developmental genes act in a strictly temporal sequence. They form a hierarchy of gene activity: The action of one set of genes is essential for the activation of the following set of genes. To my knowledge these are the first genetic backgrounds that exhibit a failure to downregulate pair-rule gene expression. But obviously the temporal over-expression of pair-rule genes leads to Wg signalling defects and consequently segment polarity defects. As described in the introduction (1.1.2, page 4 et seq.) the pair-rule genes *ftz* and *eve* activate the expression of the segment polarity gene *en*. The segment polarity gene *wg* in turn is only activated in those cells that receive little or no *ftz* or *eve*. The feed-back loop is made up of *wg* activating *en* in neighbouring cells, *en* activating *hh* which in turn activates *wg* in the adjacent cells. Obviously the expression of *ftz* and *en* negatively interferes with this feedback loop. It was visible in immuno-stainings that the temporal over-expression of Ftz in even numbered parasegments leads to a downregulation of En (Figure 25). This downregulation must be indirect as normally *ftz* activates *en*. Therefore it might be possible that the temporal over-expression of Ftz/Eve might negatively influence the expression of *wg* in neighbouring cells. As a consequence En might then be downregulated by the breakdown of the feedback loop through the absence of Wg. Taken together the observations indicate that *ftz* might be a target that is regulated by Ago2 containing miRISC. The hypothesis is further supported by the observation that in the above mentioned microarray experiment *ftz* was identified as one target that was not downregulated in *ago2*^{dop1} mutant embryos (Gehlen, Westwood, Smibert, Müller, unpublished). This is an interesting observation. If *ftz* is the direct target of a miRNA it would be interesting to know which miRNA this might be and which other transcripts might be regulated by it. More work should be invested in the future to determine the role of Ago2^{short}, Ago2^{dop1} and other Argonaute proteins in the regulation of *ftz* and its consequences for segmentation. So far it is not known what triggers the degradation of pair-rule gene products at the end of gastrulation. This work provides the possibility that the pair-rule gene products are degraded in a miRNA-dependent manner that requires the activity of Ago2^{long} and Piwi or Aubergine.

Taken together this data demonstrates that different isoforms of Ago2 are not only involved but also essential for miRNA mediated silencing. Furthermore this study indicates that key developmental processes like MBT and segment polarity establishment and maintenance are controlled by miRNA mediated silencing.

4.4 Conclusions

This thesis investigated the role of *ago2* during early embryonic development by studying the *ago2*^{dop1} mutation. The *ago2*^{dop1} mutation results in a reduced number of GRRs at

Ago2's amino-terminus. By studying the *ago2^{dop1}* allele this work has been able to reveal new functions for Ago2 in miRNA mediated silencing and embryonic development of *Drosophila melanogaster*. This work demonstrates that Ago2 is essential for development. The phenotypes that are observed in different *ago2* mutants can result from a disrupted miRNA mediated silencing pathway:

(1) Genetic interactions and biochemical data show for the first time that Ago1 and Ago2 have overlapping functions during MBT and segment polarity establishment. Therefore, the model that in *Drosophila* different Argonaute and Dicer proteins function in distinct RNA silencing pathways is challenged by the data presented in this thesis. The present data rather suggest that Ago1 and Ago2 work in concert.

(2) This work demonstrates strong evidence for the existence of a new Ago2 isoform which was named *ago2^{short}*. Ago2^{short} completely lacks the amino-terminal GRRs. The function of GRRs has not been determined. This work clearly shows the importance of GRRs for Ago2's function at different developmental stages. The analysis of the *ago2^{dop}* mutants revealed that Ago2 is essential for MBT. Small alterations in the GRR lead to severe cellularisation defects. During MBT Ago2^{dop1} might negatively interfere with Ago2^{short}. This allows the conclusion that the *ago2^{dop1}* phenotype is dependent on the availability of Ago2^{short}. These results strongly suggest that Ago2^{short} is essential for correct cellularisation.

(3) Mutations in Ago1, Piwi and Aub enhance the *ago2^{dop1}* cellularisation phenotype. Consequently, it is very likely that all Argonaute family members contribute to miRNA mediated silencing at MBT.

(4) The data presented here support the model that Ago2 is required for degradation of maternal transcripts at MBT. The phenotype of *ago2^{dop}* might reflect a requirement for *miR-9a* at MBT, because overexpression of *miR-9a* could rescue the *ago2^{dop1}* cellularisation phenotype.

(5) Proteins that are involved miRNA mediated silencing like Dcr-1 and Ago1 but also Ago2 play as well an important role in establishing segment polarity. While Ago2^{short} is essential for MBT this work provides the possibility that Ago2^{long} is required for the establishment of segment polarity. Here Ago1 and Ago2 act in a partially redundant fashion to control the expression of the segment-polarity gene *wingless* in the early embryo.

Taken together, the data presented here argue strongly against a strict separation of Ago1 and Ago2 functions and suggest that these proteins act in concert to control key steps of midblastula transition and of segmental patterning. Furthermore the *ago2^{dop1}* mutation revealed a requirement of GRRs for the normal function of Ago2.

In summary, the *ago2^{dop1}* mutation is a powerful tool to investigate RNA silencing processes in a biological well-defined system and will probably bring more insight into the complex regulatory machinery in the future.

4.5 Outlook

This work showed interesting and new functions of Ago2 in miRNA mediated silencing and probably other yet to be defined pathways. But still many questions remained unanswered, which should be addressed in the future. It would be essential to identify a real *ago2* null allele, because only elimination of all Ago2 isoforms would allow studying the requirement of the *ago2* for development. This tool would provide a handle to examine how Ago2 regulates gene expression by miRNA mediated silencing. It is as well very important to determine the targets that are misregulated by $Ago2^{dop1}$, $Ago2^{dop46}$, $Ago2^{short}$ and ΔAgo2. The microarray experiment that compares mRNA levels of *wild-type* and $ago2^{dop1}$ embryos at different developmental stages is a first step to identify Ago2 targets. But this approach will only identify those targets that are regulated on the level of transcript stability. Target specific silencing by translation inhibition will not be detected and requires a proteomic approach.

A comprehensive study on Ago2 protein isoforms is also currently hampered by the fact that none of the antibodies against Ago2 is very specific. Therefore, the generation of a functional Ago2 antibody is pivotal for further analysis. A good Ago2 antibody would allow immunostainings in ovaries and the early embryo and would reveal the location of the Ago2 protein. Importantly, an Ago2 antibody would clarify whether Ago2 localises with the miRNA machinery in the GW bodies in the embryo. Furthermore, it would forward the understanding of how the GRR contribute to Ago2's function if one could distinguish by biochemical studies between the aggregate and soluble form of Ago2 or to differentiate between $Ago2^{short}$ and $Ago2^{full}$. All this data would help to shed light on the key question: How and where do which Argonaute proteins regulate a certain miRNA and what are the targets at a particular developmental stage?

5 List of Abbreviations

α–	anti-
°C	degree Celsius
Δ	Delta (deleted)
µ	micro (10^{-6})
A	Adenine
aa	amino acids
Ab	Antibody
Ago	Argonaute
AP	alkaline phosphatase
Arm	Armadillo
Aub	Aubergine
bp	base pair
BSA	Bovine serum albumin
C	Cytosine
DABCO	1,4-Diazybicyclo(2.2.2)octane
DIG	Digoxigenin
Dcr	Dicer
dH_2O	demineralised water
DMSO	Dimethylsulfoxid
DNA	Desoxyribonucleic acid
dNTP	Desoxyribonucleotide phosphate
dop	drop out
dsRNA	double stranded RNA
e. g.	for example (lat.: exempli gratia)
En	Engrailed
Eve	Even-skipped
FA	Formaldehyde
Fig.	Figure
Ftz	Fushi-tarazu
g	gramme
G	Guanine
GRR	Glutamine rich repeat
HRP	Horse Radish Peroxidase
k	kilo (10^{3})
kb	kilo base
kDa	kilo Dalton
L	litre
LB medium	Luria Bertani broth medium
m	milli (10^{-3})

m	mouse
M	Mol
MBT	midblastula transition
min	minute
miRISC	miRNA-containing RISC
miRNA	microRNA
miRNP	miRNA-containing ribonucleoprotein
mRNA	messenger RNA
n	nano (10^{-9})
NaOCl	Sodium Hypochloride
NHS	Normal horse serum
nt	nucleotide
OD	optical density
PAGE	Polyacryl amide gel electrophoresis
PBS	Phosphate buffered saline
PBT	PBS-Tween
PCR	Polymerase chain reaction
Piwi	P-Element induced wimpy testis
PTX	PBS-TritonX-100
rasiRNA	repeat-associated small interfering RNA
rb	rabbit
RISC	RNA induced silencing complex
RNA	ribonucleic acid
RNAi	RNA interference
rpm	rotations per minute
RT	Room temperature
RT-PCR	Reverse Transcription Polymerase Chain Reaction
SDS	Sodium dedocyl sulfate
siRNA	small interfering RNA
Suppl.	supplementary
T	Thymine
Tab.	Table
Taq	Thermophilus aquaticus
TSS	Transcriptional start site
U	Unit
UAS	Upstream activating sequence
V	Volume
Wg	Wingless

6 List of References

Ambros, V. (2001). microRNAs: tiny regulators with great potential. Cell *107*, 823-826.

Aravin, A.A., Naumova, N.M., Tulin, A.V., Vagin, V.V., Rozovsky, Y.M., and Gvozdev, V.A. (2001). Double-stranded RNA-mediated silencing of genomic tandem repeats and transposable elements in the D. melanogaster germline. Curr Biol *11*, 1017-1027.

Bashirullah, A., Halsell, S.R., Cooperstock, R.L., Kloc, M., Karaiskakis, A., Fisher, W.W., Fu, W., Hamilton, J.K., Etkin, L.D., and Lipshitz, H.D. (1999). Joint action of two RNA degradation pathways controls the timing of maternal transcript elimination at the midblastula transition in Drosophila melanogaster. The EMBO journal *18*, 2610-2620.

Baulcombe, D. (2004). RNA silencing in plants. Nature *431*, 356-363.

Bernstein, E., Caudy, A.A., Hammond, S.M., and Hannon, G.J. (2001). Role for a bidentate ribonuclease in the initiation step of RNA interference. Nature *409*, 363-366.

Bernstein, E., Kim, S.Y., Carmell, M.A., Murchison, E.P., Alcorn, H., Li, M.Z., Mills, A.A., Elledge, S.J., Anderson, K.V., and Hannon, G.J. (2003). Dicer is essential for mouse development. Nature genetics *35*, 215-217.

Billy, E., Brondani, V., Zhang, H., Muller, U., and Filipowicz, W. (2001). Specific interference with gene expression induced by long, double-stranded RNA in mouse embryonal teratocarcinoma cell lines. Proceedings of the National Academy of Sciences of the United States of America *98*, 14428-14433.

Bolt, M.W., and Mahoney, P.A. (1997). High-efficiency blotting of proteins of diverse sizes following sodium dodecyl sulfate-polyacrylamide gel electrophoresis. Analytical biochemistry *247*, 185-192.

Bonnet, E., Van de Peer, Y., and Rouze, P. (2006). The small RNA world of plants. The New phytologist *171*, 451-468.

Brandt, A., Papagiannouli, F., Wagner, N., Wilsch-Brauninger, M., Braun, M., Furlong, E.E., Loserth, S., Wenzl, C., Pilot, F., Vogt, N.*, et al.* (2006). Developmental control of nuclear size and shape by Kugelkern and Kurzkern. Curr Biol *16*, 543-552.

Brennecke, J., Hipfner, D.R., Stark, A., Russell, R.B., and Cohen, S.M. (2003). bantam encodes a developmentally regulated microRNA that controls cell proliferation and regulates the proapoptotic gene hid in Drosophila. Cell *113*, 25-36.

Callaini, G., and Anselmi, F. (1988). Centrosome splitting during nuclear elongation in the Drosophila embryo. Experimental cell research *178*, 415-425.

Carmell, M.A., and Hannon, G.J. (2004). RNase III enzymes and the initiation of gene silencing. Nature structural & molecular biology *11*, 214-218.

Carmell, M.A., Xuan, Z., Zhang, M.Q., and Hannon, G.J. (2002). The Argonaute family: tentacles that reach into RNAi, developmental control, stem cell maintenance, and tumorigenesis. Genes & development *16*, 2733-2742.

Caudy, A.A., Myers, M., Hannon, G.J., and Hammond, S.M. (2002). Fragile X-related protein and VIG associate with the RNA interference machinery. Genes & development *16*, 2491-2496.

Chen, X. (2005). MicroRNA biogenesis and function in plants. FEBS letters *579*, 5923-5931.

Cox, D.N., Chao, A., Baker, J., Chang, L., Qiao, D., and Lin, H. (1998). A novel class of evolutionarily conserved genes defined by piwi are essential for stem cell self-renewal. Genes & development *12*, 3715-3727.

Cox, D.N., Chao, A., and Lin, H. (2000). piwi encodes a nucleoplasmic factor whose activity modulates the number and division rate of germline stem cells. Development (Cambridge, England) *127*, 503-514.

Crawford, J.M., Su, Z., Varlamova, O., Bresnick, A.R., and Kiehart, D.P. (2001). Role of myosin-II phosphorylation in V12Cdc42-mediated disruption of Drosophila cellularization. European journal of cell biology *80*, 240-244.

Dawes-Hoang, R.E., Parmar, K.M., Christiansen, A.E., Phelps, C.B., Brand, A.H., and Wieschaus, E.F. (2005). folded gastrulation, cell shape change and the control of myosin localization. Development (Cambridge, England) *132*, 4165-4178.

Denli, A.M., Tops, B.B., Plasterk, R.H., Ketting, R.F., and Hannon, G.J. (2004). Processing of primary microRNAs by the Microprocessor complex. Nature *432*, 231-235.

Deshpande, G., Calhoun, G., and Schedl, P. (2005). Drosophila argonaute-2 is required early in embryogenesis for the assembly of centric/centromeric heterochromatin, nuclear division, nuclear migration, and germ-cell formation. Genes & development *19*, 1680-1685.

DiNardo, S., Sher, E., Heemskerk, J.J., Kassis, J.A., and O'Farrell, P.H. (1988). Two-tiered regulation of spatially patterned engrailed gene expression during Drosophila embryogenesis. Nature *332*, 604-609.

Doench, J.G., Petersen, C.P., and Sharp, P.A. (2003). siRNAs can function as miRNAs. Genes & development *17*, 438-442.

Driever, W., and Nusslein-Volhard, C. (1988a). The bicoid protein determines position in the Drosophila embryo in a concentration-dependent manner. Cell *54*, 95-104.

Driever, W., and Nusslein-Volhard, C. (1988b). A gradient of bicoid protein in Drosophila embryos. Cell *54*, 83-93.

Driever, W., and Nusslein-Volhard, C. (1989). The bicoid protein is a positive regulator of hunchback transcription in the early Drosophila embryo. Nature *337*, 138-143.

Elbashir, S.M., Harborth, J., Lendeckel, W., Yalcin, A., Weber, K., and Tuschl, T. (2001a). Duplexes of 21-nucleotide RNAs mediate RNA interference in cultured mammalian cells. Nature *411*, 494-498.

Elbashir, S.M., Lendeckel, W., and Tuschl, T. (2001b). RNA interference is mediated by 21- and 22-nucleotide RNAs. Genes & development *15*, 188-200.

Elbashir, S.M., Martinez, J., Patkaniowska, A., Lendeckel, W., and Tuschl, T. (2001c). Functional anatomy of siRNAs for mediating efficient RNAi in Drosophila melanogaster embryo lysate. The EMBO journal *20*, 6877-6888.

Fire, A., Xu, S., Montgomery, M.K., Kostas, S.A., Driver, S.E., and Mello, C.C. (1998). Potent and specific genetic interference by double-stranded RNA in Caenorhabditis elegans. Nature *391*, 806-811.

Foe, V.E., Odell, G.M., and Edgar, B.A. (1993). Mitosis and Morphogenesis in the *Drosophila* embryo: point und counterpoint, Vol 1 (Cold Spring Harbor Laboratory Press).

Forstemann, K., Tomari, Y., Du, T., Vagin, V.V., Denli, A.M., Bratu, D.P., Klattenhoff, C., Theurkauf, W.E., and Zamore, P.D. (2005). Normal microRNA maturation and germ-line stem cell maintenance requires Loquacious, a double-stranded RNA-binding domain protein. PLoS Biol *3*, e236.

Frasch, M., Hoey, T., Rushlow, C., Doyle, H., and Levine, M. (1987). Characterization and localization of the even-skipped protein of Drosophila. The EMBO journal *6*, 749-759.

Fullilove, S.L., and Jacobson, A.G. (1971). Nuclear elongation and cytokinesis in Drosophila montana. Developmental biology *26*, 560-577.

Galewsky, S., and Schulz, R.A. (1992). Drop out: a third chromosome maternal-effect locus required for formation of the Drosophila cellular blastoderm. Mol Reprod Dev *32*, 331-338.

Giansanti, M.G., Bonaccorsi, S., Williams, B., Williams, E.V., Santolamazza, C., Goldberg, M.L., and Gatti, M. (1998). Cooperative interactions between the central spindle and the contractile ring during Drosophila cytokinesis. Genes & development *12*, 396-410.

Giraldez, A.J., Cinalli, R.M., Glasner, M.E., Enright, A.J., Thomson, J.M., Baskerville, S., Hammond, S.M., Bartel, D.P., and Schier, A.F. (2005). MicroRNAs regulate brain morphogenesis in zebrafish. Science *308*, 833-838.

Giraldez, A.J., Mishima, Y., Rihel, J., Grocock, R.J., Van Dongen, S., Inoue, K., Enright, A.J., and Schier, A.F. (2006). Zebrafish MiR-430 promotes deadenylation and clearance of maternal mRNAs. Science *312*, 75-79.

Grishok, A. (2005). RNAi mechanisms in Caenorhabditis elegans. FEBS letters *579*, 5932-5939.

Grishok, A., Tabara, H., and Mello, C.C. (2000). Genetic requirements for inheritance of RNAi in C. elegans. Science *287*, 2494-2497.

Gross, S.P., Guo, Y., Martinez, J.E., and Welte, M.A. (2003). A determinant for directionality of organelle transport in Drosophila embryos. Curr Biol *13*, 1660-1668.

Gross, S.P., Welte, M.A., Block, S.M., and Wieschaus, E.F. (2000). Dynein-mediated cargo transport in vivo. A switch controls travel distance. The Journal of cell biology *148*, 945-956.

Grosshans, J., Muller, H.A., and Wieschaus, E. (2003). Control of cleavage cycles in Drosophila embryos by fruhstart. Dev Cell *5*, 285-294.

Grosshans, J., Wenzl, C., Herz, H.M., Bartoszewski, S., Schnorrer, F., Vogt, N., Schwarz, H., and Muller, H.A. (2005). RhoGEF2 and the formin Dia control the formation of the furrow canal by directed actin assembly during Drosophila cellularisation. Development (Cambridge, England) *132*, 1009-1020.

Guo, S., and Kemphues, K.J. (1995). par-1, a gene required for establishing polarity in C. elegans embryos, encodes a putative Ser/Thr kinase that is asymmetrically distributed. Cell *81*, 611-620.

Guo, Y., Jangi, S., and Welte, M.A. (2005). Organelle-specific control of intracellular transport: distinctly targeted isoforms of the regulator Klar. Mol Biol Cell *16*, 1406-1416.

Hafen, E., Kuroiwa, A., and Gehring, W.J. (1984). Spatial distribution of transcripts from the segmentation gene fushi tarazu during Drosophila embryonic development. Cell *37*, 833-841.

Hammond, S.M. (2005). Dicing and slicing: the core machinery of the RNA interference pathway. FEBS letters *579*, 5822-5829.

Hammond, S.M., Bernstein, E., Beach, D., and Hannon, G.J. (2000). An RNA-directed nuclease mediates post-transcriptional gene silencing in Drosophila cells. Nature *404*, 293-296.

Hammond, S.M., Boettcher, S., Caudy, A.A., Kobayashi, R., and Hannon, G.J. (2001). Argonaute2, a link between genetic and biochemical analyses of RNAi. Science *293*, 1146-1150.

Han, J., Lee, Y., Yeom, K.H., Kim, Y.K., Jin, H., and Kim, V.N. (2004). The Drosha-DGCR8 complex in primary microRNA processing. Genes & development *18*, 3016-3027.

Harris, A.N., and Macdonald, P.M. (2001). Aubergine encodes a Drosophila polar granule component required for pole cell formation and related to eIF2C. Development (Cambridge, England) *128*, 2823-2832.

Herr, A.J. (2005). Pathways through the small RNA world of plants. FEBS letters *579*, 5879-5888.

Hidalgo, A., and Ingham, P. (1990). Cell patterning in the Drosophila segment: spatial regulation of the segment polarity gene patched. Development (Cambridge, England) *110*, 291-301.

Hiromi, Y., Kuroiwa, A., and Gehring, W.J. (1985). Control elements of the Drosophila segmentation gene fushi tarazu. Cell *43*, 603-613.

Huh, J.R., Vernooy, S.Y., Yu, H., Yan, N., Shi, Y., Guo, M., and Hay, B.A. (2004). Multiple apoptotic caspase cascades are required in nonapoptotic roles for Drosophila spermatid individualization. PLoS Biol *2*, E15.

Inoue, H., Nojima, H., and Okayama, H. (1990). High efficiency transformation of Escherichia coli with plasmids. Gene *96*, 23-28.

Irish, V., Lehmann, R., and Akam, M. (1989). The Drosophila posterior-group gene nanos functions by repressing hunchback activity. Nature *338*, 646-648.

Jiang, F., Ye, X., Liu, X., Fincher, L., McKearin, D., and Liu, Q. (2005). Dicer-1 and R3D1-L catalyze microRNA maturation in Drosophila. Genes & development *19*, 1674-1679.

Jones, W.M., and Bejsovec, A. (2003). Wingless signaling: an axin to grind. Curr Biol *13*, R479-481.

Kataoka, Y., Takeichi, M., and Uemura, T. (2001). Developmental roles and molecular characterization of a Drosophila homologue of Arabidopsis Argonaute1, the founder of a novel gene superfamily. Genes Cells *6*, 313-325.

Kellogg, D.R., Sullivan, W., Theurkauf, W., Oegema, K., Raff, J.W., and Alberts, B.M. (1991). Studies on the centrosome and cytoplasmic organization in the early Drosophila embryo. Cold Spring Harbor symposia on quantitative biology *56*, 649-662.

Kennerdell, J.R., Yamaguchi, S., and Carthew, R.W. (2002). RNAi is activated during Drosophila oocyte maturation in a manner dependent on aubergine and spindle-E. Genes & development *16*, 1884-1889.

Keßler, T. (2006). The function of the Drosophila caspase inhibitor DIAP1 in the control of epithelial integrity and cell polarity. In Institut für Genetik (Düsseldorf, Heinrich-Heine-Univerisität).

Klingensmith, J., and Nusse, R. (1994). Signaling by wingless in Drosophila. Developmental biology *166*, 396-414.

Krause, H.M., and Gehring, W.J. (1988). The location, modification, and function of the fushi tarazu protein during Drosophila embryogenesis. Progress in clinical and biological research *284*, 105-123.

Kuroiwa, A., Hafen, E., and Gehring, W.J. (1984). Cloning and transcriptional analysis of the segmentation gene fushi tarazu of Drosophila. Cell *37*, 825-831.

Laemmli, U.K. (1970). Cleavage of structural proteins during the assembly of the head of bacteriophage T4. Nature *227*, 680-685.

Lawrence, P.A., and Struhl, G. (1996). Morphogens, compartments, and pattern: lessons from drosophila? Cell *85*, 951-961.

Leaman, D., Chen, P.Y., Fak, J., Yalcin, A., Pearce, M., Unnerstall, U., Marks, D.S., Sander, C., Tuschl, T., and Gaul, U. (2005). Antisense-mediated depletion reveals essential and specific functions of microRNAs in Drosophila development. Cell *121*, 1097-1108.

Lecuit, T., Samanta, R., and Wieschaus, E. (2002). slam encodes a developmental regulator of polarized membrane growth during cleavage of the Drosophila embryo. Dev Cell *2*, 425-436.

Lecuit, T., and Wieschaus, E. (2000). Polarized insertion of new membrane from a cytoplasmic reservoir during cleavage of the Drosophila embryo. The Journal of cell biology *150*, 849-860.

Lee, Y., Ahn, C., Han, J., Choi, H., Kim, J., Yim, J., Lee, J., Provost, P., Radmark, O., Kim, S*., et al.* (2003). The nuclear RNase III Drosha initiates microRNA processing. Nature *425*, 415-419.

Lee, Y., Jeon, K., Lee, J.T., Kim, S., and Kim, V.N. (2002). MicroRNA maturation: stepwise processing and subcellular localization. The EMBO journal *21*, 4663-4670.

Lee, Y., Kim, M., Han, J., Yeom, K.H., Lee, S., Baek, S.H., and Kim, V.N. (2004a). MicroRNA genes are transcribed by RNA polymerase II. The EMBO journal *23*, 4051-4060.

Lee, Y.S., Nakahara, K., Pham, J.W., Kim, K., He, Z., Sontheimer, E.J., and Carthew, R.W. (2004b). Distinct roles for Drosophila Dicer-1 and Dicer-2 in the siRNA/miRNA silencing pathways. Cell *117*, 69-81.

Lehmann, R., and Nusslein-Volhard, C. (1987). hunchback, a gene required for segmentation of an anterior and posterior region of the Drosophila embryo. Developmental biology *119*, 402-417.

Lindsley, D.L., and Zimm, G.G. (1992). The genome of Drosophila melanogaster (San Diego, USA, Academic Press, Inc.).

Lingel, A., Simon, B., Izaurralde, E., and Sattler, M. (2003). Structure and nucleic-acid binding of the Drosophila Argonaute 2 PAZ domain. Nature *426*, 465-469.

Liu, J., Carmell, M.A., Rivas, F.V., Marsden, C.G., Thomson, J.M., Song, J.J., Hammond, S.M., Joshua-Tor, L., and Hannon, G.J. (2004). Argonaute2 is the catalytic engine of mammalian RNAi. Science *305*, 1437-1441.

Liu, J., Valencia-Sanchez, M.A., Hannon, G.J., and Parker, R. (2005). MicroRNA-dependent localization of targeted mRNAs to mammalian P-bodies. Nat Cell Biol *7*, 719-723.

Liu, Q., Rand, T.A., Kalidas, S., Du, F., Kim, H.E., Smith, D.P., and Wang, X. (2003). R2D2, a bridge between the initiation and effector steps of the Drosophila RNAi pathway. Science *301*, 1921-1925.

Liu, X., Jiang, F., Kalidas, S., Smith, D., and Liu, Q. (2006). Dicer-2 and R2D2 coordinately bind siRNA to promote assembly of the siRISC complexes. RNA (New York, NY *12*, 1514-1520.

Ma, J.B., Ye, K., and Patel, D.J. (2004). Structural basis for overhang-specific small interfering RNA recognition by the PAZ domain. Nature *429*, 318-322.

Mandel, M., and Higa, A. (1970). Calcium-dependent bacteriophage DNA infection. Journal of molecular biology *53*, 159-162.

Martinez Arias, A., Baker, N.E., and Ingham, P.W. (1988). Role of segment polarity genes in the definition and maintenance of cell states in the Drosophila embryo. Development (Cambridge, England) *103*, 157-170.

Mazumdar, A., and Mazumdar, M. (2002). How one becomes many: blastoderm cellularization in Drosophila melanogaster. Bioessays *24*, 1012-1022.

Megosh, H.B., Cox, D.N., Campbell, C., and Lin, H. (2006). The role of PIWI and the miRNA machinery in Drosophila germline determination. Curr Biol *16*, 1884-1894.

Meister, G., Landthaler, M., Patkaniowska, A., Dorsett, Y., Teng, G., and Tuschl, T. (2004). Human Argonaute2 mediates RNA cleavage targeted by miRNAs and siRNAs. Mol Cell *15*, 185-197.

Mermall, V., and Miller, K.G. (1995). The 95F unconventional myosin is required for proper organization of the Drosophila syncytial blastoderm. The Journal of cell biology *129*, 1575-1588.

Miller, K.G., and Kiehart, D.P. (1995). Fly division. The Journal of cell biology *131*, 1-5.

Miyoshi, K., Tsukumo, H., Nagami, T., Siomi, H., and Siomi, M.C. (2005). Slicer function of Drosophila Argonautes and its involvement in RISC formation. Genes & development *19*, 2837-2848.

Müller, H.-A.J. (2001). Of mice, frogs and flies: Generation of membrane asymmetries in early development. Development Growth and Differentiation *in press*.

Nakayashiki, H. (2005). RNA silencing in fungi: mechanisms and applications. FEBS letters *579*, 5950-5957.

Napoli, C., Lemieux, C., and Jorgensen, R. (1990). Introduction of a Chimeric Chalcone Synthase Gene into Petunia Results in Reversible Co-Suppression of Homologous Genes in trans. Plant Cell *2*, 279-289.

Nusslein-Volhard, C., Frohnhofer, H.G., and Lehmann, R. (1987). Determination of anteroposterior polarity in Drosophila. Science *238*, 1675-1681.

Okamura, K., Ishizuka, A., Siomi, H., and Siomi, M.C. (2004). Distinct roles for Argonaute proteins in small RNA-directed RNA cleavage pathways. Genes & development *18*, 1655-1666.

Pal-Bhadra, M., Bhadra, U., and Birchler, J.A. (2002). RNAi related mechanisms affect both transcriptional and posttranscriptional transgene silencing in Drosophila. Mol Cell *9*, 315-327.

Pankratz, M.J., and Jäckle, H. (1993). Blastoderm segmentation, Vol 1 (Cold Spring Harbor Laboratory Press).

Perrimon, N. (1994). The genetic basis of patterned baldness in Drosophila. Cell *76*, 781-784.

Pilot, F., Philippe, J.M., Lemmers, C., Chauvin, J.P., and Lecuit, T. (2006). Developmental control of nuclear morphogenesis and anchoring by charleston, identified in a functional genomic screen of Drosophila cellularisation. Development (Cambridge, England) *133*, 711-723.

Postner, M.A., and Wieschaus, E.F. (1994). The nullo protein is a component of the actin-myosin network that mediates cellularization in Drosophila melanogaster embryos. J Cell Sci *107*, 1863-1873.

Preston, C.R., and Engels, W.R. (1996). P-element-induced male recombination and gene conversion in Drosophila. Genetics *144*, 1611-1622.

Qi, Y., and Hannon, G.J. (2005). Uncovering RNAi mechanisms in plants: biochemistry enters the foray. FEBS letters *579*, 5899-5903.

Rand, T.A., Ginalski, K., Grishin, N.V., and Wang, X. (2004). Biochemical identification of Argonaute 2 as the sole protein required for RNA-induced silencing complex activity. Proceedings of the National Academy of Sciences of the United States of America *101*, 14385-14389.

Rehwinkel, J., Behm-Ansmant, I., Gatfield, D., and Izaurralde, E. (2005). A crucial role for GW182 and the DCP1:DCP2 decapping complex in miRNA-mediated gene silencing. RNA (New York, NY *11*, 1640-1647.

Rehwinkel, J., Natalin, P., Stark, A., Brennecke, J., Cohen, S.M., and Izaurralde, E. (2006). Genome-wide analysis of mRNAs regulated by Drosha and Argonaute proteins in Drosophila melanogaster. Mol Cell Biol *26*, 2965-2975.

Riggleman, B., Schedl, P., and Wieschaus, E. (1990). Spatial expression of the Drosophila segment polarity gene armadillo is posttranscriptionally regulated by wingless. Cell *63*, 549-560.

Rivas, F.V., Tolia, N.H., Song, J.J., Aragon, J.P., Liu, J., Hannon, G.J., and Joshua-Tor, L. (2005). Purified Argonaute2 and an siRNA form recombinant human RISC. Nature structural & molecular biology *12*, 340-349.

Rivera-Pomar, R., and Jackle, H. (1996). From gradients to stripes in Drosophila embryogenesis: filling in the gaps. Trends Genet *12*, 478-483.

Roignant, J.Y., Carre, C., Mugat, B., Szymczak, D., Lepesant, J.A., and Antoniewski, C. (2003). Absence of transitive and systemic pathways allows cell-specific and isoform-specific RNAi in Drosophila. RNA (New York, NY *9*, 299-308.

Rose, L.S., and Wieschaus, E. (1992). The Drosophila cellularization gene nullo produces a blastoderm- specific transcript whose levels respond to the nucleocytoplasmic ratio. Genes & development *6*, 1255-1268.

Saiki, R.K., Scharf, S., Faloona, F., Mullis, K.B., Horn, G.T., Erlich, H.A., and Arnheim, N. (1985). Enzymatic amplification of beta-globin genomic sequences and restriction site analysis for diagnosis of sickle cell anemia. Science *230*, 1350-1354.

Saito, K., Ishizuka, A., Siomi, H., and Siomi, M.C. (2005). Processing of Pre-microRNAs by the Dicer-1-Loquacious Complex in Drosophila Cells. PLoS Biol *3*, e235.

Sanson, B. (2001). Generating patterns from fields of cells. Examples from Drosophila segmentation. EMBO reports *2*, 1083-1088.

Sasaki, T., Shiohama, A., Minoshima, S., and Shimizu, N. (2003). Identification of eight members of the Argonaute family in the human genome small star, filled. Genomics *82*, 323-330.

Schejter, E.D., and Wieschaus, E. (1993). bottleneck acts as a regulator of the microfilament network governing cellularization of the Drosophila embryo. Cell *75*, 373-385.

Schmidt, A., Palumbo, G., Bozzetti, M.P., Tritto, P., Pimpinelli, S., and Schafer, U. (1999). Genetic and molecular characterization of sting, a gene involved in crystal formation and meiotic drive in the male germ line of Drosophila melanogaster. Genetics *151*, 749-760.

Schreiber, S. (2003). Zellbiologische und molekularbiologische Untersuchungen zur Charakterisierung des *drop out*-Genlokus in *Drosophila melanogaster*. In Institut für Genetik (Düsseldorf, Heinrich-Heine Universität).

Schweisguth, F., Lepesant, J.A., and Vincent, A. (1990). The serendipity alpha gene encodes a membrane-associated protein required for the cellularization of the Drosophila embryo. Genes & development *4*, 922-931.

Si, K., Lindquist, S., and Kandel, E.R. (2003). A neuronal isoform of the aplysia CPEB has prion-like properties. Cell *115*, 879-891.

Sigova, A., Rhind, N., and Zamore, P.D. (2004). A single Argonaute protein mediates both transcriptional and posttranscriptional silencing in Schizosaccharomyces pombe. Genes & development *18*, 2359-2367.

Sijen, T., Fleenor, J., Simmer, F., Thijssen, K.L., Parrish, S., Timmons, L., Plasterk, R.H., and Fire, A. (2001). On the role of RNA amplification in dsRNA-triggered gene silencing. Cell *107*, 465-476.

Simmonds, A.J., dosSantos, G., Livne-Bar, I., and Krause, H.M. (2001). Apical localization of wingless transcripts is required for wingless signaling. Cell *105*, 197-207.

Sisson, J.C., Field, C., Ventura, R., Royou, A., and Sullivan, W. (2000). Lava Lamp, a Novel Peripheral Golgi Protein, Is Required for Drosophila melanogaster Cellularization. The Journal of cell biology *151*, 905-918.

Small, S., and Levine, M. (1991). The initiation of pair-rule stripes in the Drosophila blastoderm. Current opinion in genetics & development *1*, 255-260.

Smardon, A., Spoerke, J.M., Stacey, S.C., Klein, M.E., Mackin, N., and Maine, E.M. (2000). EGO-1 is related to RNA-directed RNA polymerase and functions in germ-line development and RNA interference in C. elegans. Curr Biol *10*, 169-178.

Song, J.J., Liu, J., Tolia, N.H., Schneiderman, J., Smith, S.K., Martienssen, R.A., Hannon, G.J., and Joshua-Tor, L. (2003). The crystal structure of the Argonaute2 PAZ domain reveals an RNA binding motif in RNAi effector complexes. Nat Struct Biol *10*, 1026-1032.

Song, J.J., Smith, S.K., Hannon, G.J., and Joshua-Tor, L. (2004). Crystal structure of Argonaute and its implications for RISC slicer activity. Science *305*, 1434-1437.

Stein, J.A., Broihier, H.T., Moore, L.A., and Lehmann, R. (2002). Slow as molasses is required for polarized membrane growth and germ cell migration in Drosophila. Development (Cambridge, England) *129*, 3925-3934.

Struhl, G., Johnston, P., and Lawrence, P.A. (1992). Control of Drosophila body pattern by the hunchback morphogen gradient. Cell *69*, 237-249.

Szakmary, A., Cox, D.N., Wang, Z., and Lin, H. (2005). Regulatory relationship among piwi, pumilio, and bag-of-marbles in Drosophila germline stem cell self-renewal and differentiation. Curr Biol *15*, 171-178.

Theurkauf, W.E. (1994). Actin cytoskeleton. Through the bottleneck. Curr Biol *4*, 76-78.

Thomas, G.H., and Kiehart, D.P. (1994). Beta heavy-spectrin has a restricted tissue and subcellular distribution during Drosophila embryogenesis. Development (Cambridge, England) *120*, 2039-2050.

Tijsterman, M., May, R.C., Simmer, F., Okihara, K.L., and Plasterk, R.H. (2004). Genes required for systemic RNA interference in Caenorhabditis elegans. Curr Biol *14*, 111-116.

Tomari, Y., and Zamore, P.D. (2005). Perspective: machines for RNAi. Genes & development *19*, 517-529.

Tuite, M.F. (2000). Yeast prions and their prion-forming domain. Cell *100*, 289-292.

Turner, F.R., and Mahowald, A.P. (1976). Scanning Electron Microscopy of Drosophila Embryogenesis. 1. The Structure of the Egg Envelope and the Formation of the Cellular Blastoderm. Developmental biology *50*, 95-1108.

Vagin, V.V., Sigova, A., Li, C., Seitz, H., Gvozdev, V., and Zamore, P.D. (2006). A distinct small RNA pathway silences selfish genetic elements in the germline. Science *313*, 320-324.

van Eeden, F., and St Johnston, D. (1999). The polarisation of the anterior-posterior and dorsal-ventral axes during Drosophila oogenesis. Current opinion in genetics & development *9*, 396-404.

Welte, M.A., Gross, S.P., Postner, M., Block, S.M., and Wieschaus, E.F. (1998). Developmental regulation of vesicle transport in Drosophila embryos: forces and kinetics. Cell *92*, 547-557.

Wienholds, E., Koudijs, M.J., van Eeden, F.J., Cuppen, E., and Plasterk, R.H. (2003). The microRNA-producing enzyme Dicer1 is essential for zebrafish development. Nature genetics *35*, 217-218.

Wilkie, G.S., and Davis, I. (2001). Drosophila wingless and pair-rule transcripts localize apically by dynein-mediated transport of RNA particles. Cell *105*, 209-219.

Williams, R.W., and Rubin, G.M. (2002). ARGONAUTE1 is required for efficient RNA interference in Drosophila embryos. Proceedings of the National Academy of Sciences of the United States of America *99*, 6889-6894.

Xu, K., Bogert, B.A., Li, W., Su, K., Lee, A., and Gao, F.B. (2004). The fragile X-related gene affects the crawling behavior of Drosophila larvae by regulating the mRNA level of the DEG/ENaC protein pickpocket1. Curr Biol *14*, 1025-1034.

Yan, K.S., Yan, S., Farooq, A., Han, A., Zeng, L., and Zhou, M.M. (2003). Structure and conserved RNA binding of the PAZ domain. Nature *426*, 468-474.

Yeom, K.H., Lee, Y., Han, J., Suh, M.R., and Kim, V.N. (2006). Characterization of DGCR8/Pasha, the essential cofactor for Drosha in primary miRNA processing. Nucleic acids research *34*, 4622-4629.

Zamore, P.D., Tuschl, T., Sharp, P.A., and Bartel, D.P. (2000). RNAi: double-stranded RNA directs the ATP-dependent cleavage of mRNA at 21 to 23 nucleotide intervals. Cell *101*, 25-33.

7 Appendix

7.1 Genomic Sequence of *ago2*

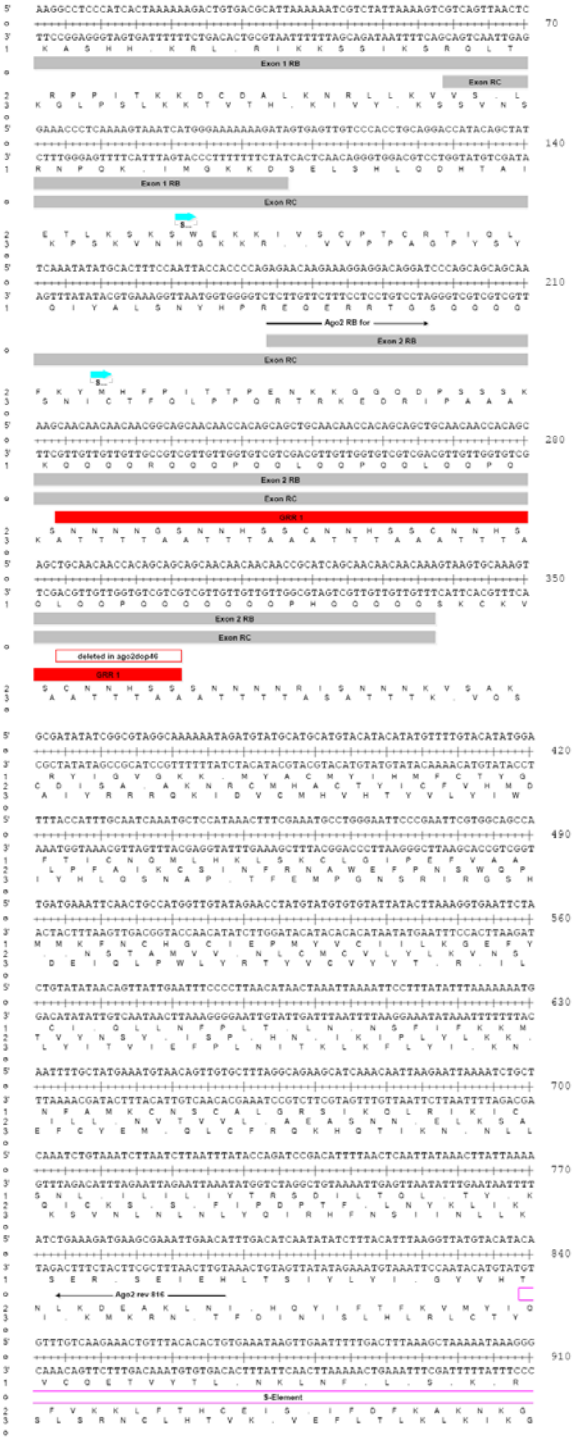

Figure 27 continued

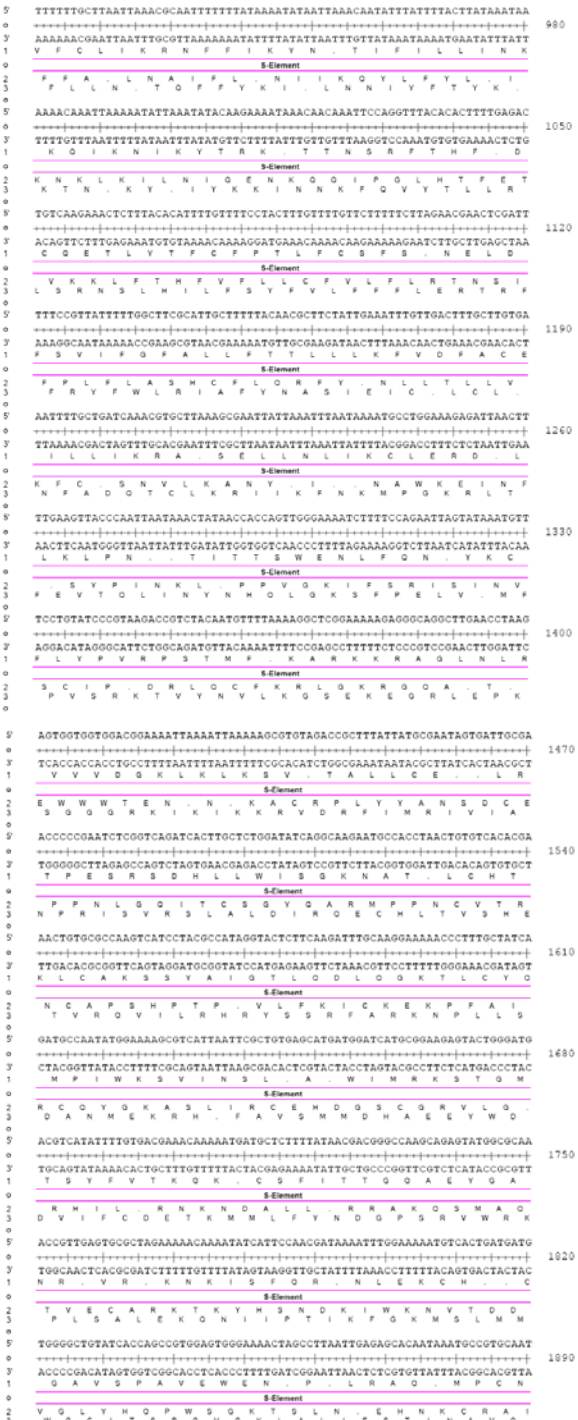

Figure 27 continued

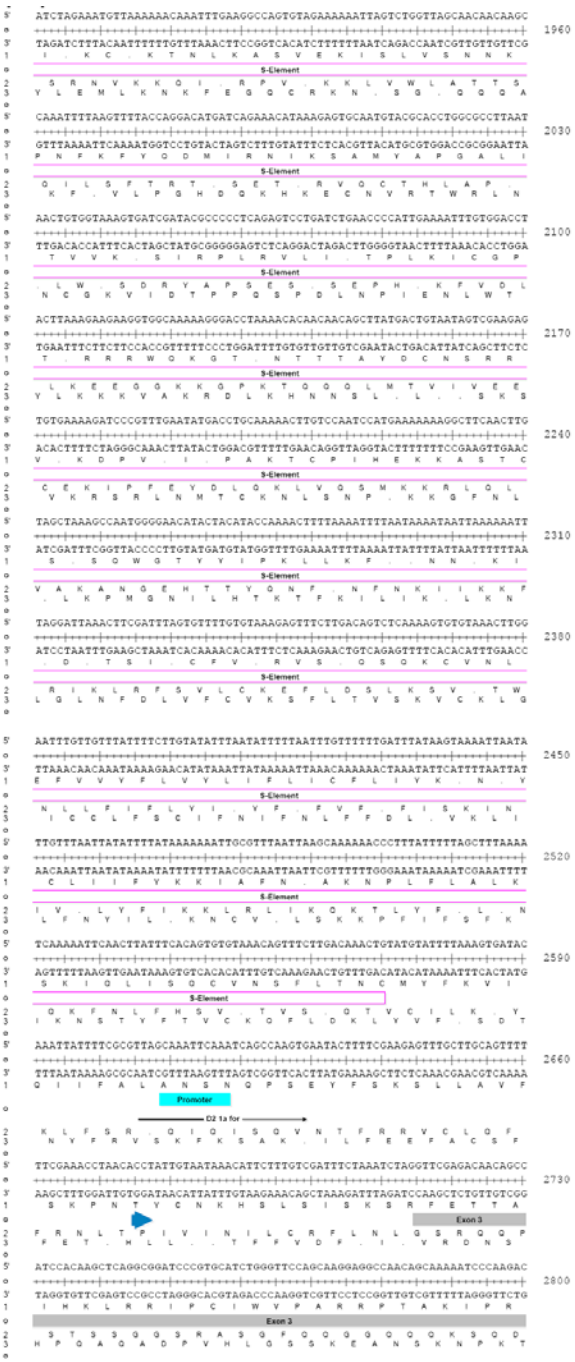

Figure 27 continued

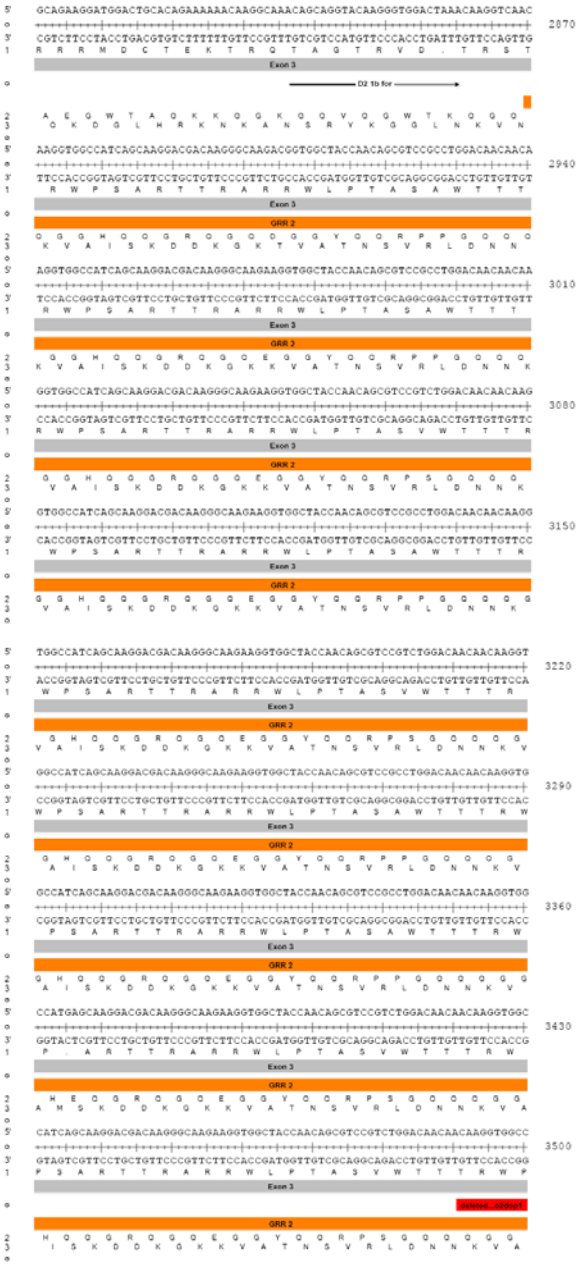

Figure 27 continued

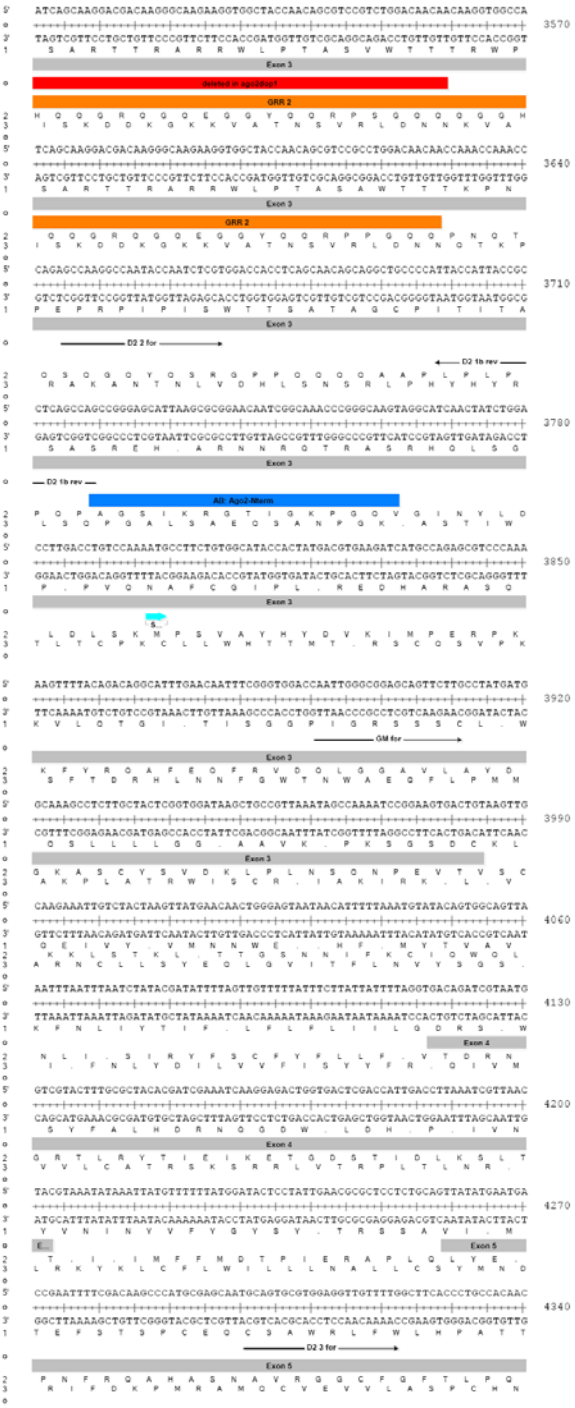

Figure 27 continued

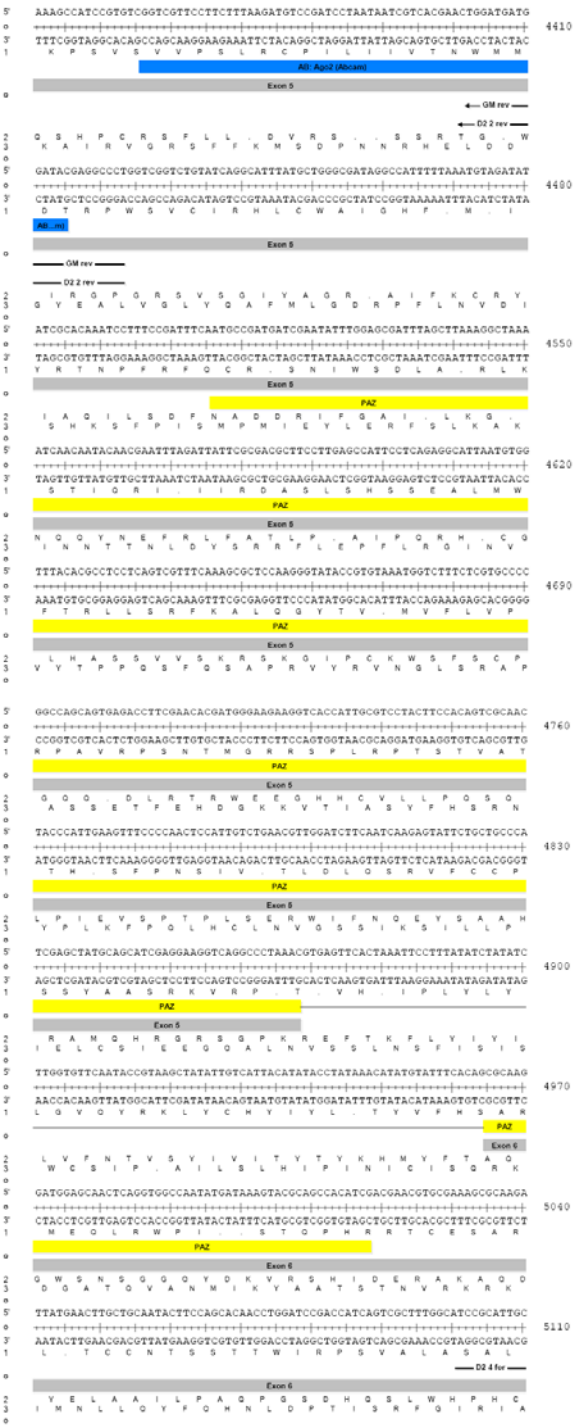

Figure 27 continued

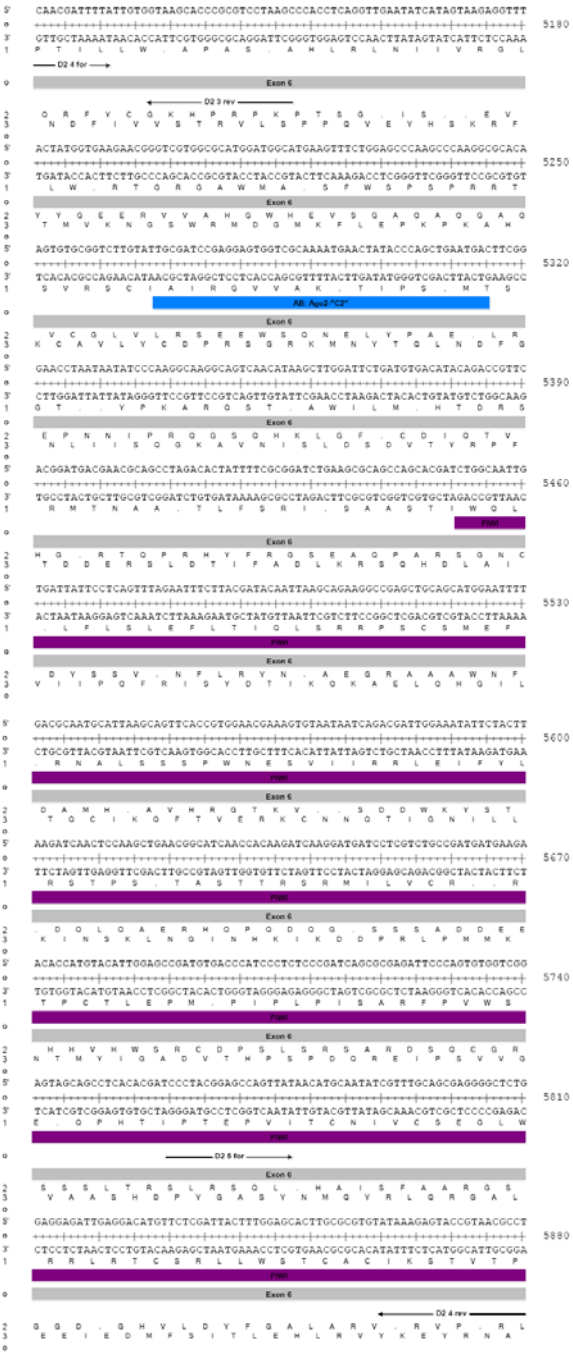

Figure 27 continued

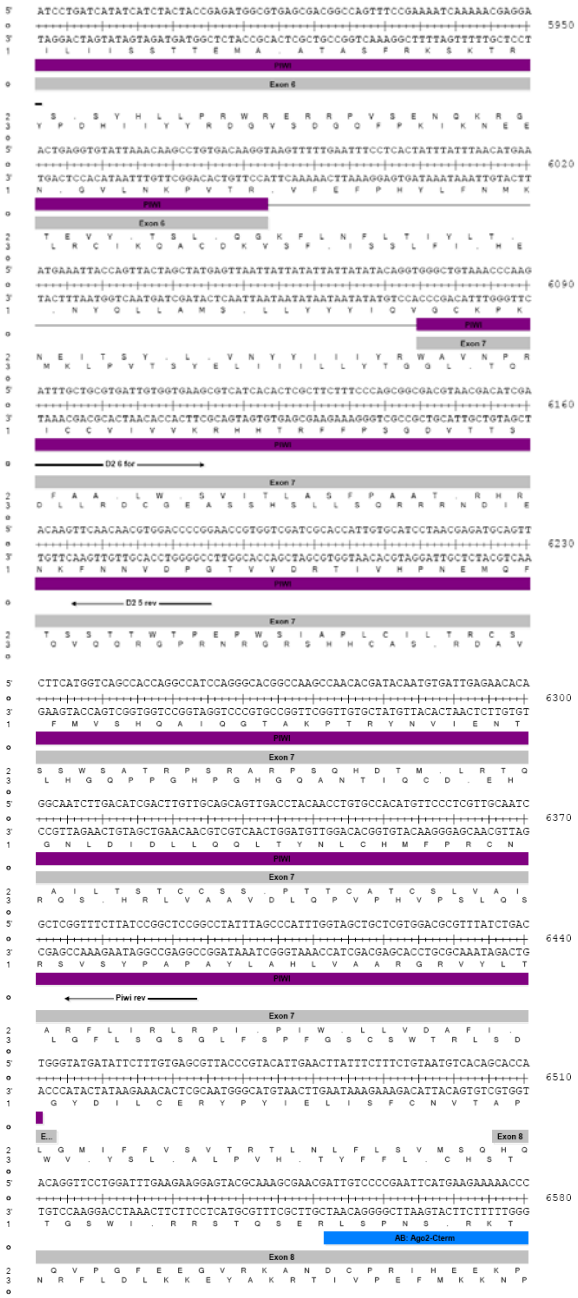

Figure 27 continued

Figure 27: Genomic sequence of *ago2*

The genomic sequence of *ago2* is shown. The 8 *ago2* exons are marked in grey. The regions that encode for the different Ago2 domains are indicated in different colours: GRR1 is indicated in red, GRR2 in orange, PAZ in yellow and the PIWI domain is purple. The deletions in *ago2*^{dop1} and *ago2*^{dop46} are marked with a red box. The location of oligonucleotides that were used in this work are represented by a black arrow (see as well Table 1). The oligonucleotides Ago2for203 and D2 6rev lay outside of *ago2*'s transcript and are not shown in this figure. The promoter for *ago2*^{short} is indicated with a turquoise box. The transcriptional start site (TSS) for *ago2*^{short} is marked with a blue arrow. The translational start sites for all isoforms are marked with turquoise arrows. The natural S-element is marked in pink. Binding sites for Ago2 antibodies are indicated by blue boxes. NB: Find the original sequencing data on CD which is attached to this thesis.

7.2 Analysis of Ago2 using different Ago2 antibodies

To study the subcellular localisation of Ago2 different Ago2 antibodies there generated. Immunolabelling were performed as followed: The fixed embryos were divided into two samples. One part was incubated with Ago2 antibody, the other half was incubated with Ago2 antibody and peptide [50 µg ml^{-1}] against which the antibody was generated. By comparing the antibody stainings, this approach allowed to determine whether the staining would be an unspecific background staining or if it would really recognise the epitope of the peptide. The settings of the confocal microscope were adjusted using the embryos that were incubated with antibody and peptide as a negative control. Using the same confocal microscope settings the embryos that were immunolabelled with the Ago2 antibodies only were investigated (Figure 28A - D). The immunolabelling of Ago2 using two different Ago2

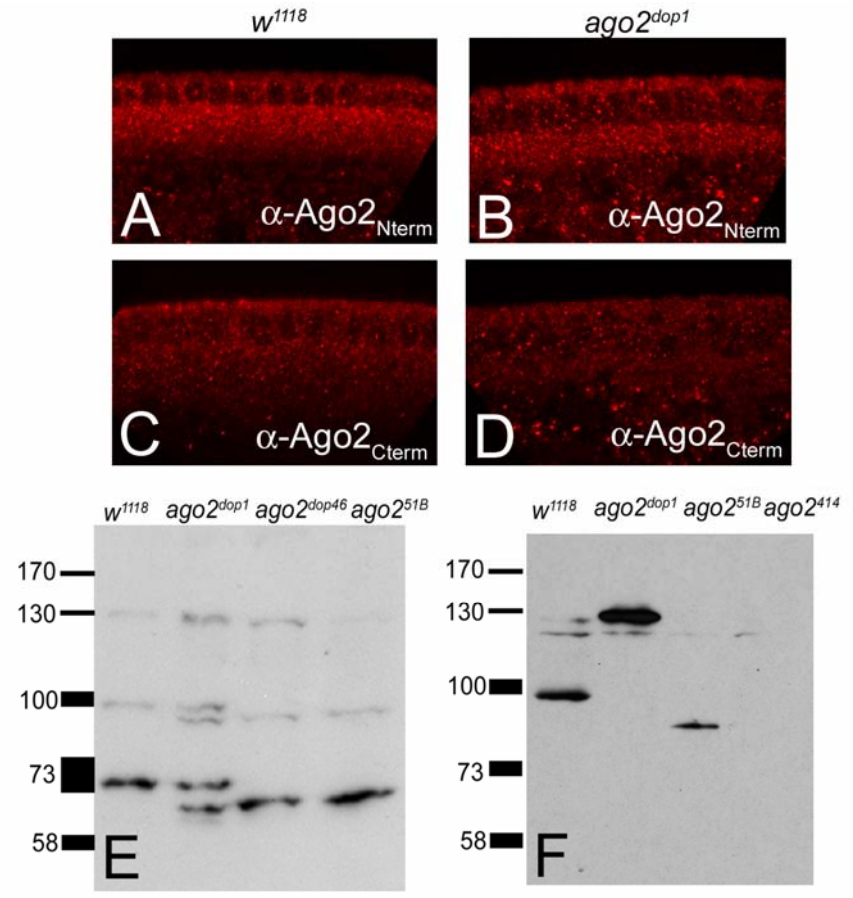

Figure 28: Investigation of Ago2 protein

Localisation studies and biochemical analysis of Ago2 using different Ago2 antibodies: Immunolabelling of early *wild-type* (A; C) and *ago2*^{dop1} mutant (B, D) embryos using Ago2$_{Nterm}$ and Ago2$_{Cterm}$ antibodies shows that dotty staining pattern for Ago2. The dots seem to be bigger in *ago2*^{dop1} mutant embryos (B, D). Biochemical analysis using different Ago2 antibodies identified different bands in a Western blot analysis. Crude protein preparations using Ago2$_{Cterm}$ antibody identified different protein isoforms for *wild-type, ago2*^{dop1}, *ago2*^{dop46} and *ago2*^{51B} (E). Using protein extracts and an Ago2 antibody from Q. Liu (University of Texas, Dallas, USA) identified a different protein pattern than Ago2$_{Cterm}$ (F).

antibodies (Ago2$_{Cterm}$ and Ago2$_{Nterm}$) in early embryos showed a dot-like staining pattern (Figure 28). This shows that Ago2^{long} might localise to distinct subcellular compartments. As in *ago2*^{dop1} embryos the dots seem to be bigger and to be localised more basally than in *wild-type* embryos might reflect an altered recruitment of Ago2^{dop1} to subcellular compartments. This might show that the altered GRRs of Ago2^{dop1} might have a higher potential to form aggregates or that the GRRs of Ago2^{dop1} have a higher affinity to be localised to subcellular compartments. In the future it would be essential to determine the nature of these putative subcellular compartments, e. g. one could test whether these compartments are GW bodies. GW bodies are cytoplasmic processing bodies. It was

shown that GW bodies concentrate miRNAs (Rehwinkel et al., 2005). Moreover, it would be necessary to reveal the process how Ago2, Ago2^{dop1} and if at all Ago2^{short} are localised there.

Western Blot experiments identified different Ago2 protein isoforms (Figure 28E, F). Crude protein preparations using Ago2$_{Cterm}$ antibody identified in *wild-type* a band of 130 kDa, which would correspond to Ago2^{long}, one band at approx. 100 kDa, which might correspond to Ago2^{short}, and a band at about 73 kDa, which might be an Ago2 degradation product (Figure 28E, left lane): The same bands are observed for *ago2^{dop1}* crude protein preparations (Figure 28E, left middle lane). But additionally to the three bands two smaller bands are detected: One is slightly smaller than 100 kDa and one is between 73 and 58 kDa. It is not clear what these bands represent. Interestingly, in *ago2^{dop46}* crude protein preparations only the smaller bands but not the bands that were detected in *wild-type* appear (Figure 28E, middle right lane). In crude protein preparations from *ago2^{51B}* ovaries Ago2 protein is present: a short protein of about 100 kDa and one band at approx. 70 kDa were detected. Using protein extracts and an Ago2 antibody from Q. Liu, PhD, University of Texas, Dallas, USA, detected a weak band at 130 kDa and band at 100 kDa (Figure 28F, left lane). For *ago2^{dop1}* protein extracts only a 130 kDa band is detected (Figure 28F, middle left lane). In *ago2^{51B}* extracts a band between 100 and 73 kDa is detected (Figure 28E, middle right lane). No protein was detected in *ago2^{414}* protein extracts (Figure 28E, right lane). Both antibodies that where used here identified Ago2^{long} and Ago2^{short}. However, in different experiments the results that were obtained with these two Ago2 antibodies were not consistent with each other. It therefore remains unclear which of the bands corresponds really to which Ago2 isoform and which band represents an Ago2 degradation product. What do the bands represent that were detected by α-Ago2$_{Cterm}$ that are slightly smaller than 100 kDa and 73 kDa, respectively (Figure 28E)? Using the Ago2 antibody from Q. Liu, PhD, University of Texas, Dallas, USA, why would Ago2^{short} be smaller in *ago2^{51B}* protein extracts than in extracts from *wild-type* (Figure 28F)? These questions should be addressed in the future.

8 Acknowledgements

Diese Dissertation wurde im Institut für Genetik der Heinrich-Heine Universität Düsseldorf unter der Anleitung von Herrn Dr. H. Arno J. Müller angefertigt. Ihm möchte ich für die Überlassung des Themas, die sehr gute Betreuung und stetige Unterstützung und für angeregte Diskussionen danken.

Herrn Prof. Dr. Rüdiger Simon danke ich für die freundliche Übernahme des Koreferats.

Michael Welte, PhD danke ich sehr für die Zusammenarbeit und die Unterstützung.

Bei Frau Prof. Dr. Elisabeth Knust als Leiterin des Instituts bedanke ich mich für die Bereitstellung des Arbeitsplatzes.

Bei Herrn Prof. Dr. Hans Bünemann möchte ich mich herzlich für die Bereitstellung des Arbeitsplatzes in seinem Labor bedanken. Außerdem danke ich ihm und Cornelia Gieseler für die freundliche Atmosphäre in der VIP-Lounge und den super Kaffee, der wahrlich alle Lebensgeister in einem geweckt hat!

Thorsten Volkmann danke ich sehr für seine engagierte Mitarbeit am Ago2-Projekt, für seine außerordentliche Hilfsbereitschaft in technischen Dingen und bei Computerproblemchen und für das Fachsimpeln über unser „Illuminatengen“.

Allen Mitgliedern des Instituts für Genetik bin ich für ihre außerordentliche Hilfsbereitschaft, das Engagement und die angenehme Arbeitsatmosphäre sehr dankbar. Für die stetige Diskussionsbereitschaft danke ich besonders Dr. Thomas Kessler, Dr. André Bachmann und Andreas van Impel.

Bedanken möchte ich mich herzlich bei den Mitgliedern der AG Müller für die schöne Zeit, die gute Stimmung und den Zusammenhalt. Mein besonderer Dank gilt Sirin Otte, Annika Raupach, Thomas Keßler, Mirjana Keßler, Anna Klingseisen und Andreas van Impel.

Ich danke besonders meinen Eltern Adda und Werner Meyer und meinen Geschwistern Maike und Reeno für ihre stetige Unterstützung.

Von ganzem Herzen danke ich meinem Mann Eduardo Márquez Oropeza für seine Liebe, Geduld und Unterstützung in jeder Hinsicht.

Erklärung:

Ich versichere, dass ich die von mir vorgelegte Dissertation eigenständig und ohne unerlaubte Hilfe angefertigt, die benutzten Quellen und Hilfsmittel vollständig angegeben und die Stellen der Arbeit, die anderen Werken im Wortlaut oder dem Sinn nach entnommen sind, in jedem Fall als Entlehnung kenntlich gemacht habe.

Die Dissertation wurde in der vorgelegten oder in ähnlicher Form noch bei keiner anderen Institution eingereicht. Ich habe bisher keine erfolglosen Promotionsversuche unternommen.

Die Bestimmungen der geltenden Promotionsordnung sind mir bekannt. Die von mir vorgelegte Dissertation ist von Herrn PD Dr. H. Arno J. Müller betreut worden.

Wibke Meyer Düsseldorf im März 2007

Teile dieser Arbeit wurden bereits veröffentlicht:

Meyer, W. J., Schreiber, S., Guo, Y., Volkmann, T., Welte, M. A., and Müller, H. A. (2006). Overlapping functions of argonaute proteins in patterning and morphogenesis of *Drosophila* embryos. PLoS genetics *2*, e134.